Role of Galectin-1 in Pancreatic Cancer Stroma, a small but mischievous protein with a novel nuclear function

Judit Vinaixa Forner

Director - **Dr. Pilar Navarro Medrano**
Co-Director – **M.D. Martín E. Fernandez Zapico**
Tutor – **Dr. Antonio García de Herreros**

Doctoral thesis UPF

Pilar Navarro Medrano (Director)	Martín E. Fernandez-Zapico (Co-director)	Antonio García de Herreros (Tutor)	Judit Vinaixa Forner (PhD candidate)

Cancer Research Program

(IMIM, Institut de Recerca Hospital del Mar)

PhD Programme in Biomwdicine

Barcelona, January 2019

“And the day came when the risk to remain tight in a bud was more painful than the risk it took to blossom”

Anaïs Nin

A Sandra
i Juli

ACKNOWLEDGEMENTS

En primer lugar, me gustaría dar las gracias a mi directora de tesis Pilar Navarro, por aceptarme a formar parte de tu grupo, por todas las oportunidades que me has ofrecido, pero sobretodo, por haber tenido siempre la puerta abierta a cualquier tipo de duda que nos haya ido surgiendo durante la tesis. Es una suerte contar con ese tipo de apoyo, muchas gracias Pilar! Por otra parte, también me gustaría agradecer a mi co-director de tesis Martín Fernández-Zapico por haberme acogido en un lugar tan lejano como es Rochester, por ayudarme a adaptarme tan rápido a tu laboratorio, por todas las cosas nuevas que aprendí durante mi estancia en la Mayo y por haber querido formar parte de este proyecto. ¡Estos cuatro años han supuesto un tiempo de aprendizaje enorme, muchísimas gracias a los dos!

Neus, la "post-doc meravella" i una gran companya de laboratori!! Gràcies per tot el que m'has ensenyat, per la paciència que has tingut en explicar-me tot el que no entenia, per (tot i les milions de coses que tens sempre a fer) sempre tindre un momentet per a mi, per preocupar-te, pel teu interès i per ajudar-me cada vegada que m'ha fet falta. A Mireia, l'alegria (i bogeria) del laboratori (i dels "mimis"), tan disposada a ajudar i sempre amb un somriure a la cara; gràcies pels teus "truquitos de la abuelita", per fer-me de metgessa més d'una vegada, i per estar sempre tan present. A les dos, moltíssimes gràcies per les forces i els ànims que m'heu donat durant toooota la tesi i sobretot en l'etapa final, sou glòria!

Amb tu Joan no sabria per on començar! Eres una persona que admire moltíssim i sóc més que conscient de la sort que he tingut en tindre un company con tu en el lab, m'has ensenyat molt! Mil gràcies per tot l'interés que has posat en el meu projecte, per

fer-me pensar, pel teu suport fins al final d'aquesta etapa i per les classes gratuïtes de bioinformàtica (per fi sé fer servir alguna cosa més que el "paint" en l'ordenador, qui ho diria!). A Carlos, ¡ay pobre Carlitos! Lo que te tocó aguantar en el laboratorio y, por si fuera poco, también en casa, verdad? Has sido un buen compañero, gracias por tus protocolos para dummies, por escucharme, y por darme a galectina-1 en herencia, ¡espero haber sabido cuidarla bien! I com no, a l' adquisició més recent del grup: Nayomi! Xiqueta, amb el poc temps que hem estat juntes al lab i el carinyo que t'has guanyat. De veres espere que tingues moltíssima sort amb tot el que t'espera, t'ho mereixes molt!! Ah, i per a que quede constancia: gràcies també pels "modelitos" que portes cada dia, els trobaré a faltar quan me'n vaja del lab!!

A todos los estudiantes de máster y carrera que han pasado por el lab: A Pedro, nuestro corresponsal de Girona, por las veces (aunque no muchas) que has conseguido sacarme de fiesta, por la ratona que me regalaste para mi "*in vivo*" y sobretodo por el tráfico de markers (la de eppis que hubiesen quedado sin rotular), gracias! A Bernat, per totes les rises, les carreres pel passadís del PRBB i pel senyor Dorín (recordes?). A Mireia xicoteta i a Núria, dos super mini-tècnics que espere que hagen aconseguit els seus objectius. A Núria, per les vesprades que passarem juntes al lab. A Alba, que tot i que les coses no han eixit sempre com esperaves no te rendires mai; continua aixina! Y en especial a Marta que, a pesar de los momentos de estrés, espero que te lleves un buen recuerdo de "la jefa", que te enseñó que la vida es dura (pero no tanto ;P!).

Continue amb els veïns, Snail lab, a vosaltres vos he d'agrair, des del primer dia en que vaig arribar, que sempre m' hageu fet sentir com una més del vostre grup. Començaré pels Chromatin Team: Joan Paut, Laura Pascual, Gemma i Jess, esteu com una cabra (alguns en especial) i, per això mateix, dir-vos que ha sigut una sort

haver-vos tingut al costat, amb vosaltres el riure estava més que assegurat. A Lorena, que primero fue Snail y después PN (menos mal que no soy la única), gracias por todo! A Raúl, por saber responder a todas mis dudas y por los todos reactivos prestados, ¡qué paciencia! =P. A Rubén, Héctor, Jordi, Aida, Willy, Raulillo y Rian pel temps compartit durant estos anys (for your company during you stay in Barcelona). A Marina, la més recent del grup, ànims amb aguantar a tota la tropa XD. Mil gràcies també al "trío calavera" de la UAB: Bea, Willy Strong y Neus ("la percha del PRBB"). M' encanteu els tres, i ho sabeu! També m'agradaria donar les gràcies a Laura Palacios, per tota l'alegria, que junt a Marta, portares al PRBB; et desitge el millor allà on vages reina!

Gràcies també a Bigas Lab, Laura, Jess, David, Leonie, Irene... Specially, I would like to mention Cristina Porcheri for your advices y también a Sara, por ser una fantasía de muchacha! A Xavier Mayol, per donar-me totes les cells que m'han fet falta (inclòs a destemps). A Estela, por tu buen sentido del humor, por los ánimos que vas repartiendo por ahí y porque das unos abrazos como nadie, mil gracias!! A Marta Garrido, porque de mayor quiero ser como tú! A Pilar y Rosi, por vuestra compañía y por todo lo que me habéis cuidado, sobretodo durante los últimos meses, muchísimas gracias de corazón; sois una maravilla! A més a més, a tota la gent del passadís de l'IMIM: Jeni, Dani, Laura, Anna, Cristina, Aïda, Ali, Evelyn, Miguel... als que ja se n'han anat Judith, Maria, Laura... i a molts més que segur em deixe... a tots gràcies, sobretot pels tornejos de volley platja, no haurem guanyat molts partits, però ganes no han faltat i trofeu tampoc! ;P I no sols de l'IMIM, sinó del PRBB en general, gràcies a totes aquelles persones que han posat el seu granet de sorra per fer que aquesta tesi anara endavant.

Gràcies també als organitzadors i organitzadores del Open Day, tindre l' oportunitat de compartir i ensenyar la feina que fem al

laboratori d' una manera tan amena és un regal. S'ho curreu moltíssim!

Gràcies a totes aquelles persones que ens faciliten i complementen la feina al laboratori. A la unitat de proteòmica del CRG/UPF, per aconsellar-nos i ajudar-nos tant amb la part experimental com amb l' anàlisi d'espectrometria de masses. Sobretodo, agradecer a Ivonne los "trainings" que nos hiciste hasta que conseguimos las muestras definitivas para el MS. A la unitat de genòmica de la UPF, Raquel, Roger i Núria gràcies per resoldre i buscar solucions alternatives als xicotets obstacles amb els que ens hem anat trobant durant la tesi. A la unitat de genòmica del CRG, per la seqüenciació del ChIP-seq. I a la unitat de microscòpia avançada (ALMU) del CRG per tota la seua ajuda amb el confocal durant l'últim període de la tesi.

Als meus companys de pis i veïns de laboratori: Rumi (Laura Sala) y Daví (Mi arma). A los dos deciros que sois más que geniales, que me ha encantado vivir con vosotros, y que lo volvería a hacer mil y una veces. Una parte muy importante que me llevo de Barcelona viene de vosotros dos, os adoro! Rumi, eres una dolçor de persona, el teu bon rollo és contagiós; t'ho mereixes tot perla! Contigo Daví, sobran las palabras (a veces ni me salen, literalmente!), vales oro no lo olvides!

I was also very lucky to meet lot of special people in the other side of the world, during my stay in Rochester. Me gustaría empezar con mis compañeros de casa internacionales: Luis y Renzo, por lo bien que os portasteis siempre conmigo, por todos los buenos (y no tan buenos) momentos que pasamos y que nos hicieron aprender, por las noches de salsa y por hacer de la ciudad de Rochester un hogar: gracias! Al grupo de españoles que nos encontramos tan lejos de casa: Javi, Candela, Núria, Santi, Marta, Kons… gracias por hacer

que la llegada a Rochester fuese tan cálida, quién diría que comería fabada asturiana casera al otro lado del charco! I would like also say thanks to my lab mattes at Mayo Clinic: Ezequiel, Luciana, Elisa, Rachel, Paola, Stephany, David, Luis, Renzo, Eriko, Tara, Aryan and Anne. For your interest and for your help inside and outside the lab. I have learnt a lot from each of you, thanks! Reeja, Koji, Kiran, Poorval and Luis, thanks for seasoning my time in Rochester with so many great moments, you guys have been very good friends. All of you made me feel like home. THANK YOU!

Tornant un poc la vista enrere, també m'agradaria rememorar el temps que vaig estar en la Universitat de València. Marce i Mercé, vosaltres vau ser els primers que m'iniciareu en l'extraordinari món que és la ciència. Als dos, moltíssimes gràcies per tot el que me vareu ensenyar!

Als amics de "tota la vida", David, Lorena, Raquel, Mario, Piesito,... gràcies per fer que tornar al poble sempre siga una alegria. A Enric i a Mire, que encara que no ens vejam molt seguit, amb vosaltres és com si el temps no passara. A Sergio, a Adrián..., i en especial, gràcies a Rocío, Alba i Ángel per entendre tot el que de vegades ha sigut difícil de comprendre. Y a Eloísa y a Anchel, a vosotros gracias por ser como sois.

A la meua família un milió de gràcies, perquè part del que sóc ara és gràcies a vosaltres. A mon pare, per posar tot de la teua part i donar-me suport durant aquesta etapa. A ma mare, per estar quan més ho he necessitat i per animar-me sempre a seguir endavant. Als dos mil gràcies per fer-me creure que sempre podia intentar-ho una vegada més! *Sis-ter*, a tu te podria dir mil coses, però crec que elegiré esta: T'has posat les serps als peus?! (Sempre seràs la meua mitja taronja, ja ho saps). Gràcies als meus tios, ties, cosins, cosines i a Joan, l'alegria de la casa; però en especial als meus

cosins Aida, Andrés i Joel (tot i que me venjaré per lo del flam! ¬ ¬). Als meus "uelos", Vicente i Visantica, i als meus iaios, José i Amparito, perquè m'encateu i perquè me feu riure més que ningú. També a Carlos, Laura i Alba, gràcies per acollir-me en casa quan no tenia on anar. I a Juli, Vicent i Maria, a vosaltres gràcies per demostrar-me que l'estima va molt més enllà dels llaços familiars. Ah, i Maria va per tu: llentilles/llenties/lentejes, cúspide, i no recorde qué més! XD

I també gràcies a la música en general, no me vaig a posar a recitar la meua llista del spotify; però xe!, qui no s'anima posant-li un poc de ritme al dia a dia!

Finally, thanks to the tribunal committee for reading and assessing this project. I hope you enjoy reading it as well as I enjoyed writing it.

Una xicoteta reflexió sobre el PhD/ Una pequeña reflexión sobre el PhD/ A little thought about PhD

Pensant en el primer dia quan una comença el doctorat, veus que realment no saps el que t' espera durant aquesta etapa. Al principi et veus preparadíssima per a endinsar-te en un projecte nou, amb ganes d'aprendre i de "descobrir moltes coses". Saps, perquè ja t'ho han avisat, que és una feina moltes vegades frustrant, que no tot ix com t'agradaria i que l'esforç moltes vegades no es veu del tot reflectit amb els resultats que una voldria aconseguir, però tu pots amb tot (no serà per a tant). I és ben cert (ambdues coses ho són), la ciència és una feina que implica dedicació i esforç, dos qualitats que continue veient molt importants per seguir endavant en aquest àmbit. La frustració és un factor vital en tota la història, no ens enganyem, cap feina resulta ser un camí de roses i la ciència

no és una excepció. Però no siguem tan negatius, al final tot porta la seua recompensa, perquè si la frustració sobre "el temps que he perdut" és dura (i segurament una de les coses que més ens costa acceptar), el fet de sobrepassar-la i de resoldre problemes que abans no sabies com afrontar ho compensa exponencialment. I és que, la motivació i les ganes de superar-se són essencials en moments en que ho enviaríem tot "a pastar fang". I no sols ens afecta en l' àmbit professional, al cap i a la fi, la tesi és un període en el que "ens posem a prova" i que moltes vegades ens influeix a un nivell més intern. Conseqüències? Com a mínim una ben bona, i és que una persona evoluciona i canvia amb el seu pas pel doctorat i, ja siga més o menys "exitós" el seu projecte, sempre t'emportes un missatge a casa, i és ahí on resideix el vertader èxit que implica un Ph.D.

Pensando en el primer día en que una empieza el doctorado, creo que la mayoría de nosotros no sabemos muy bien que es lo que nos espera durante esta etapa. Al principio te ves preparadísima para adentrarte en un proyecto nuevo, con ganas de aprender y de "descubrir muchas cosas". Sabes, porque ya te han avisado, que es un trabajo muchas veces frustrante, que no todo sale como a te gustaría i que el esfuerzo muchas veces no se ve reflejado con los resultados que una consigue, pero tú puedes con todo (no será para tanto). Y es muy cierto (ambas cosas lo son), la ciencia es un trabajo que implica dedicación y esfuerzo, dos cualidades que continúo viendo muy importantes para seguir adelante en este ámbito. La frustración es un factor vital en toda la historia, no nos engañemos, ningún trabajo resulta ser un camino de rosas y la ciencia no es una excepción. Pero no seamos tan negativos, al final todo tiene su recompensa, porque si la frustración sobre "el tiempo que he perdido" es dura (i seguramente una de las cosas que más nos cuesta aceptar), el hecho de superar-la y resolver problemas que antes no sabías como afrontar lo compensa exponencialmente. Y es

que la motivación y las ganas de superarse son esenciales en momentos en los que lo mandaríamos todo a “tomar vientos”, Y no solo nos afecta en el ámbito profesional, al fin y al cabo, la tesis es un periodo en el que “nos ponemos a prueba” y que muchas veces nos influye a un nivel más interno. ¿Consecuencias? Por lo menos una muy buena, y es que una persona evoluciona y cambia a lo largo de su doctorado y, ya sea más o menos “exitoso” su proyecto, siempre te llevas un mensaje a casa, i es ahí donde reside el verdadero éxito que implica un Ph.D.

Thinking about your first day of your thesis, you would think you had no clue about what are you going to life during your thesis. At the beginning, you are ready for starting a new project, happy to learn and for “discovering lot of things”. You already know, because somebody advise you, that science isn’t that easy, since most of the time you don’t get the desired results, but you can do it! And that’s true (both of them), science is a job that requires lot of effort and vocation, two very important qualities (at least for me). Frustration is an essential part of the whole story; perfect job doesn’t exist and science is not a “bed of roses” neither. However, every effort is rewarded, because of the satisfaction you feel when you overcome the frustration and start solving problems. Definitely, motivation is essential during the hardest moments. On the other hand, thesis challenge you every day and this can also affect ourselves. Any consequence? A very good one, people evolve along their projects and, with more or less results, you always learn something, and that’s the real success of a Ph.D.

ABSTRACT

Pancreatic ductal adenocarcinoma (PDA) is one of the most aggressive tumors and it is predicted to become the second cause of cancer related death by 2030. This is mostly due to its lack of symptoms, resulting in late diagnosis, and also to the presence of an aggressive tumor microenvironment, which favors the resistance to current and emerging therapies. Galectin-1 (Gal-1), a glycan-binding protein highly expressed in the PDA stroma compartment, exerts a crucial role in modulating tumor-stroma crosstalk in this disease. In particular, our group has demonstrated that Gal-1 promotes tumor proliferation, metastasis, angiogenesis and immune evasion in PDA. Importantly, Gal-1 is mainly produced by PDA stellate cells (PSC), however the intrinsic role of this protein in PSC biology is poorly understood. In the present study, we define a novel role of endogenous Gal-1 in the biology of pancreatic cancer stroma using a combination assays in Human PSC (HPSC) models. We determine the impact of Gal-1 in HPSC proliferation, migration, invasion, activation and extracellular matrix organization. Using high throughput analysis (microarrays) we have defined the molecular mechanisms underlying Gal-1 functions in HPSC. Finally, considering that Gal-1 is highly expressed in HPSC nuclei, we elucidate the involvement of nuclear Gal-1 in the regulation of gene expression in these cells.

RESUM

El càncer de pàncrees representa un dels tumors més agressius, del qual es preveu que serà la segona causa de mort deguda al càncer en 2030. Aquesta mortalitat, principalment, s'explica per la falta de símptomes, la conseqüent tardana diagnosi i per la presència d' un microambient tumoral agressiu que afavoreix la resistència del tumor als tractaments actuals. Galectina-1 (Gal-1), una proteïna que reconeix carbohidrats i que es troba altament expressada en el estroma del càncer de pàncrees, exerceix un paper fonamental en modular la interacció tumor-estroma. Concretament, el nostre grup ha demostrat que Gal-1 promou la proliferació tumoral, la metàstasi, l'angiogènesi i l' evasió de l' efecte anti-tumoral del sistema immune. Gal-1 es produïda principalment per les cèl·lules estelades del càncer de pàncrees, tot i així, la funció biològica d'aquesta proteïna en les pròpies cèl·lules estelades continua sent desconeguda. En aquest estudi, hem definit una nova funció biològica de Gal-1 endògena en el estroma de càncer de pàncrees utilitzant una combinació d'assajos amb cèl·lules estelades de càncer de pàncrees humanes. D' aquesta manera hem determinat la importància de Gal-1 en la proliferació, migració, invasió, activació i en l'organització de la matriu extracel·lular d' aquestes cèl·lules. Mitjançant anàlisis genètics, hem determinat els mecanismes moleculars amb els que Gal-1 controla aquestes funcions en les cèl·lules esmentades. Finalment, considerant que Gal-1 es troba altament expressada en el nucli de les cèl·lules estelades de càncer de pàncrees, hem definit la contribució de Gal-1 nuclear al control de la expressió gènica en aquestes cèl·lules.

CONTENTS

INTRODUCTION

1.1. The Pancreas

1.1.1 Anatomy and physiology of pancreas

The human pancreas (from Greek *pan* ("all") and *kreas* ("flesh")) is a slender organ located in the abdominal cavity which can be divided into four distinct regions: head, neck, body and tail. In mice, pancreas is observed as a less defined organ diffusely distributed throughout the duodenal mesentery[1,2]. This gland is composed of exocrine and endocrine cells, which are in charge of two essential functions in the metabolism: nutrient digestion and glucose homeostasis, respectively. The exocrine compartment, corresponding to the bulk of the adult organ mass (> 80%), comprises acinar cells that are responsible for digestive enzyme production and secretion, and duct cells which form a tubular network in charge of enzyme transport to the duodenum[3,4]. Acinar cells are pyramidal-polarized cells with a high secretory capacity due to the presence of zymogen granules placed in the lumen-proximal region[5]. These cells are organized in epithelial rosettes (acini) surrounding a central lumen and placed at terminal ends of an interconnected channels formed by hydrogen bicarbonate-producing ductal cells (Fig. 1). Pancreatic ductal network is composed of highly branched channels which progressively converge into larger ducts transporting pancreatic fluid through the accessory duct of Santorini and the main pancreatic duct of Wirsung, which finally drains pancreatic juice containing proenzymes that catalyze the lysis of carbohydrates, proteins and lipids into the duodenum[3]. An oval-to-cuboidal shaped cells, called centroacinar cells, are located at the terminal end duct that interface with acini. Embedded within the exocrine tissue, the endocrine section (1 - 4 % of pancreatic mass in humans) is distributed in highly vascularized grouped-cells named islets of Langerhans, which are composed of different hormone-producing cell types[1]. These includes: α-cells

(responsible for glucagon generation), β-cells (in charge of insulin and amylin synthesis), somatostatin-producing δ-cells, pancreatic polypeptide-producing PP-cells and ghrelin-producing ε-cells[1,6].

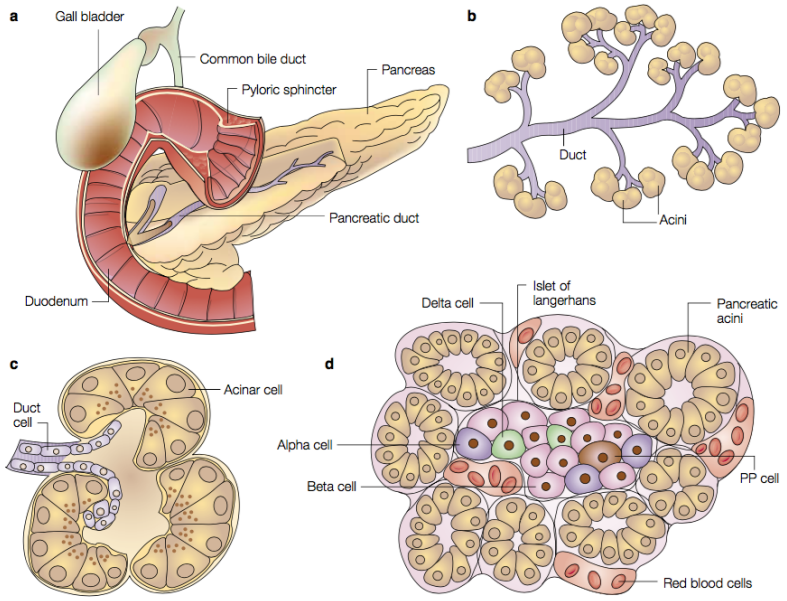

Figure 1. Anatomy of the pancreas. A) Gross anatomy of the pancreas. B) Ductal network and acini diagram. C) A detailed acinar cell rosette. D) Islet of Langerhans embedded within exocrine tissue. Extracted from *Bardeesy and DePinho. Nat Rev Cancer (2002)*[7].

1.1.2 Pancreatic organogenesis in mice

A highly regulated gene network is necessary for progenitor pancreatic identity maintenance as well as proper cell specification. Expression of pancreatic and duodenal homeobox-1 (*Pdx1*), pancreas-specific transcription factor 1a (*Ptf1a*) and sry-box 9 (*Sox9*), among other factors, are essential for the maintenance and expansion of multipotent pancreatic progenitors. At the primary

transition, pancreatic progenitor cells proliferate and evaginate from a pancreatic bud which results in cell stratification surrounding central microlumens. These microlumens, placed in the middle of rosettes, start to enlarge and fuse generating a primitive tubular network composed of bipotent *Nkx6.1*$^{+}$ "trunk" domains and multipotent *Ptf1a*$^{+}$ "tip" domains (Fig. 2)[3,5].

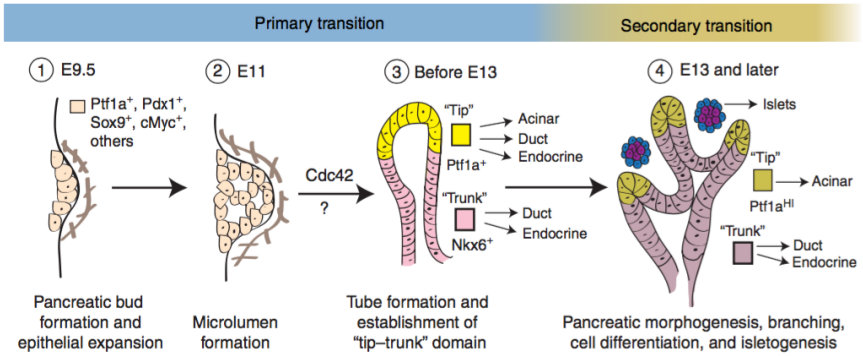

Figure 2. Mouse pancreatic morphogenesis. Pancreatic development consists in two transition waves: a primary transition from embryonic day (E) 9.5 to E12.5 and a secondary transition from E13 to birth. 1) Pancreatic bud formation and proliferation of pancreatic progenitor cells expressing *Ptf1a*, *Pdx1*, *Sox9*, *cMyc* transcription factors among others. 2) Microlumen formation (white spaces), proper pancreatic morphogenesis is coordinated by interactions and signals from other cells, such as mesenchymal cells (brown crosshatch). 3) Multipotent "tip" and bipotent "trunk" establishment. *Ptf1a*$^{+}$ "tip" progenitors give rise to acinar, ductal and endocrine cells, whereas *Nkx6*$^{+}$ (*Nkx6.1* and *Nkx6.2* factors) "trunk" progenitors derive ductal and endocrine cells. This process is simultaneous with the tubular network formation. 4) Pancreatic branching cell expansion and specification. "Tip" domain only will generate acinar cells, while "trunk" domain will produce ductal and endocrine cells, last will group together into islets known as Islets of Langerhans. Extracted from *Benitez et al. Cold Spring Harb Perspect Biol. (2012)*[5].

During pancreatic morphogenesis, branching is concomitant with proper regulatory gene changes leading to lineage segregation (Fig. 3). In a secondary transition, expressing *Ptf1a*, *cMyc* and *Cpa1*

distal tip domains become unipotent giving rise to acinar cells specification. While expressing *Nkx6.1*, *Hnf1b*, *Sox9*, *Hnf6* and *Hes1* central trunk is bipotent generating endocrine as well as ductal cells. Acinar differentiation requires the formation of PTF1a-RBP-J_L protein complex, and the expression of *Nr5a2* and *Mist1* genes which respectively control the generation of acinar proenzymes and acinar cell polarization, this results in the acinar compartment which corresponds to near 90% of adult pancreas. Ductal cells preserve the expression of most of the trunk-specific markers leading to the development of mature interconnected ducts. Endocrine specification depends on NEUROG3 transcription factor expression, facilitated via low levels of Notch signaling, and takes place in two major steps during pancreatic organogenesis: in the primary transition, in which progenitor cells can evolve into α-cells expressing *Arx*, *Brn4*, *MafB* genes; and in the secondary transition, in which "trunk" domain gives rise to the majority of endocrine precursors, simultaneously to ductal cell remodeling and maturation. Unipotent endocrine cell precursors disassembled from ductal neighboring cells and gradually differentiate towards mature endocrine cells. Finally, delaminated endocrine cells cluster into islets of Langerhans[3,5].

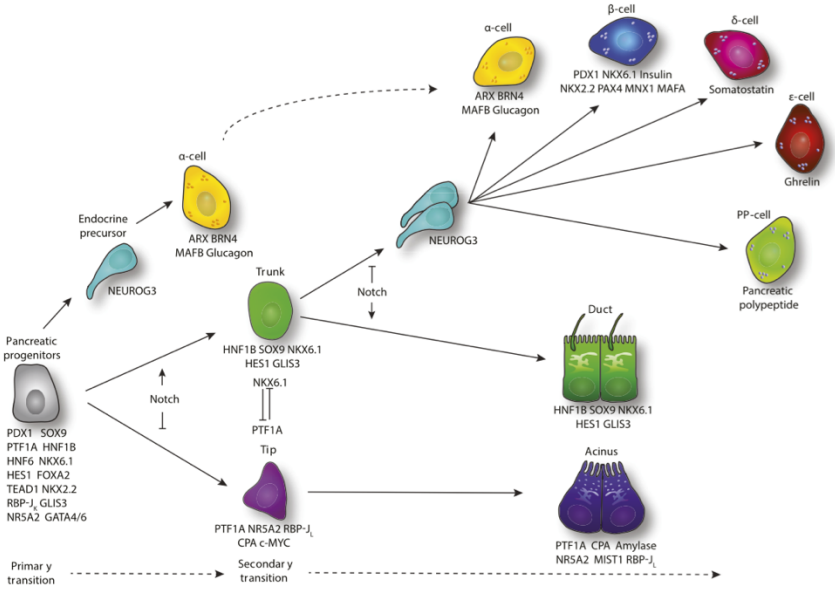

Figure 3. Pancreatic lineage segregation. A set of transcription factors are expressed by pancreatic progenitors to maintain their multipotent properties. During primary transition α-cells could emerge from scattered pancreatic progenitors after expressing *Neurog3* endocrine marker. The segregation of the expression of *Ptf1a* (acinar cells progenitors) and *Nkx6.1* (ductal and endocrine cells progenitors), in conjunction with Notch signaling, generate tip-trunk domains formation. During secondary transition the expression of PTF1a-RBP-J_L protein complex leads to acinar cell maturation expressing *Nr5a2* and *Mist1* genes. While ductal cells retain most of the trunk domain markers, endocrine cell specification is determined by *Neurog3* expression. Extracted from *Larsen and Grapin-Botton. Semin Cell Dev Biol (2017)*[3].

1.2 Pancreatic ductal adenocarcinoma (PDA)

Since cellular diversity is a remarkable characteristic of pancreas, multiple neoplasms of the pancreas have been defined in accordance to its histological and molecular features. Pancreatic neoplasms can be classified as pancreatic neuroendocrine tumors

(PanNET), which account for about 6% of all pancreatic tumors, or as exocrine pancreatic tumors (94%) including pancreatic ductal adenocarcinoma (PDA), acinar cell carcinoma, mucinous cystic neoplasms (MCN), intraductal papillary mucinous neoplasms (IPMN), solid-pseudopapillary neoplasms (SPN), serous cystadenomas (SCA) and pancreoblastoma among others[8–10]. PDA is by far the most common type of pancreatic tumor, comprising more than 80% of all pancreatic cancers. More than 1.7 million new cancer cases were estimated to be diagnosed in 2019 in United States, 56.770 of them were predicted to develop pancreatic cancer corresponding to 3.34% of all cancer cases. In spite of its low incidence, PDA represents the third leading cause of all cancer cases, being previewed to become the second one by 2030[11], with a 5-year relative survival rate about 9%[12,13]. Although causes of pancreatic cancer still remain unknown, it has been observed diverse factors that could affect the risk of pancreatic cancer, such as age, obesity, low physical activity, diet, tobacco consumption, diabetes, and even ABO blood type[14,15]. The overlapping inflammatory events that occur between chronic pancreatitis (CP) and PDA, evidence CP as a well-established risk factor for pancreatic cancer development[16]. In addition, around 10% of pancreatic cancer cases are hereditary due to cancer-associated germline mutations in genes like *BRCA2*, *CDKN2A*, *P53*, *APC* and *PRSS1* among others[17,18]. Huge mortality lead by PDA could be explained by its aggressiveness, in which even primary stages of the disease are able to develop metastasis [18]. An important hallmark of PDA is desmoplasia, which is a dense fibrotic deposition mainly driven by pancreatic stellate cells (PSC) accounting for more than 80% of the tumoral mass in PDA. It has been reported that desmoplasia represents a physical barrier contributing to therapy resistance of PDA making difficult to develop an effective treatment (see section *1.3 The relevance of stroma compartment in PDA*). Moreover, since symptoms usually do not appear until disease progress to a more advanced stage, early

diagnosis had become troublesome (see section *1.2.2 PDA symptoms and diagnosis*). For this reason, a special interest should be done on developing new promising treatments as well as better approaches for early diagnosis for PDA.

1.2.1 PDA development and genetics

PDA is characterized by the accumulation of multiple genetic alterations during disease progression (Fig. 4). Activating point mutation in *KRAS* oncogene at codon 12 represent the most common genetic mutation which appears sporadically in pancreas tissue. It is found in nearly 30% of early neoplasms and its frequency is increased as disease progress, thus more than 95% of advanced PDA presents mutated KRas[7,18]. This genetic abnormality generates a constitutively activated KRas molecule promoting cell proliferation and survival independently of the presence of any growth factor stimuli. Mutated *KRAS* involves activation of several downstream pathways, like epidermal growth factor (EGF) signaling which stimulates cell growth via PI3K pathway[18]. Interestingly, it has been described that *KRAS* mutation is not only an initiating event for PDA generation, but also its expression is determining for PDA maintenance and progression[18]. Mutations in *CDKN2A* tumor suppressor gene are also very frequent (80-95%) in PDA and usually appear in moderately-advanced lesions. *CDKN2A* encodes for *INK4A* and *ARF,* two overlapping tumor suppressors located in 9p21 locus (being $p16^{INK4A}$ and $p19^{ARF}$ their respective protein products). Implying that mutations in *INK4A* and *ARF* appear together in many pancreatic cancers[7]. However, the loss of those tumor suppressors follows different mechanisms to tumorigenesis contribution. While $p16^{INK4A}$ inhibits CDK4 and CDK6 and consequently, blocks the entry to S phase in cell cycle; $p19^{ARF}$ induces cell arrest hindering p53

proteolysis driven by MDM2. Interestingly, it seems that KRas cooperates with the loss of $p16^{INK4A}$ exacerbating chromosome instability and pancreatic malignant cell progression, since cells lacking of $p16^{INK4A}$ are uncapable to become senescent[18,19]. On the other hand, *TP53*, another tumor suppressor gene, is mutated in 80-85% of PDA cases[19], usually at very advanced stages of the disease when significant dysplasia emerges. Upon telomeric erosion and genetic damage, loss of p53 allows survival and cell growth, as well as favoring chromosomal rearrangements through breakage-fusion-bridge cycles[7]. Loss of *SMAD4* is found at the later stages of pancreatic cancer promoting non-canonical TGF-β-mediated signaling growth[19]. Hedgehog (Hh), Notch and Wnt, three signaling pathways crucial for pancreatic embryogenesis, have been found aberrantly activated during PDA development and progression. Special interest has been done in defining Hh signaling pathway since its activation in pancreatic stellate cells (PSC) have been shown to contribute to desmoplasia, a hallmark of PDA[20,21]. Alterations on Notch and Wnt signaling activation have been described in tumor compartment mediated by secreted factors at the tumor microenvironment (TME)[22].

PDA usually originates in the head of the pancreas exhibiting a glandular duct-like structures with diverse degrees of cellular atypia and differentiation. Muscinous cystic neoplasms (MCN), intraductal papillary muscinous neoplasms (IPMN), and pancreatic intraductal neoplasms (PanINs) have been identified as PDAC precursor lesions[19,23]. Among them, PanINs represent the classical and most common injuries from which PDAC arises. Mutation frequency and variability, and consequent cytological atypia, increases within advanced PanINs degree. Thus, PanINs are classified in three stages encompassing from PanIN-1 (low-grade dysplasia) to PanIN-3 (high-grade dysplasia). During early stages, PanINs are histologically identified by ductal cell elongation and

mucin production (PanIN-1A), then pseudo-papillary structures start to arise (PanIN-1B) usually accompanied by the overexpression of *ERBB2* and *EGFR* (receptors of the EGF-family ligands), and mutant *KRAS* activation. Nuclear abnormalities, such as pleomorphism and crowding, appear as PanIN lesions enlarged (PanIN-2) in which mucinous epithelium frequency is reduced and mutations in *CDKN2A* can be detected. PanIN-3 are characterized by drastic nuclear atypia, frequent mitosis, budding into lumen, and intraluminal apoptotic cell debris; these lesions normally present mutations in *TP53* and *SMAD4* genes and are already considered *in situ* carcinomas. PanINs eventually turn into frank well-established adenocarcinoma with invasive growth beyond base membrane accompanied by a robust stromal inflammatory reaction (Fig. 4 B)[7,18,19].

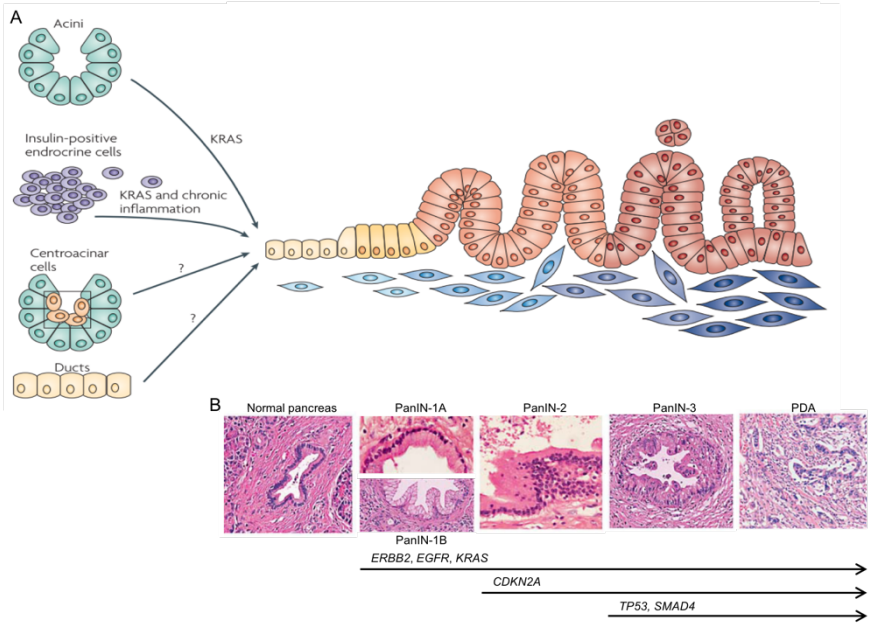

Figure 4. Cell of origin and progression of PDA. A) Acinar, ductal, endocrine and centro-acinar cells have been proposed to be the cell of origin of PDA. Acini and endocrine cells bearing activated *KRAS* have been shown to generate PanINs.

Ductal cells have been proposed to follow different pathophysiology during PDA progression. Giving their location and cellular features, centro-acinar cells could also be the source of PDA. B) PDA progression through PanIN neoplastic stages (from PanIN-1 to PDA) Arrows indicated frequent gene alteration found in each stage. *ERBB2*, *EGFR* and *KRAS* alterations appear in early lesions. Inactivation of *CDKN2A* are usually found as of PanIN-2. While *TP53* and *SMAD4* are lost in advanced lesions. Several gene mutations accumulate throughout PDA progression giving rise to a well-established pancreatic tumor. Panel A was extracted from *Morris et al. Nat Rev Cancer (2010)*[20]. And panel B from *Hernández-Muñóz et al. Pancreatology (2008)*[24].

The cell of origin that gives rise to pancreatic ductal adenocarcinoma has also been a matter of concern (Fig. 4 A). Because of the similarity of PDA histology to pancreatic ductal structures it was initially proposed that ductal cells give rise to this malignancy. Moreover, this thought is sustained by the detection of duct cell antigens in PDA injuries[7,18]. However, detection of non-ductal markers supports that developmental plasticity might have a role in tumorigenic process might[7]. According to this fact, one of the currently most well-accepted hypothesis about PDA origin is that acinar cells transdifferentiate generating duct-like tubular structures in a process called acinar-to-ductal metaplasia (ADM)[25,26]. Recently, Ferreira *et al*. demonstrated by performing lineage tracing studies that PDA could emerge from both acinar and ductal cells, but following distinct pathophysiology and presenting different marker expression[27]. Nevertheless, some other studies supported an endocrine origin of pancreatic cancer, since mouse islet cells expressing the polyoma virus middle T (PyMT) oncogene are able to generate pancreatic tumors in mice[28]. Centro-acinar cells (CAC) have been also proposed as the PDA initiating cells due to their localization at the interface between acinar and ductal compartments, ultrastuctural ductal features, and the exhibition of an active Notch pathway signaling when they proliferate[29]. On the other hand, an additional well-explored question related to cancer

origin[7,18] is the existence of a cancer stem cell (CSC) defined as a cell that holds the potential to self-renew and to develop into different cell lineages in the adult tissue, favoring tumor generation in pathological conditions. This model has been well described in leukemia[30] and it was suggested for other tumors such as lung[31] and prostate[32] cancers. However, a more dynamic process has been also proposed for cancer origin in which stem-ness could arise by dedifferentiation from other cell identities instead of the existence of a stem cell entity *per se*[33]. That is, the emerge of a facultative stem cell could be favored under particular conditions, such as cell stress. Different studies based on partial pancreatectomy in rats have been described dedifferentiated duct cells expressing Pdx1 progenitor cell marker[34].

1.2.2 PDA symptoms and diagnosis

Accurate diagnosis of pancreatic cancer is necessary since depending on the stage of the disease different treatments should be performed. Surgical resection is the only curative treatment for PDA, however it can be applied only when the tumor is localized and has not spread to other tissues, a situation that is found in less than 20% of patients at the time of diagnosis, highlighting the relevance of early detection. Several imaging techniques have been developed to improve pancreatic cancer detection and staging, such as computer tomography (CT), magnetic resonance imaging (MRI) or endoscopic ultrasonography (EUS)[9]. However, the lack of symptoms during the early stages of PDA leads to a late diagnosis of the disease. Moreover, signs of pancreatic cancer are quite unspecific and they vary depending on tumor location. If tumor mass is localized at the head of the pancreas (~75 %), weight loss, jaundice, nausea and vomiting are the most common symptoms. While if the

tumor is at the body/tail of the pancreas, patients usually have abdominal pain that radiates to the back[9]. Lot of efforts have been made on searching specific biomarkers that allows an early detection of PDA using non-invasive analysis. Carbohydrate antigen 19-9 (CA19-9), which is a sialylated tetrasaccharide related to the Lewis Antigen[A], is the most widely used biomarker in PDA diagnosis. However, since CA19-9 has several limitations, as it can give to false positive or negative results since this antigen is overexpressed in chronic inflammation and 10% of Caucasians are Lewis-negative[9], therefore better biomarkers for PDA diagnoses must be found. Carcinoembryonic antigen (CEA), osteopontin (OPN), macrophage inhibitory cytokine 1 (MIC1), S100A6, circulating DNA encoding pancreatic cancer mutations and even exosomes carrying proteins, nucleic acids and microRNAs have been proposed as PDA biomarkers[23]. However, lack of specificity and sensitivity of all these molecules as early PDA biomarkers makes crucial to search for alternative evidences indicative for PDA development.

1.2.3 PDA treatment

Dismally, despite it has been done a considerable progression on deciphering the molecular basis of pancreatic cancer, to date non-efficient therapeutic strategy has been developed. Usually PDA can be defined as resectable, borderline resectable or unresectable, based on tumor location, staging and the involvement of major arteries and veins. As mentioned, surgery resection still represents the only potentially curative option for PDA, however only 20% of patients are operable and 80% of them will finally relapse[9,23]. Therefore, most of the patients are diagnosed with locally advanced unresectable tumors or even with metastasis to the liver and peritoneum. Chemotherapy, alone or in combination

with other drugs, is the conventional treatment in this context. Gemcitabine was approved by the US FDA as PDA therapy in 1997, and various drug combinations that increase survival or palliative effects have been approved since then. FOLFIRINOX, a combination of folinic acid, 5-fluorouracil [5-FU], irinotecan, and oxaliplatin, is used in patients with an advanced disease; it exhibits a robust activity but with considerable toxicities[9,35]. As an alternative, gemcitabine plus albumin-bound paclitaxel (GEM/NAB-paclitaxel) has also shown an improved efficacy with a considerable but safely secondary effects[36]. More recently, pancreatic cancer cells have been targeted using different cytotoxic agents like TH-302 (also named evofosfamide) which is activated under hypoxic conditions and whose combination with gemcitabine leads to an improved PFS (progression-free-survival). Inhibitors of KRas or JAK pathways have been tested too. Or even drugs targeting tumor metabolism, such as inhibiting enzymes that regulate glycolysis impairing cancer cell nutrition and proliferation[37]. Regarding radiotherapy, it is often used as a palliative treatment to kill cancer cells in unresectable locally advanced tumors. Usually, side effects results from this treatment because of the affected surrounding normal tissues, however recent innovations have allowed more effective and tolerated treatment[9,38]. Lamentably, all of these possibilities only have been able to slightly increment, if so, PDA patient survival during last decades. However, as described, PDA is defined as malignant cells surrounded by a large stromal compartment, a hallmark that has recently change the focus of attention in PDA therapy towards this target (see section *1.3.5 Targeting tumor stroma microenvironment for PDA therapy*).

1.3 The relevance of stroma compartment in PDA

Classically, most efforts in cancer research have been done to study and treat malignant cancer cells themselves. However, increasing evidences from scientists around the world have demonstrated the remarkable contribution of TME or stroma in cancer progression. Cancer cells does not act alone, but they get along with a rich TME that provides an optimum niche for tumor growth[39]. Actually, PDA is one of the cancers with more abundant stroma, representing more than 80% of the tumor mass[40]. Stromal makeup can notably vary not only between tumors, but also from different locations into the same tumor[41]. In spite of the observed TME heterogeneity, stroma is basically composed of a fibroblastic compartment, which is the main responsible of the huge fibrotic deposition; endothelial cells and pericytes, which give rise to blood vessels; and immune cells, comprising macrophages, lymphocytes, neutrophils, and dendritic cells, in charge of the tumoral immunity. The stroma also includes an acellular compartment, the extracellular matrix (ECM), mainly produced by activated fibroblasts and whose architecture and protein composition also influences in tumor progression[42]. Hence, high abundancy of TME compartment, as well as, several interactions established between malignant cells and stroma (also known as tumor-stroma crosstalk) are crucial for the development, progression and aggressiveness of PDA malignancy as well as resistance against conventional therapies (Fig. 5).

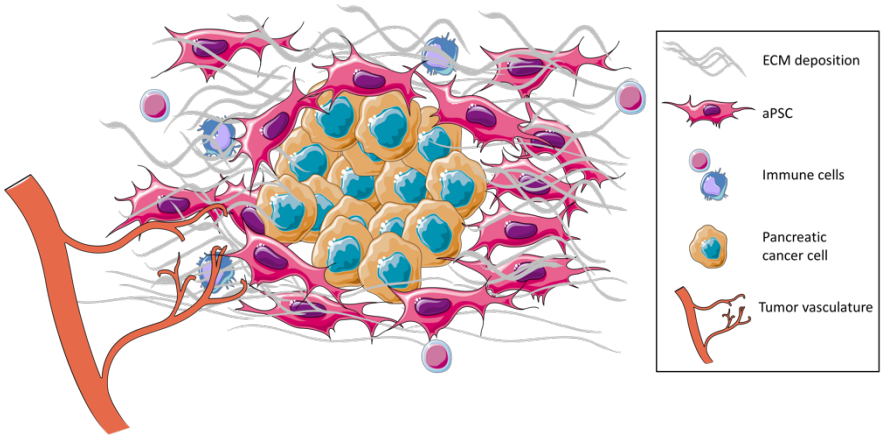

Figure 5. The stromal compartment in PDA. Pancreatic tumor cells are surrounded by a dense stromal compartment composed of activated pancreatic stellate cells (aPSC; see section *1.3.4 Pancreatic stellate cells (PSC)*), immune cells, endothelial cells and a strong extracellular matrix (ECM) deposition (fibrosis). aPSC are the major responsible for ECM deposition which leads to an hypovascularized pancreatic tumor forming a physical barrier impeding proper anti-tumoral drug delivery. Individual cell representation was extracted from Servier Medical Art Website (https://smart.servier.com).

In spite of the deep characterization of the malignant effects of stroma, its pro-tumoral contribution in a well-established tumor has been supposed a paradox, since it has been reported an exacerbated progression of tumors after stroma depletion[43,44] (see section *1.3.5 Targeting tumor stroma microenvironment for PDA therapy*). Indicating a dual function of stroma compartment through a balance of signals that promote but also inhibit tumor progression, emphasizing on the complexity of tumor-stroma crosstalk. Consequently, stroma and epithelial compartments cannot be analyzed as separate entities since it is the interaction between all components which give rise to the PDA phenotype.

1.3.1 Extracellular matrix (ECM) in PDA

The ECM is the principal non-cellular component in PDA, it is composed of fibrous proteins, such as collagens, growth factors, cytokeratins, as well as, glycoproteins, proteoglycans and glycosaminoglycans, and other proteins like osteopontin, periostin and serine protein acidic and rich in cysteine (SPARC)[45,46]. All of these elements interplay in the stroma-tumor crosstalk during PDA progression. For example, it has been reported that type I collagen signaling upregulates Snail1 and LEF-1 expression leading to EMT in malignant cells[47]. Fibronectin binds, predominantly, to integrin receptors and collagens favoring cell adhesion, migration and proliferation. Indeed fibronectin, in conjunction with laminins, contributes to apoptosis resistance favoring tumor cell survival[48]. Another interesting component of ECM is hyaluronic acid (HA), whose capacity for retaining water conduces to an increase of interstitial pressure creating a physical barrier for proper drug delivery[42,49].

1.3.2 PDA vasculature

PDA vasculature is mainly formed by endothelial cells (ECs), pericytes, and vascular smooth muscle cells (vSMCs). Malignant cancer and stromal cells secrete several anti- and pro- angiogenic factors, like endostatin and vascular endothelial growth factor (VEGF), to the TME modulating vessel remodeling and formation. ECM composition also influences in this process, since the high interstitial pressure carried by the dense fibrotic deposition impedes the formation of new vessels[45]. All of these factors generate hypovascularized pancreatic tumors which induces to metabolic stress because of nutrient and oxygen deprivation (hypoxia)[50]. In

response to this situation, malignant cells develop adaptive changes by modifying its own metabolism. Nutrition of *KRAS* mutated cells is promoted by the uptake of proteins and lipids from the extracellular compartment by scavenging or macropinocytosis[51,52]. Moreover, activated PSC are able to secrete exosomes containing metabolites[53] or even undergo autophagy[54] to serve as a source of nutrients for tumoral cells. On the other hand, the characteristic hypoxic condition of PDA promotes hypoxia inducible factor 1α (HIF-1α) to handle with cellular stress. It is known that HIF-1α not only promotes cancer cell migration and invasion, but also it is a mediator of chemoresistance through upregulating Hedgehog (Hh) pathway, stimulating NF-kβ or ERK signaling, and by suppressing the production of reactive oxygen species (ROS)[45].

1.3.3 The immune system in PDA

PDA development and progression can be positively or negatively modulated by the immune system; however, in established tumor several methods have been developed by cancer cells to escape from immune control. One of them is known as immunoediting, in which malignant cells take an advantage on their genomic instability promoting the loss of antigens recognized by T cells[55]. Moreover, tumor and stroma cells secrete a set of cytokines, like IL-6, IL-10, TGF-β or TNF-α, that also influence in immune system modulation towards an immune suppressive phenotype. In this context, myeloid-derived suppressor cells (MDSC) population is increased within the tumor[56], tumor associated macrophages (TAMs) tent to polarize to the immune suppressive M2-like phenotype, which has been associated with poor prognosis in PDA[57]. Tumor infiltrated lymphocytes (TILs) populations are also affected, in which immunomodulatory Th2 and T regulatory (Treg) cell

population are increased[45,58]. Indeed, the activation of immune checkpoints can also explain the observed switch to an immunosuppressive TME; among them, programmed cell death protein 1 (PD1/PDL1 (or B7-H1))[59] and cytotoxic T-lymphocyte-associated antigen 4 (B7-1 (or CD80), B7-2 (or CD86) /CTLA4)[60] are the most well-characterized. Interestingly, tumor associated neutrophils (TANs) are able to trap circulating tumor cells facilitating their extravasation and metastasis to distant organs by suppressing peripheral leucocyte activation in blood stream[61]. All of these strategies leads to the inhibition of activated $CD4^+$ or $CD8^+$ T lymphocytes and natural killer cells (NK) which, in conjunction with the creation of an immunosuppressive niche, contributes to tumor cell progression and metastasis[62]. Finally, galectin family plays also a key role in the immune evasion of PDA, as described below (see section *1.5 Galectins in cancer*).

1.3.4 Pancreatic Stellate Cells (PSC)

The fibroblastic-like component of PDA comprises different cell types with distinct origins. Cancer-associated fibroblasts (CAFs) have been described as a population of fibroblastic activated cells that hold a huge dynamic participation in determining tumor progression[63]. In PDA, CAFs represent the main stromal component responsible for the characteristic abundant extracellular matrix deposition in this malignancy[45,64,65]. There are evidences supporting the presence of different populations of CAFs in PDA stroma[66]. Moreover, multiple precursors, such as resident fibroblasts, bone marrow-derived cells (BMDC), pancreatic stellate cells (PSCs), and even epithelial cells which has undergone epithelial-to-mesenchymal transition (EMT) have been proposed to give rise to CAF population[63,65]. Taking in account the complexity of this

population and considering that PSCs are the principal source of CAFs in PDA[65], from this point we will center our attention on the implication of PSCs as main CAF population in PDA progression .

As noticed, PSCs are the most abundant cell component in PDA stroma and the major source of extracellular matrix deposition, specially type I collagen which represents near 90% of protein content[46,67]. In a healthy pancreas, PSCs are in a quiescent state (qPSCs) encompassing 4-7 % of the parenchymal tissue[68]. In this context qPSCs, characterized by the expression cytoplasmic vitamin A droplets, are the responsible for the normal ECM turnover by the secretion of metalloproteinases (MMPs) and their inhibitors (TIMPs)[65,69]. Upon injury, qPSCs get into an activated state (aPSC) identified by the loss of the vitamin A droplets, the expression of activated-fibrotic markers, such as α smooth muscle actin (α-SMA), and the acquirement of a spindled shape resembling to a myofibroblast phenotype[68]. When the damage is repaired, aPSCs undergo apoptosis and, finally, the normal architecture of pancreatic tissue is restored[70]. But, in cancer, the injury is constantly sustained and PSCs are continuously activated. Actually, the tumor was described by Dvorak in 1986 as a "wound that never heals"[71]. In this situation, the balance between ECM proteins synthesis and degradation is severely disrupted favoring an excessive ECM deposition and leading to an extend fibrosis (desmoplasia)[45,72].

In PDA, PSCs become activated by several factors such as cytokines, chemokines, growth factors and other molecules secreted by cancer cells, immune cells and endothelial cells resident within TME[73]. In turn, aPSCs secret factors that not only maintain their own activation via autocrine signaling, but also affect cancer cells and the other components of the TME in a paracrine way[46,74]. Interestingly, it has been reported that CAFs also have the ability to migrate and invade in conjunction with tumoral cells favoring

metastasis in colon[75] and pancreatic cancers[76]. In this manner, a complex cross-talk is established between stroma and tumor cells, creating a supporting niche for malignant cells and favoring tumor growth, progression and metastasis (Fig. 6).

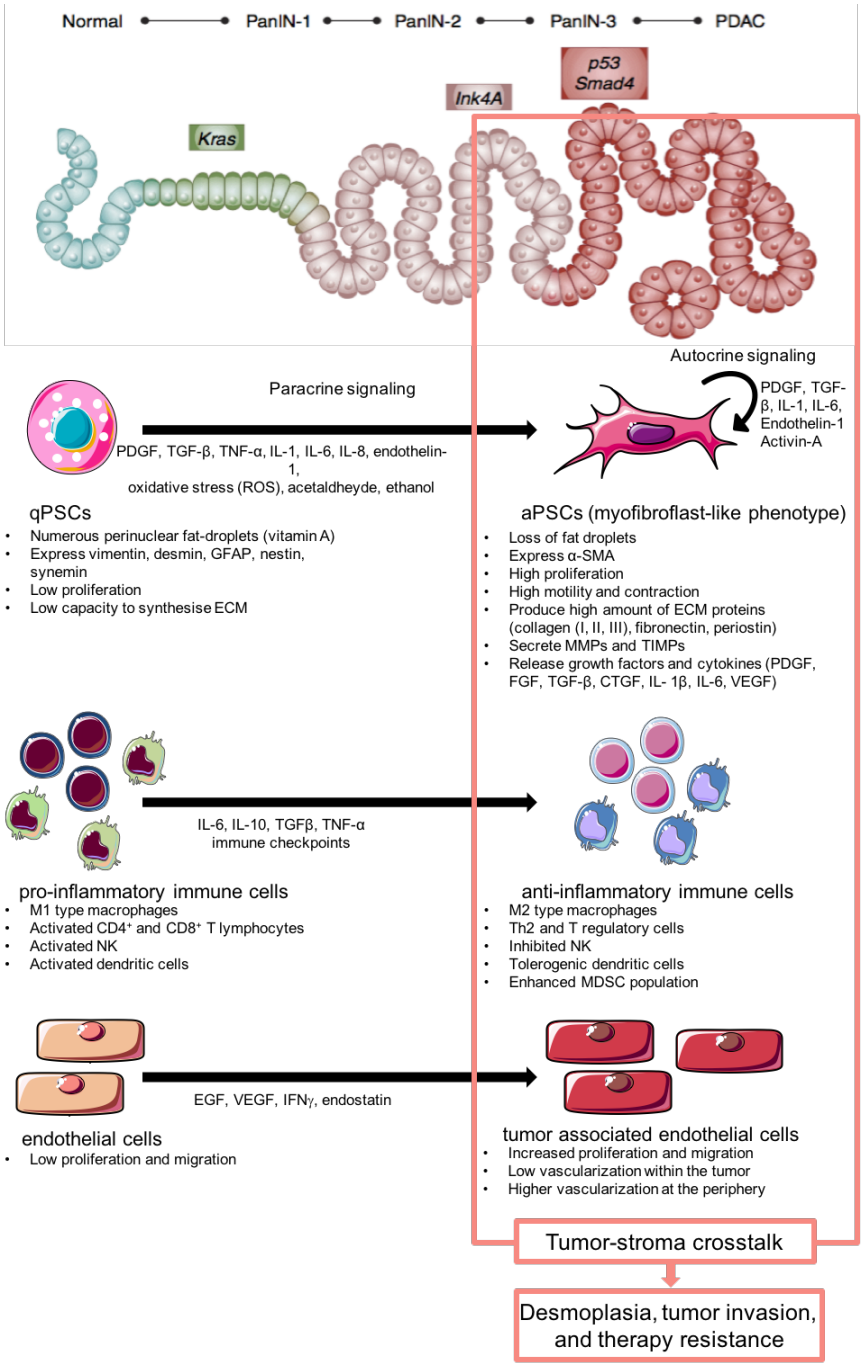
Normal
PanIN-1
PanIN-2
PanIN-3
PDAC
p53
Smad4
Ink4A
Kras
Autocrine signaling
Paracrine signaling
PDGF, TGF-β, IL-1, IL-6, Endothelin-1 Activin-A
PDGF, TGF-β, TNF-α, IL-1, IL-6, IL-8, endothelin-1, oxidative stress (ROS), acetaldheyde, ethanol
qPSCs
Numerous perinuclear fat-droplets (vitamin A)
Express vimentin, desmin, GFAP, nestin, synemin
Low proliferation
Low capacity to synthesise ECM
aPSCs (myofibroflast-like phenotype)
Loss of fat droplets
Express α-SMA
High proliferation
High motility and contraction
Produce high amount of ECM proteins (collagen (I, II, III), fibronectin, periostin)
Secrete MMPs and TIMPs
Release growth factors and cytokines (PDGF, FGF, TGF-β, CTGF, IL- 1β, IL-6, VEGF)
IL-6, IL-10, TGFβ, TNF-α immune checkpoints
pro-inflammatory immune cells
M1 type macrophages
Activated CD4+ and CD8+ T lymphocytes
Activated NK
Activated dendritic cells
anti-inflammatory immune cells
M2 type macrophages
Th2 and T regulatory cells
Inhibited NK
Tolerogenic dendritic cells
Enhanced MDSC population
EGF, VEGF, IFNγ, endostatin
endothelial cells
Low proliferation and migration
tumor associated endothelial cells
Increased proliferation and migration
Low vascularization within the tumor
Higher vascularization at the periphery
Tumor-stroma crosstalk
Desmoplasia, tumor invasion, and therapy resistance

Figure 6. Tumor-stroma crosstalk. Most representative changes described in TME cell populations (PSC, immune cells and endothelial cells) as PDA progress. In a healthy pancreas, qPSC are responsible for normal ECM architecture maintenance, when cancer occurs several secreted factors activate PSC which in turn secrete other factors that affect whole tumor subsets and start to generate an excessive ECM deposition. Secreted factors during tumor progression tilt immune subset population to an immunosuppressive state, so favoring tumor cell survival. Finally, endothelial cells get activated in PDA favoring their proliferation, although strong desmoplasia induces hypovascularized tumors, PDA vasculature is enough to mediate cancer cell invasion and metastasis. Top image and figure design extracted from *Neesse et al. Gut (2015)*[77]. Information extracted from *Erkan et al. Gut (2012)*[68] and from *Omary et al. J Clin Invest (2007)*[74]. Individual cell representation was extracted from Servier Medical Art Website (https://smart.servier.com).

1.3.5 Targeting tumor stroma microenvironment for PDA therapy

Despite of huge efforts have been made on generating new potent drugs and advanced strategies, pancreatic cancer treatment remains inefficient and unfortunately, patient death survival rates are still pretty similar to PDA incidences. One of the main reasons that explain pancreatic cancer resistance to the most conventional therapies is its strong desmoplasia reaction. The copious fibrotic deposition surrounding malignant cells represents a physical barrier which impedes drug delivery and creates a hypoxic niche by blocking intratumoral vasculature. Indeed, several TME components implicated in tumor-stroma cross-talk also contributes to boycott the effects of applied therapies. Thus, development of new approaches targeting stroma compartment has been assessed[78,79].

Since PSCs are the major responsible for desmoplasia generation and maintenance, this population has been one of the major targets for stromal-directed therapy in PDA. Hh signaling has been one of the first targeted pathways since it is well-reported its ability to activate PSCs. An oral administration of IPI-926, a

smoothened antagonist, produced a considerable depletion of stroma compartment, an increased intratumoral vasculature and an enhanced gemcitabine uptake within KPC mice tumors[80], pointing that elimination of tumoral stroma may be a good strategy for increasing PDA therapy delivery and improve patient outcome. However, two independent studies from Özdemir *et al.* and Rhim *et al.* in 2014 demonstrated that the ablation of stromal compartment in murine mouse models by elimination of α-SMA positive fibroblasts[43] or knocking out Sonic Hedgehog (SHH) ligand[44] increased disease progression and reduced animal survival, indicating that new approaches for PDA treatment should be based on reprogramming PSCs to a quiescent phenotype able to promote an anti-tumoral effect rather than total ablation of these cells. Different strategies have been proposed favoring their quiescent state. Vitamin D and A analogs were used by different researchers to induce qPSCs[81]. Antifibrotic agents, such as pirfenidone, and angiotensin II inhibitors demonstrated a reduction in PSC-mediated fibrosis and tumor growth suppression[82,83]. Silencing overexpressed microRNAs is an alternative strategy to promote qPSCs phenotype[78]. Regarding to other components present within TME, hyaluronic acid (HA) has been described as a crucial contributor to the increased interstitial fluid pressure (IFP) hampering intratumoral vasculature and consequently leading to a hypoxic environment and an inefficient drug delivery[84] (see section *1.3.1 Extracellular matrix (ECM) in PDA*). It has been reported that enzymatic degradation of HA could favor the re-expansion of tumor vessels favoring drug delivery[85]. Efficacy of PEGPH20, a PEGylated recombinant hyaluronidase, has been observed in animal pre-clinical trials[86,87], and is currently being explored in clinics[88]. In the context of immunotherapy, CTLA4 and PD-1/PD-L1 are the most targeted checkpoints, however immune therapies blocking only one of them have not achieved good results for PDA[62]. Combination of different immunotherapies has exhibited promising results. For example,

blocking interaction between CXCL2 and its receptor CXCR4, which promotes accumulation of cytotoxic T cells in the TME, in combination with anti-PDL1 treatment leads to a highly decreased tumor growth[62]. Targeting CD40 pathways in conjunction with anti-PD1 or anti-CTLA4, or both, increased $CD8^+$/Treg ratio resulting in tumor regression[62]. Novel therapies, such as cancer vaccines[37] or CAR-T cells[62] could also be promising therapies. Finally, despite the low vascularization of pancreatic cancers, angiogenesis inhibitors have been also studied in PDA patients[89]. In this regard, our group demonstrated the effectiveness of sunitinib, a multi-kinase inhibitor with a potent anti-angiogenic effect, in promoting pancreatic cancer cell death and reducing subcutaneous pancreatic tumors volume in xenografts. However, this drug had none effect on established tumors from *Ela-myc* mice, indicating that the presence of a strong desmoplasia in these tumors is the responsible for treatment resistance. These results strength the role of the stromal compartment as a physical barrier contributing to the resistance of PDA treatment[90].

1.4 Galectins

Galectins are a class of lectins defined by the presence of a highly conserved carbohydrate recognition domain (CRD)[91] with comprises ~130 amino acid (aa) responsible for their affinity for β-galactosides[92]. Up to now, 15 members (from galectin-1 to 15) have been defined in mammals which, according to their structure and the number of CRDs, are classified as 1) prototypical galectins (galectins-1, -2, -7, -10, -11, -13, -14, and -15) that contain one CRD, 2) chimera-type galectins (galectin-3) with one CRD and an amino-terminal polypeptide tail rich in proline, glycine, and tyrosine residues, which allow its oligomerization into multivalent complexes

up to pentamers, and 3) tandem-repeat galectins (galectins-4, -8, -9, and -12) composed by two homologous CRD connected with a peptide linker which can measure from 5 to more than 50 amino acids[93]. In spite of some galectins are biologically active as monomers, such as galectins-5, -7 and -10, most of them are capable to form dimers, like galectins-1, -2, -11, -13, -14, -15, or even oligomers through their N-terminal region, which is the case of galectin-3 (Gal-3) (Fig. 7 A). This increase in glycan binding valency allows the formation of cell surface lattices[94], homo- and heterotypic cell interactions, cell-ECM bindings as well as interactions between ECM components, all of them required for many of their biological effects[95–99]. In spite of the highly conserved amino acidic sequence of CRD along galectins, unique subsites localized on either sites of CRD confer to each galectin a determined affinity for specific glycoconjugates containing different oligosaccharide modifications (N- and O-linked glycans) mediating specific functions and ligands for each member of the family[95,100]. Since galectins lack of a signal sequence, it has been proposed that this lectins are synthesized and accumulated in the cytoplasm before a non-classical secretion mediated by disrupted vesicles or autophagy in which β-galactoside-binding activity seems to be required for galectin export[101,102]. Interestingly, galectins are also found intracellularly, both in the cytoplasm and in the nucleus, in which mainly protein-protein interactions are engaged to carry out their activities inside the cell[95]. In this context, it has been reported that CRD is necessary for some intracellular galectin interactions that occur independently of carbohydrate-recognition[103]. However, in spite of, there is no evidence of the relevance of the carbohydrate-binding for intracellular galectin functions[104–106]; an intracellular lectin activity cannot be discarded. Despite multivalency has been commonly described for extracellular galectins, the functionality of intracellular dimeric galectins cannot be neither dismissed[107,108]. Unfortunately, non-common domains

have been identified between intracellular galectin protein partners[95]. Through these properties, galectin family is implicated in numerous functions such as cell adhesion and migration, cell proliferation, differentiation, apoptosis, as well as, inflammation processes, modulation of immune responses, and even regulation of pre-mRNA splicing.

1.4.1 Galectin-1 structure and its physiological functions

Galectin-1 (Gal-1) is a lectin protein encoded by *LGALS1* gene, which is located at the chromosome 22q12. Initially, Gal-1 was defined as a S-type lectin because of the presence of thiol groups (in cysteine amino acids) whose reduction are essential for the lectin-dependent activities[106]. Gal-1 can act as a monomer of 14.5KDa, but usually it exerts its functions as a homodimer, which is the result of a non-covalent binding of the well-conserved hydrophobic core located at the interface of two CRD subunits. So, leaving glycan-binging pockets arranged on opposing sites[104,105]. Each form, mono- and dimeric, is associated with different biological activities[104]. Crystallography studies determined that Gal-1 structure consists of six-stranded and five-stranded antiparallel β sheets organized in a β-sandwich folding pattern[109] (Fig. 7B). Sugar recognition is driven via van der Waals and hydrogen bound interactions between Gal-1 binding pocket and its ligand[110]. As a lectin, Gal-1 is especially affine to glycoconjugates (glycoproteins or glycolipids) displaying disaccharide N-acetyllactosamine (Gal-β1-3/4 GlcNAc, also named LacNAc II) present at the cell surface and in the ECM. As well as other galectins, Gal-1 is not only present at the extracellular compartment but also found in the nucleus and in the cytoplasm.

Gal-1 is expressed during mice embryogenesis and plays a role in embryonic implantation[111,112] as well as in the formation of the neural network of the olfactory bulb[113,114]. Interestingly, Gal-1 knockout mice does not present any apparent phenotypical abnormality, being these mice fertile and perfectly viable with the only minor defects on olfactory axon guidance and a reduced thermal sensitivity[115,116]. This observation could be explained because the expression of other galectins could compensate the lack of Gal-1. In the adult, Gal-1 is usually barely expressed in most tissues, but its expression is frequently enhanced after different stimuli, such as inflammation[104].

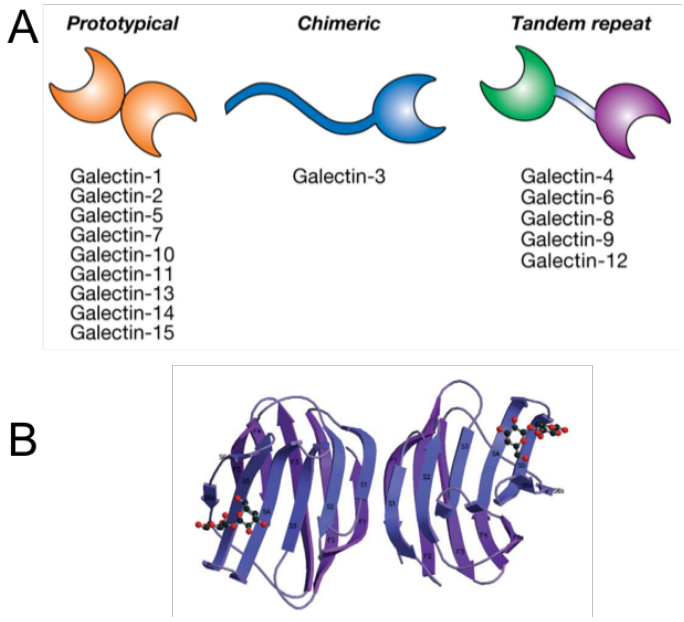

Figure 7. Galectin family structure. A) Galectin family classification. Prototypical galectins exist as a balance between monomeric and dimeric forms. Most of them usually act as dimers. Chimeric Gal-3 can form up to pentamers for increasing its multivalency. Tandem repeat galectins are formed by two non-identical CRD connected by a peptide linker. B) Ribbon diagram of Gal-1 homodimer structure. Panel A was extracted from *Essentials of Glycobiology, Third Edition (2017). Cold*

Spring Harbor Laboratory Press U.S. Panel B was extracted from *López-Lucendo et al. J Mol Biol (2004)*[110].

1.4.1.1 Extracellular functions of Gal-1

Gal-1 is able to recognize, through its carbohydrate-binding ability, several components of the ECM (Fig. 8), such as laminin and fibronectin, affecting to ECM assembly and remodeling[117,118]. It is also involved in cell adhesion and motility by modulating cell-cell and cell-ECM interactions, probably through integrins, one of the most well-studied cell surface glycoproteins[119]. For example, Gal-1 is able to modulate the adhesion, spreading and migration of vascular smooth muscle cells along extracellular laminin fibers by its binding to $\alpha 1\beta 1$ integrin[120]. Indeed, secreted Gal-1 can trigger intracellular signaling pathways after recognizing proper cell surface proteins affecting cell proliferation[121] and differentiation[122]. In spite of the widespread functions of Gal-1, the most investigated effect of this lectin is its implication as immune system modulator. It has been well-reported that Gal-1 regulates T cell homeostasis by modulating cytokine production, affecting cell proliferation and inducing apoptosis signaling pathways[123,124] as well as controlling several functions in other immune cells (see section *1.5.1.3 Modulation of immune system by Gal-1*).

1.4.1.2 Intracellular functions of Gal-1

Gal-1 is synthetized by free ribosomes[125], it is acetylated at the N-terminus[126] and lacks of glycosylation[127] which are typical characteristics of cytosolic proteins. Up to now, Gal-1 has been described as a scaffold for two cytosolic proteins activating different

signal pathways. First, cytosolic Gal-1 can interact with HRas guanosine triphosphate (HRas-GTP) and translocate it to the inner leaflet of plasma membrane. Gal-1 overexpression promotes membrane-anchoring of activated HRas, promoting Raf-1 recruitment and triggering the activation of ERK pathway leading to malignant cellular transformation[128]. Second, Gal-1 can also bind protocadherin-24 (Pro-24) which impedes PI3K pathway activation inhibiting cell proliferation in cancer colon cells[129].

The most well-defined function of nuclear Gal-1 is its role as a pre-mRNA splicing factor in HeLa cells, described for the first time by Vyakarnam and colleges in 1997[108]. This function was also linked to Gal-3[130], both lectins presented redundant functions since any of them could recover splicing activity in nuclear extracts depleted for Gal-1 and Gal-3[108]. Interestingly, both lectins have been found associated to survival motor neuron (SMN) complex by its direct interaction with Gemin4[131]. SMN-containing complexes are implicated in the delivery of small nuclear ribonucleoproteins (snRNP) promoting spliceosome assembly, thus Gal-1 and Gal-3 have been related to this process[131,132]. This activity is inhibited by lactose, suggesting that the lectin activity could be essential for galectin-mediated mRNA splicing[108]; however, mutated Gal-1 (Gal-1 (N46D)), which is not able to recognize carbohydrates, is still functional as a splicing factor[103]. This data exhibited an interesting characteristic of Gal-1 in which CRD and its carbohydrate-binding ability could be dissociated for proper lectin function. Gal-1 has been also reported to interact with FOXP3, a transcription factor with a tumor suppressive function in breast cancer. In this context, overexpression of Gal-1 in breast cancer cells impairs DNA-binding ability of FOXP3 inhibiting its tumor suppressive properties[133]. Interestingly, nuclear repartitioning of Gal-1 have been observed in mammary gland cells in response to cell-surface glycan patterning[134]. Some nuclear functions of Gal-3 have been also

described, besides its function as a splicing factor as described above, it has been also reported Gal-3 favors cell proliferation by binding to thyroid-specific transcription factor (TTF-I) in papillary thyroid cancer cells[135] or by enhancing/stabilizing protein-DNA complex on cyclin D promoter in breast epithelial cells[136] (Fig. 8).

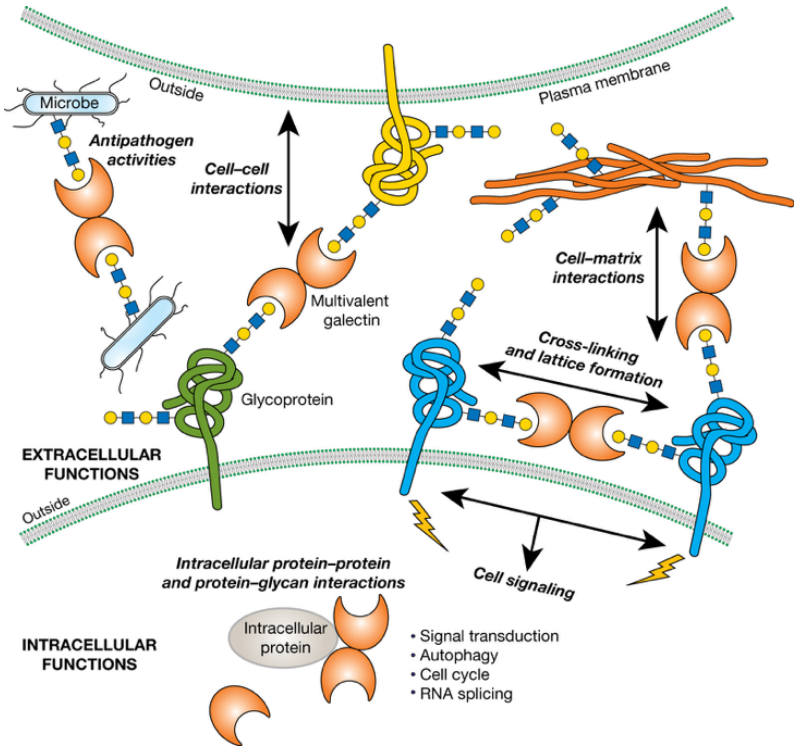

Figure 8. Gal-1 extracellular and intracellular interactions. Extracellularly, Gal-1 exerts its functions through its carbohydrate-recognition ability affecting cell-cell and cell-ECM interactions as well as triggering cell signals. Intracellularly, Gal-1 mainly establish protein-protein interactions inducing activating signaling pathways, regulating pre-mRNA splicing or even affecting gene expression. Extracted from *Essentials of Glycobiology, Third Edition (2017). Cold Spring Harbor Laboratory Press U.S.*

1.5 Galectins in cancer

Due to the wide diversity of functions that galectins can exert, in particular its role in immune evasion, their dysfunction or altered expression are usually linked to disease, such as cancer[100,137]. Gal-1, Gal-3 and galectin-9 (Gal-9) are the most studied galectins in cancer context, since their expression is altered in several types of cancer. Usually, Gal-1 is frequently overexpressed in tumor tissues compared with their normal counterparts, interestingly high levels of this lectin have been often found within the stroma compartment surrounding tumor cells in many cancers, such as prostate[138], colon[139], liver[140] and pancreic[141] cancers. Otherwise, Gal-1 can also be expressed simultaneously in both stroma and cancer cells such as in breast[142], thyroid[143] or skin[144] cancers. Only few studies observed a decreased expression of Gal-1 in malignant cells, however other several studies contradict these results. In comparison to Gal-1, the expression of Gal-3 is more heterogeneous among cancers. For example, Gal-3 is normally increased in melanoma[145] but decreased in basal and squamous cell carcinomas[146]. Interestingly, changes in subcellular location have been reported for Gal-3 in colon cancer, in which this lectin shifts from a nuclear to a cytoplasmic expression in malignant cells as cancer progresses[139]. With these observations, it should be noticed that not only expression levels of galectins are important, but also which type of cells (malignant or stromal) and even subcellular localization of galectins in each tumor type should be taken into account to determine its role in tumor progression[137]. Regarding to Gal-9, most of the studied cancer tissues presented a decreased expression of this lectin whose downregulation has been linked to tumor cell adhesion and metastasis in solid tumors. Thus, expression of Gal-9 has been correlated with a better prognosis for some cancers such as melanoma[147], breast cancer[148] and hepatocellular carcinoma[149].

Importantly, one of the deeply studied pro-tumoral functions of galectins is their immunomodulatory activity facilitating tumor immune evasion[62]. Gal-1 has been characterized by promoting apoptosis of activated T cells, enhancing Treg immunosuppressive cells. Likewise, other immunosuppressive immune cell populations are favored by this lectin (see section *1.5.1.3 Modulation of immune system by Gal-1*). Gal-3 is also able to modulate T cell and NK responses impairing their anti-tumoral effect. Regarding Gal-9, this lectin induces Treg differentiation as well, and favors expansion of immunosuppressive MDSCs. It seems Gal-9 has a pro-tumoral effect when it modulates the immune system in the TME, contribution of this lectin to tumor immune evasion is specially known by its interaction with TIM-3 receptor resulting in Th1 and $CD8^+$ apoptosis. Figure 9 summarizes the immunomodulatory properties of Gal-1, Gal-3 and Gal-9 in cancer.

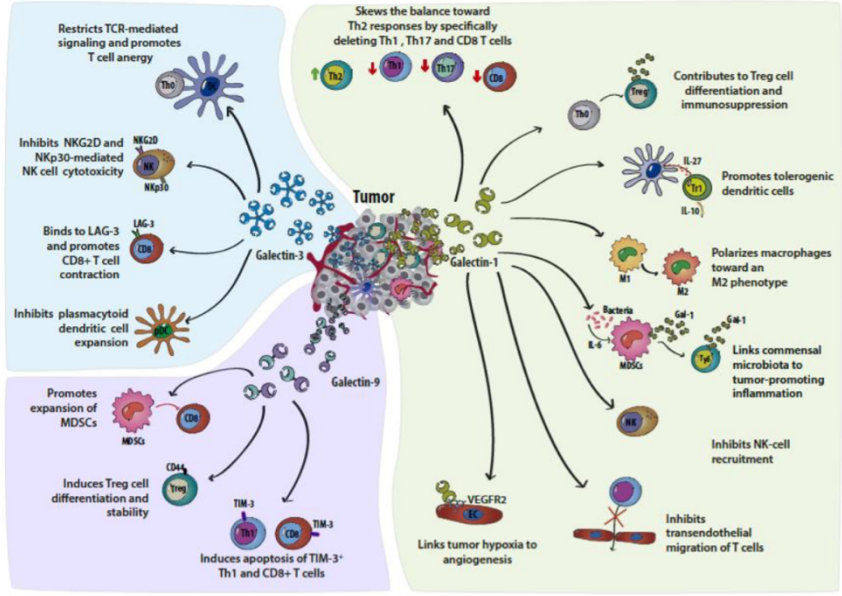

Figure 9. Role of Gal-1, Gal-3 and Gal-9 on immune system modulation. Gal-1 tilts the balance toward Th2 profile, enhances Treg population, promote

tolerogenic dendritic cells functionality, polarizes macrophages toward an anti-inflammatory M2-phenotype and inhibits NK recruitment and T cell transendothelial migration. Moreover, Gal-1 expand MDSC and preserves angiogenesis in hypoxic tumors. Gal-3 promotes T cell anergy by restricting T cell receptor (TCR), impairs NK anti-tumor activity and promotes plasmacytoid dencritic cell expansion. Finally, Gal-9 confers immune privilege to tumor cells through TIM-dependent or -independent signaling, promotes MDSC and Treg cell expansion. Extracted from *Rabinovich and Conejo-García. J Mol Biol (2016)*[150].

1.5.1 Gal-1 in cancer

It has been extensively reported a significant overexpression of Gal-1 in cancer, in which its upregulation has been detected in malignant cancerous cells, in stroma surrounding tumor cells as well as in both compartments[105,106,151]. Moreover, circulating Gal-1 has been also detected in patients with Hodgkin lymphoma[152], high-grade glioma[153], colorectal[154], epithelial ovarian[155], thyroid[156] or pancreatic[157]cancer. Due to the pleiotropic functions exerted by Gal-1, this lectin has shown contribution in multiple aspects of cancer biology (Fig. 9). Thus, Gal-1 not only influences on cancer cell behavior, but also interacts with other cells present in TME affecting tumor angiogenesis and tumor immune surveillance. Table 2 presents cancer-associated Gal-1 binding partners known up to date.

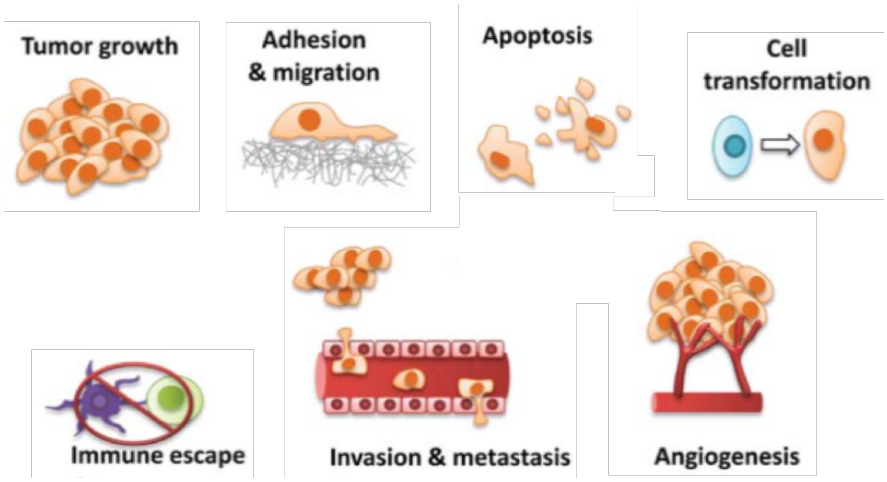

Figure 9. Gal-1 functions in cancer. Gal-1 expression favors cancer cell growth, cell adhesion and migration, T cell apoptosis, cell transformation mediated by its interaction with HRas, immune scape by affecting T cells and other immune cell populations, invasion and metastasis as well as angiogenesis. Adapted from *Vladoiu et al. Int J Oncol (2014)*[158].

Table 2. Galectin-1 and cancer: associated partners and biological activities*

Location	Binding Partner	Biological Activities	Cell Type
Intracellular	HRas	HRas/MEK/ERK cascade activation	Bladder cancer
	Pro-24	β-catening signaling inhibition	Colon cancer
	Gemin4	Pre-mRNA splicing modulation	Cervical cancer
	TFII-I	Pre-mRNA splicing modulation	Cervical cancer
	FOXP3	Gene transcription	Breast cancer
Extracellular	90K/Mac-2BP	Homotypic cell adhesion	Melanoma
	Mucin1	Cell adhesion	Prostate cancer
	Laminin	Cell-ECM adhesion	Endothelial
	Fibronectin	Cell-ECM adhesion	Endothelial
	Neuropilin-1	Proliferation, migration and adhesion	Endothelial
	VEGFR	Neovascularization	Endothelial
	CD45	Membrane redistribution and T cell death	T cell
	CD43	Membrane redistribution and T cell death	T cell
	CD7	T cell death	T cell

* Information extracted from *Cousin and Cloninger. Int J Mol Sci (2016)*[105], *Gao et al. Cell death dis (2018)*[133], and *Voss et al. Arch Biochem Biophys (2008)*[103].

1.5.1.1 Gal-1 and tumor growth

Opposing effects of Gal-1 have been found on tumor cell growth. Some studies described that extracellular Gal-1 induces cell cycle arrest in different tumor cell lines like hepatocarcinoma and melanoma cells[159]. On the contrary, other groups reported that exogenous Gal-1 is able to promote tumor cell growth[160,161]. Interestingly, Adams and colleagues have observed a dose-dependent effect of Gal-1 on cell proliferation[162]. Therefore, cell type, the presence of specific cell surface glycoproteins, intracellular Gal-1 interactions and/or the ratio between monomeric and dimeric forms of the lectin have been proposed to explain these ambiguous outcomes.

1.5.1.2 Angiogenesis mediated by Gal-1

Angiogenesis, the formation of new blood vessels out of preexisting capillaries, is a key event for tumor growth and progression. Endothelial cells (EC) are important players during angiogenesis in which they must become activated and extend the vascular network by forming interconnected tubes. This activation results from angiostimulatory growth factors such as vascular endothelial growth factor (VEGF), epidermal growth factor (EGF) and basic fibroblast growth factor (bFGF), secreted by tumor or stroma cells after metabolic and hypoxic stress[163,164].

Gal-1 has been found overexpressed in the vasculature of several tumors. Its expression and localization in ECs are affected by several factors such as interactions with other cells or with ECM, secretion of cytokine stimulatory molecules like IFNγ, IL-1β and TNF-α, metabolic stress and hypoxic conditions[165,166]. In quiescent ECs, Gal-1 is mainly localized in the nucleus, but its localization switches to the extracellular compartment when ECs become activated[167].

Gal-1 has been described as an angiogenic stimulator[168] since it binds to glycosylated receptors exposed by ECs, such as vascular endothelial growth facto receptors (VEGFRs) and Neuropilin-1 (NRP1), promoting activating signaling pathways as well as cell proliferation and migration[169,170]. Moreover, ECs activation can also be stimulated intracellularly via Gal-1 and HRas interaction[171]. More interestingly, Gal-1 mediates connections between endothelial cells and ECM acting as a scaffold and favoring ECs capacity to form tube-like structures[165,166]. In this manner, Gal-1 not only promotes angiogenesis by activating endothelial cells, but also working as a physical support through carbohydrate interactions with ECM favoring neovasculature formation. All these effects seem to be dose dependent because higher concentrations of the lectin block this phenotype[168].

1.5.1.3 Modulation of immune system by Gal-1

One of the most characterized effects of Gal-1 in cancer is the modulation on immune responses. In the tumor microenvironment, malignant epithelial cells as well as stromal cells secrete Gal-1 to promote homeostatic signals to favor the shut-off of immune surveillance[166,172]. Extracellular secreted Gal-1 is able to inhibit T cell growth[173], hamper T cell activation by blocking the production of proinflammatory cytokines such as TNF-α or INF-γ[174] and even promote apoptosis of activated T cells[123,175]. In this process, Gal-1 binds to specific glycoconjugates displayed by activated T cells, like CD7, CD43 and CD45, whose cross-linking results in segregation and redistribution into clustered membrane microdomains[105,127]. This process is critical to transduce apoptotic signaling pathway on activated T cells[176,177], favoring tumor evasion from immune response[178]. Pro-apoptotic activity of Gal-1 mediates polarization of effector T cells (type I T helper (Th1) and Th17 $CD8^+$

T cells) towards an immunosuppressive TME and favoring Th2 and Foxp3$^+$ Treg cells expansion[179,180]. M2 type macrophages and MDSCs, other tumor-friendly cell subsets, are also favored by extracellular Gal-1[150,181]. Other immune cells are also affected by Gal-1 such as dendritic cells which become tolerogenic upon extracellular Gal-1 overexpression[182]. Interestingly, Gal-1 also hampers NK recruitment[150] and leukocyte transendothelial trafficking[183,184].

1.5.1.4 Gal-1 and tumor metastasis

During tumor cell metastasis malignant cells separates from the primary tumor site to attach to ECM at distal sites. This process implies several changes in cell-cell and cell-ECM interactions in which cell migration, invasion, intra- and extravasation as well as colonization of a new niche must take place[106,127]. Bearing in mind functions of Gal-1 described in section *Galectin-1 structure and functions*, this lectin has been proposed as a modulator of tumor metastasis since it is implied in many of these processes[105,106,127].

Gal-1 is able to arbitrate cancer cell adhesion and detachment by modulating cell-ECM interactions. In the primary tumor, Gal-1 favors cell adhesion by mediating the cross-link between ECM proteins, such as laminins or fibronectin[185,186], and cell-surface glycoconjugates, like integrins[187]. After an increase on extracellular Gal-1 levels, migration of tumor cells is favored by a competitively binding of Gal-1 on glycosylated molecules involved in mentioned cell-ECM interactions. Finally, in the secondary invasive site, Gal-1 should be exerting, again, a pro-adhesive mechanism[97,105]. Moreover, it was also reported that Gal-1 stimulates secretion of proteolytic enzymes, such as matrix metalloproteinases (MMP), and activation of tissue-plasminogen

activator (tPA), which degrade ECM proteins favoring cell migration and invasion[188,189]. These processes can also promote migration of non-tumor cell types, such as endothelial cells which further contributes to cell metastasis[168,190].

Homotypic tumor cell aggregation and heterotypic cancer cell adhesion to microvascular endothelium have been described as two essential and coordinated steps of the metastatic cascade[191,192]. Gal-1 is capable to promote homotypic tumor cell aggregates through the recognition of aberrantly glycosylated cell-surface proteins, such as Mucin-1[193]; as well as, heterotypical cell interactions between cancer and endothelial cells[194]. Indeed, not only an increase of Gal-1 levels have been observed at the tumor invasion front[195]; but also, Gal-1 have been detected in metastatic lung lesions derived from breast cancer[180], supporting, that Gal-1 could be an important player in tumor metastatic processes.

1.6 Gal-1 in PDA

In the context of PDA high expression of Gal-1 has been reported by several groups. Berberat et al., was the first one to describe overexpressed levels of Gal-1 in pancreatic cancer tissues in comparison with normal samples[141]. Particularly, Gal-1 was found in the ECM and in the fibroblast compartment surrounding tumor mass, but Gal-1 expression was not found in pancreatic cancer cells neither on metastatic sites. Interestingly, tumors poorly differentiated showed increased Gal-1 mRNA levels in comparison with well differentiated tumors. These results pointed to Gal-1 having an important role in desmoplasia, a hallmark of PDA. Later, and considering pancreatic stellate cells are the major compartment in PDA, other groups determined the relevance of Gal-1 in the

activation and the cytokine production of PSCs. Fitzner and colleagues described for the first time that Gal-1 expression is enhanced in PSCs activated by growth factors such as PDGF and fetal calf serum (FCS). In turn, Gal-1 also stimulates PSCs activation in a glycan-binding dependent manner through ERK1/2 signaling, promoting their proliferation and collagen synthesis[196]. On the other hand, it was also reported that Gal-1 is able to induce the production of monocyte chemoattractant protein 1 (MCP1) and cytokine-induced neutrophil chemoattractant-1 (CINC1) cytokines by PSCs in a glycan and dose dependent manner mainly through the activation of NF-κB pathway, indicating the ability of this lectin to promote PSCs-mediated cytokine production[197].

Interestingly, our group identified Gal-1 as a novel receptor of tissue plasminogen activator (tPA), a serin-protease that is overexpressed in PDA and display pro-tumoral functions[188]. In this way, it was observed that Gal-1, in a glycan and dose dependent manner, mediated tPA-induced proliferation and invasion in pancreatic cells by ERK1/2 pathway activation. Using *c-myc* driven mouse model of PDA (*Ela-myc*), it was observed that tPA and Gal-1 colocalized in the interface between cancer cells and surrounding stromal fibroblasts, suggesting Gal-1 could be a key player on the tumor-stroma cross-talk. These observations, encourage our group to focus our attention in Gal-1 functions in pancreatic ductal adenocarcinoma since this small lectin seems to be a possible stromal-related target for such a fatal disease.

1.6.1 Gal-1 as a diagnostic marker

As mentioned previously, circulating Gal-1 has been detected in several tumors such as colorectal carcinoma[198], classical

Hodgkin lymphoma[199], and neuroblastoma[200]. Gal-1 was also proposed as a biomarker for PDA, in which increased plasma levels of the lectin have been detected in patients diagnosed with PDA compared to healthy controls. Despite sensitivity and specificity between Gal-1 and CA19-9 are similar, the combination of these two biomarkers greatly reduce the number of false negatives in PDA with an increase of sensitivity and specificity up to 96% and 100% respectively. Moreover, a trend was detected for higher Gal-1 plasma levels in those patients with short-term survival[157].

1.6.2 Gal-1 effects in *Ela-myc* driven pancreatic cancer mouse model

Gal-1 effects on PDA desmoplastic stroma were first described using the *Ela-myc* mouse model of PDA. A significant increase in survival and a significant decrease on tumor growth were observed after total or partial abrogation of Gal-1 expression on these mice. This model is characterized by the formation of ductal tumors originated from transdifferentiated acinar cells which undergo ADM. Interestingly, both total knockout (KO) and Gal-1 heterozygous mice (Gal-$1^{-/-}$ and Gal-$1^{+/-}$, respectively) showed a reduction in ductal component compared to WT mice, indicating that total or partial inhibition of Gal-1 expression impaired ADM. It was also demonstrated that Gal-1 held the ability to modulate TME since tumor vascularization and the number of aPSCs were decreased in tumors from *Ela-myc*:Gal-$1^{-/-}$ mice. In contrast, intratumoral T-lymphocytes and neutrophils were increased in those animals, supporting the hypothesis of Gal-1 as a negative modulator of the anti-tumor immune system response in this model. The underlying molecular mechanism was also identified, showing that the expression of some genes involved in Hedgehog

(Hh) pathway, an essential cell signaling pathway implicated in the initiation of PDA development, were modulated by Gal-1 on pancreatic cancer cells, demonstrating that Gal-1 could exert its effects by activating Hh pathway in PDA[201].

1.6.3 Gal-1 effects in *Ela-KRAS* driven pancreatic cancer mouse model

KRAS driven mouse models of PDA are currently considered the best models to mirror human pathology, because mutations in this oncogene are the most frequent genetic alteration in human tumors (>95%)[7,18] Therefore, our group decided to confirm phenotype shown above using the *Ela-KRAS* driven pancreatic cancer mouse model (*KRAS*$^{+/LSL.G12V}$*;Elas-tTA/tetO-Cre;p53*$^{lox/lox}$)[202,203], which develop the full spectrum of pancreatic tumor progression, from metaplastic and preneoplastic lesions to adenocarcinoma and metastasis[202,204–208]. Remarkably, it was observed that genetic ablation of Gal-1 in the *KRAS* driven mouse knockout exhibited an increased survival, delayed tumor progression and reduced metastasis, compared to control mice. Looking at the TME, abolishment of Gal-1 in *Ela-KRAS* pancreatic tumors resulted on tumors with an impaired PSCs activation, less vessel formation and increased immune surveillance by enhancing T lymphocytes recruitment. While tumors of control mice presented high proportion of myeloid cells, the lack of Gal-1 resulted in enhanced $CD4^+$ and $CD8^+$ T cell population and reduced myeloid cell subset. Indicating the ability of Gal-1 to promote immunosuppressive microenvironment in PDA[209].

1.6.4 Gal-1 effects in human pancreatic cancer models

To further investigate the role of Gal-1 in human pancreatic tumor cells as well as in the tumor-stroma crosstalk, our group has used *in vitro* models by using human pancreatic cell lines and human pancreatic stellate cells (HPSC) derived from PDA patients, and *in vivo* models using orthotopic xenografts. First, the underlying molecular mechanism of Gal-1 in pancreatic epithelial cancer cells was identified by performing microarray studies in PANC1 cells after Gal-1 downregulation. We found that the expression of some genes involved in Hh pathway, an essential cell signaling pathway implicated in the initiation of PDA development, were modulated by Gal-1 on pancreatic cancer cells, demonstrating that Gal-1 could exert its effects by activating Hh pathway in PDA[201]. In addition, since PSCs were defined as the major source of Gal-1 in PDA, the paracrine effect of HPSC on pancreatic cancer cells were further determined. Conditioned media (CM) from WT HPSC increased proliferation, migration and invasion of pancreatic cancer cells *in vitro*, while these activities were not found using CM from Gal-1 knockdowns (KD). Orthotopic co-injection was performed in immunodeficient mice using BxPC-3 cancer cells alone, BxPC-3 with WT HPSC or BxPC-3 with HPSC depleted for Gal-1. Interestingly, BxPC-3 and WT HPSC co-injection generated larger tumors than those tumors generated after injecting BxPC-3 alone or co-injecting BxPC-3 in conjunction with HPSC depleted for Gal-1. Besides confirming the relevance of stroma for PDA progression, these results demonstrated that stromal Gal-1 exerts a significant paracrine role in mediating pancreatic tumor growth and aggressiveness. All these data supports stroma Gal-1 as a key player in the tumor-stroma cross-talk in PDA and proposed this lectin as an interesting target for the treatment of this malignancy[209].

OBJECTIVES

Previous data about galectin-1 (Gal-1) role in PDA has been mostly focused on its paracrine effects in tumor epithelium during cancer-stroma crosstalk, as well as in the modulation of immune system surveillance. However, little is known about the effects of the endogenous Gal-1 in stromal fibroblasts themselves. The general aim of this Ph.D. project has been to dissert the role of endogenous Gal-1 in the biology of pancreatic cancer stroma. To investigate this, three specific objectives have been addressed:

2.1 To define the impact of Gal-1 on cancer-associated human pancreatic stellate cells (HPSC) biological functions, activation state and ECM organization

2.2 To determine the molecular mechanisms underlying Gal-1 mediated effects on HPSC

2.3 To decipher the role of nuclear Gal-1 in HPSC in the aforementioned processes

RESULTS

2.1. Characterization of the role of Gal-1 in human pancreatic stellate cells

2.1.1 Expression and localization of Gal-1 in pancreatic ductal adenocarcinoma (PDA)

The high expression of galectin-1 (Gal-1) in the stroma of pancreatic ductal adenocarcinoma (PDA) has been already described in numerous studies[141,188,201,209,210]. Previously, in our laboratory, it was determined the expression and localization of Gal-1 in human PDA and tumors from a *KRAS* driven pancreatic cancer mouse model (*KRAS*$^{+/LSL.G12V}$*;Elas-tTA/tetO-Cre;p53*$^{lox/lox}$) (Fig. 1). In comparison with healthy pancreas, in which Gal-1 was barely expressed (Fig 1. A and C), Gal-1 expression in pancreatic cancer tissues was severely increased at the stroma compartment (Fig. 1 B and D). Gal-1 expression was located at the extracellular matrix, cytosol and, remarkably, strong levels of this protein were also detected in the nucleus of pancreatic stellate cells (Fig. 1, insets black arrows). These findings demonstrated that stromal fibroblasts are the major source of Gal-1 in pancreatic tumors and encouraged our group to characterize the function of this protein in this specific population. To this aim, we have used pancreatic stellate cells from human PDA samples (HPSC) which have been immortalized with SV40 large T antigen and human telomerase (hTERT)[64]. Immunofluorescence of Gal-1 in HPSCs not only corroborated that this protein was highly expressed by HPSC (Fig. 1 E), but also that Gal-1 was notably found in the nucleus of our system of work (Fig. 1 E, white arrows).

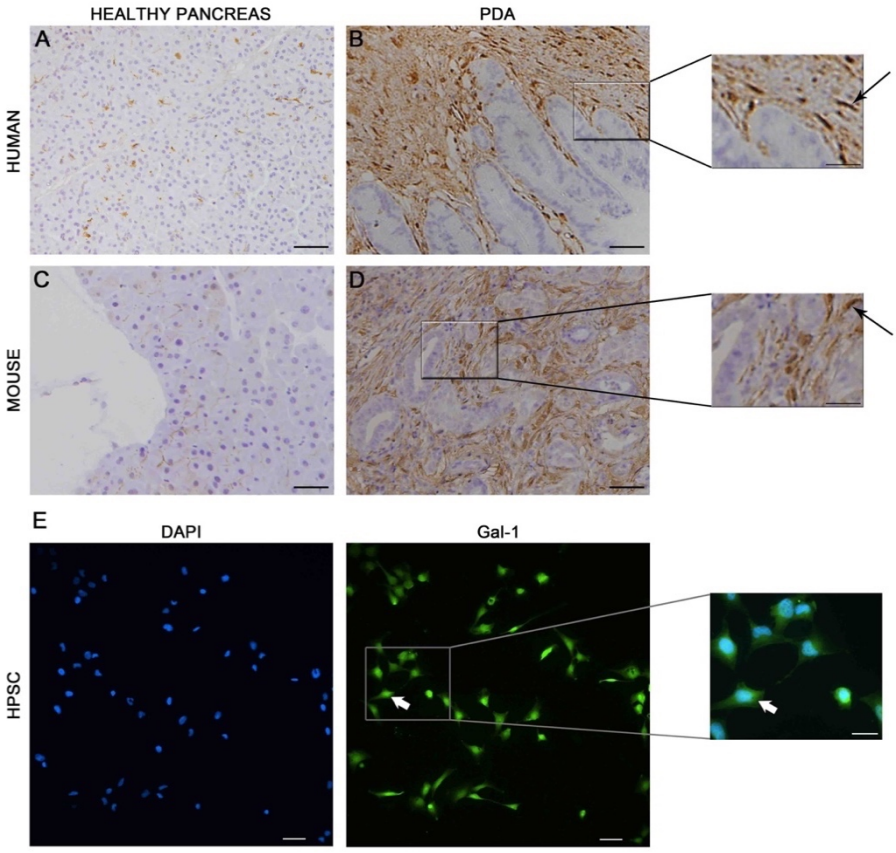

Figure 1. Comparison of Gal-1 expression between healthy and tumor pancreatic tissues. IHC of Gal-1 in human (A) and mouse (C) healthy tissues and in human (B) and mouse (D) PDA tissues. Immunofluorescence of Gal-1 (green) in HPSC (E), nuclei were stained with DAPI (blue). Gal-1 was highly detected in tumor stroma with a strong signal in pancreatic stellate cell nuclei (black arrows). Strong nuclear staining of Gal-1 was also found in the nucleus of HPSC (white arrows) Scale bars correspond to 50μm (images A to E) and 25μm (B, D, E, insets with amplified images).

2.1.2 Effects of Gal-1 downregulation in HPSC proliferation, migration, and invasion

Recent published work from our group demonstrated the implication of HPSC-secreted Gal-1 in promoting pancreatic cancer cells (PCC) aggressiveness. Those results, made our group propose that this small lectin could be described as a key factor in the tumor microenvironment crosstalk[209]. However, intrinsic functions of Gal-1 in HPSC *per se* still remain to be elucidated. To describe the role of Gal-1 in HPSC, our lab downregulated this protein in HPSC by using two strategies: small interference RNA (siRNA) for a transient downregulation of Gal-1, as well as short hairpin RNA (shRNA) for generating stable Gal-1 knockdowns (KD). For studies performed with stable Gal-1 KD, two different *LGALS1*-specific shRNA sequences were used (shGal-1_1 and shGal-1_2). In both cases, the reduction of Gal-1 expression was corroborated at mRNA and protein levels by performing Real Time quantitative PCR (RTqPCR) and Westen Blot (WB) respectively (Fig. 2).

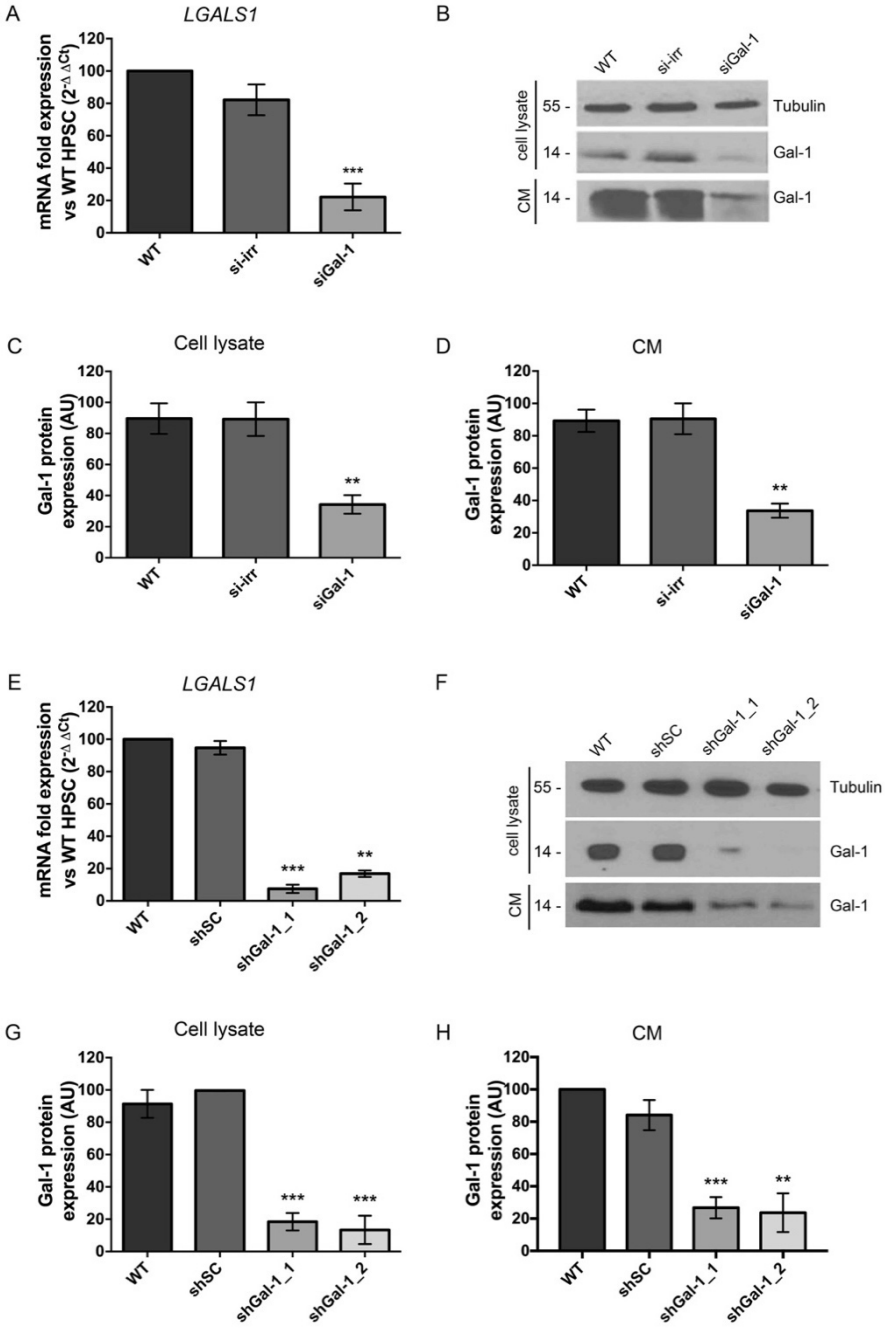
A
LGALS1
mRNA fold expression vs WT HPSC (2^-Δ ΔCt)
120
100
80
60
40
20
0
***
WT
si-irr
siGal-1
B
WT
si-irr
siGal-1
cell lysate
55 -
Tubulin
14 -
Gal-1
CM
14 -
Gal-1
C
Cell lysate
Gal-1 protein expression (AU)
**
WT
si-irr
siGal-1
D
CM
Gal-1 protein expression (AU)
**
WT
si-irr
siGal-1
E
LGALS1
mRNA fold expression vs WT HPSC (2^-Δ ΔCt)
***
**
WT
shSC
shGal-1_1
shGal-1_2
F
WT
shSC
shGal-1_1
shGal-1_2
cell lysate
55 -
Tubulin
14 -
Gal-1
CM
14 -
Gal-1
G
Cell lysate
Gal-1 protein expression (AU)
***
***
WT
shSC
shGal-1_1
shGal-1_2
H
CM
Gal-1 protein expression (AU)
***
**
WT
shSC
shGal-1_1
shGal-1_2

Figure 2. Downregulation of Gal-1 by siRNA and shRNA in HPSC. A) RTqPCR comparing *LGALS1* mRNA levels in non-transfected HPSC and HPSC transfected with an irrelevant small interference RNA sequence (si-irr) or with a small interference RNA sequence against *LGALS1* (siGal-1). B) WB of Gal-1 protein levels in cell extracts (cell lysate) and cell conditioned media (CM) from non-transfected HPSC, HPSC transfected with si-irr sequence and HPSC transfected with siGal-1. Tubulin was used as a loading control. C and D) WB quantification of Gal-1 levels from cell lysate and CM samples upon siRNA transfection. E) RTqPCR comparing *LGALS1* mRNA levels in uninfected HPSC and HPSC infected with a scramble short hairpin RNA sequence (shSC) or with a specific short hairpin RNA sequence against *LGALS1* (shGal-1_1 or shGal-1_2). F) WB of Gal-1 protein levels in cell lysate and cell CM from uninfected HPSC, shSC HPSC, shGal-1_1 HPSC, and shGal-1_2 HPSC. Tubulin was used as a loading control. G and H) WB quantification of Gal-1 levels from cell lysate and cell CM samples upon shRNA infection. Deviation is given as standard error of the mean (SEM) of three independent experiments. *p<0.05, **p<0.01, ***p<0.001 relative to WT. Panels A-C correspond to data from Carlos Alberto Orozco Castaño thesis manuscript[211]. Panels E-H were extracted from *Orozco et al. PNAS (2018)*[209].

Then, we performed an immunofluorescence of Gal-1 in wild type (WT) HPSC, shSC HPSC, and HPSC downregulated for Gal-1 (shGal-1_1 and shGal-1_2) (Fig. 3). This experiment allowed us to confirm that the expression of this protein was highly reduced in Gal-1 shRNA infected cells. Again, high nuclear expression of Gal-1 was detected in control HPSC (WT and shSC) (Fig. 3, white arrows).

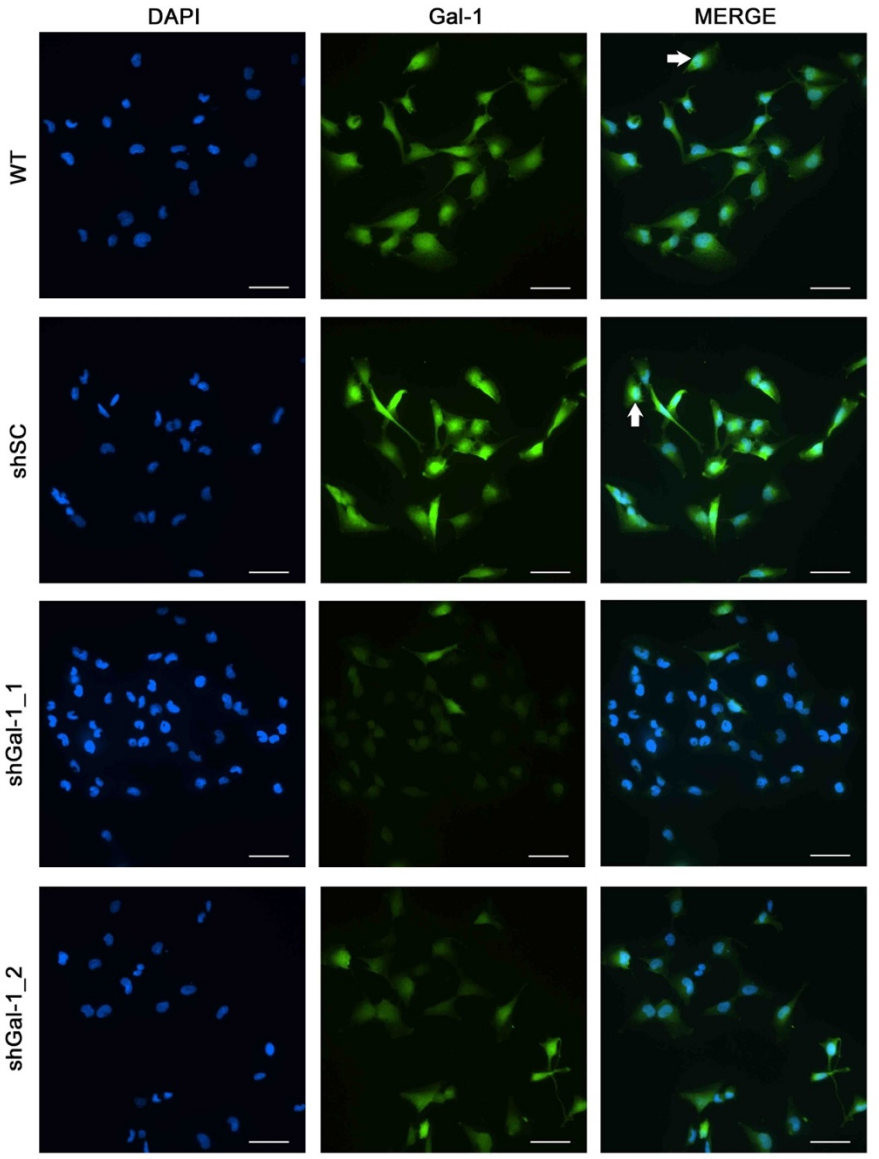

Figure 3. Downregulation and localization of Gal-1 in HPSC controls and in HPSC Gal-1 KD. Immunofluorescence staining for Gal-1 (green) in WT HPSC or infected with shSC, shGal-1_1 or shGal-1_2 sequences. Levels of Gal-1 were highly diminished upon Gal-1 knockdown. Nuclei were stained with DAPI (blue). White arrows indicate nuclear localization of Gal-1 in HPSC. Scale bar corresponds to 50μm.

Next, we explored whether Gal-1 may modulate biological functions of HPSC. To do so, we analyzed HPSC proliferation, migration and invasion after Gal-1 downregulation. As it is shown in figure 4 A, Gal-1 did not affect cell proliferation since no differences were detected between control HPSC (WT and shSC) and Gal-1 KD (shGal-1_1 and shGal-1_2) in MTT assays. However, Gal-1 KD significantly impaired HPSC migration and invasion (Fig 4. B and C).

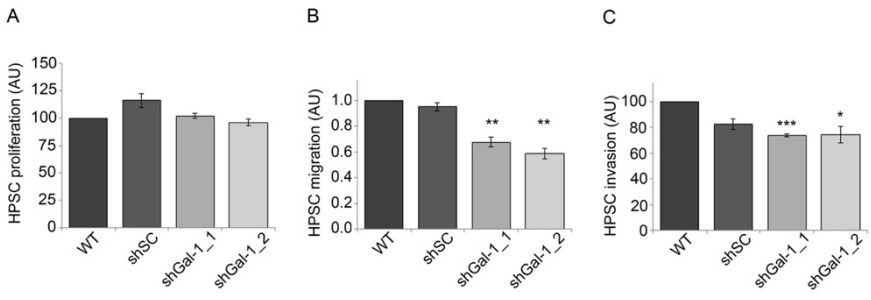

Figure 4. Gal-1 downregulation effects on HPSC proliferation, migration and invasion. A) MTT assay measuring effects of Gal-1 knockdown in HPSC proliferation. B) Wound-healing assay quantification indicating Gal-1 KD effects in HPSC migration. C) Matrigel-coated Transwell assay quantification determining Gal-1 KD effects in HPSC invasion. Deviation is given as standard error of the mean (SEM) of three independent experiments. *p<0.05; **p<0.01; ***p<0.001 relative to WT. Data extracted from *Orozco et al. PNAS (2018)*[209].

2.1.3 Effects of Gal-1 downregulation in HPSC activation

For a further characterization of the effect of Gal-1 downregulation in HPSC, molecular studies were performed. Activation of HPSC is a crucial event linked to inflammation and tumor progression[212]. Several molecular changes take place upon fibroblast activation, including overexpression of smooth muscle

actin alpha (α-SMA), fibroblast activation protein (FAP), glial fibrillary acidic protein (GFAP), alpha-1 type I collagen (COL1A1) and fibronectin (FN) among others. So, to determine whether Gal-1 was involved in HPSC activation, the expression of different activation markers was analyzed in control and Gal-1 knockdown HPSC. Figure 5 (A-D) shows that *ACTA2* (codifying gene for α-SMA), *GFAP*, *FAP* and *COL1A1* mRNA levels were significantly reduced after Gal-1 knockdown. At the protein level, we found a significant decrease in α-SMA, GFAP, FAP and FN expression (Fig. 5 E).

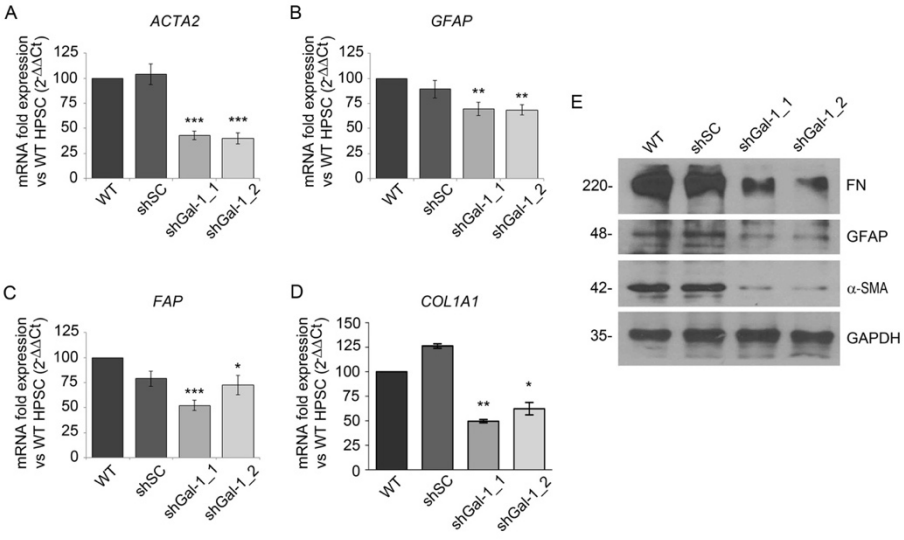

Figure 5. Gal-1 downregulation effects on HPSC activation. RTqPCR quantification of mRNA levels of fibroblast-activation markers *ACTA2* (A), *GFAP* (B), *FAP* (C) and *COL1A1* (D) in control HPSC (WT and shSC) and Gal-1 KD (shGal-1_1 and shGal-1_2). E) Protein levels detected by WB of α-SMA, GFAP and FN in control HPSC and Gal-1 knockdowns. GAPDH was used as a loading control. Deviation is given as standard error of the mean (SEM) of three independent experiments. *p<0.05; **p<0.01; ***p<0.001 relative to WT. Data extracted from *Orozco et al. PNAS (2018)*[209].

Moreover, this alteration in the expression of activation markers were accompanied by morphological changes; it was noticed that HPSC morphology switch from a spindle shape to a more epithelial-like appearance (Fig 6. A). To corroborate this observation, phalloidin toxin conjugated to a fluorescent label was used to selectively stain actin filaments (f-actin), which allowed us to have a better perception of cell morphology. It was clearly observed that while control HPSC presented more spindled shape, Gal-1 downregulated HPSC adopted a less fibroblastic aspect (Fig 6. B). All of these results suggested that Gal-1 could be promoting HPSC activation state through affecting molecular levels of different activation markers such as α-SMA, FAP, and FN hence, favoring fibroblast spindled shape when it (Gal-1) is expressed.

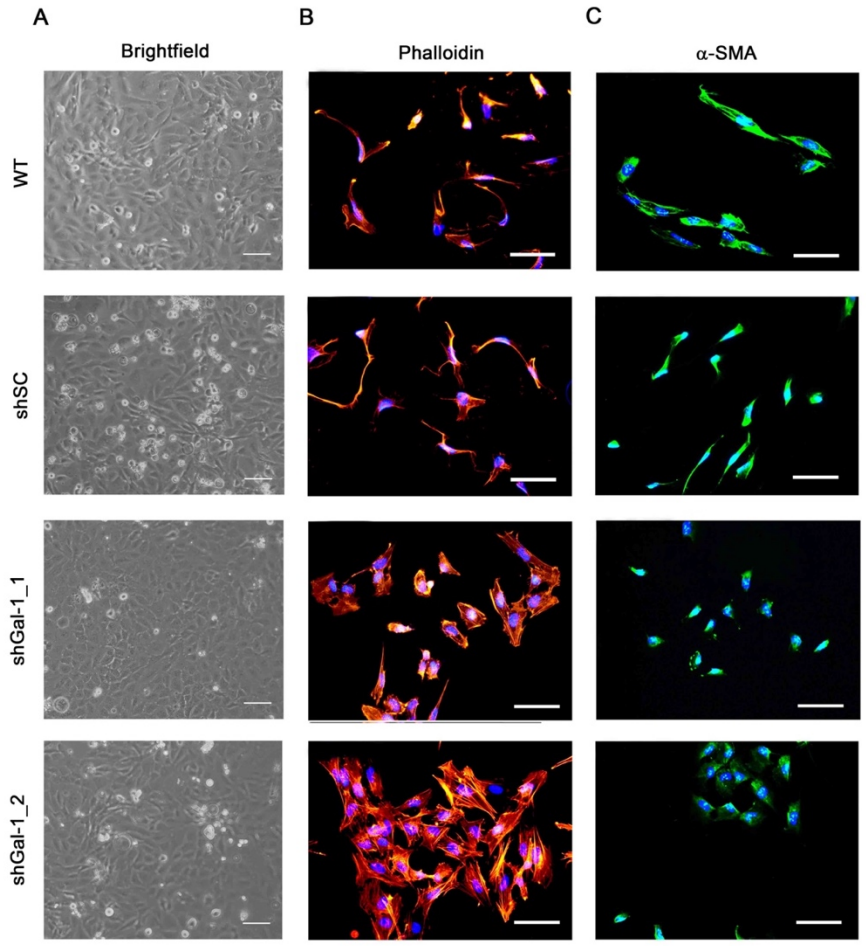

Figure 6. Morphological changes in HPSC upon galectin-1 downregulation. A) WT, shSC and Gal-1 KD (shGal-1_1 and shGal-1_2) HPSC morphology at light microscopy (brightfield). Scale bar corresponds to 50μm. B) Immunofluorescence staining of phalloidin in WT, shSC and Gal-1 KD HPSC. C) Immunofluorescence staining of α-SMA in WT, shSC and Gal-1 KD HPSC. Scale bars correspond to 50μm (A) and 100μm (B and C). Panels B and C were extracted from *Orozco et al. PNAS (2018)*[209].

These data demonstrate that Gal-1 has not only a key effect on pancreatic stellate cells migration and invasion, but also on their

capability to become activated, providing new insights into the autocrine effects of this protein in pancreatic cancer stroma.

2.1.4 Effects of galectin-1 downregulation in HPSC ECM organization

It is well known that ECM organization can control cell shape and growth[213]. Moreover, it has been demonstrated that cancer-associated fibroblasts (CAFs) are able to promote extracellular fibronectin alignment favoring cancer cell migration[214]. Consequently, we wondered whether the expression of Gal-1 could be important for determining the ECM organization of HPSC. For this porpoise, we compared ECM deposition of uninfected HPSC (WT), infected with shSC or HPSC downregulated for Gal-1 (shGal-1_1 and shGal-1_2) after 9 days of cell culture. Fiber alignment was observed at confocal microscopy after fluorescent staining of both FN and cell nuclei. Since fibroblasts were aligned as well as FN fibers, we decided to quantify the percentage of aligned nuclei to determine ECM organization. It was observed that WT and shSC HPSCs were able to generate an organized ECM while fiber alignment was clearly abrogated in Gal-1 KD HPSCs (Fig. 7). These results suggested that stromal Gal-1 levels could affect tridimensional ECM architecture.

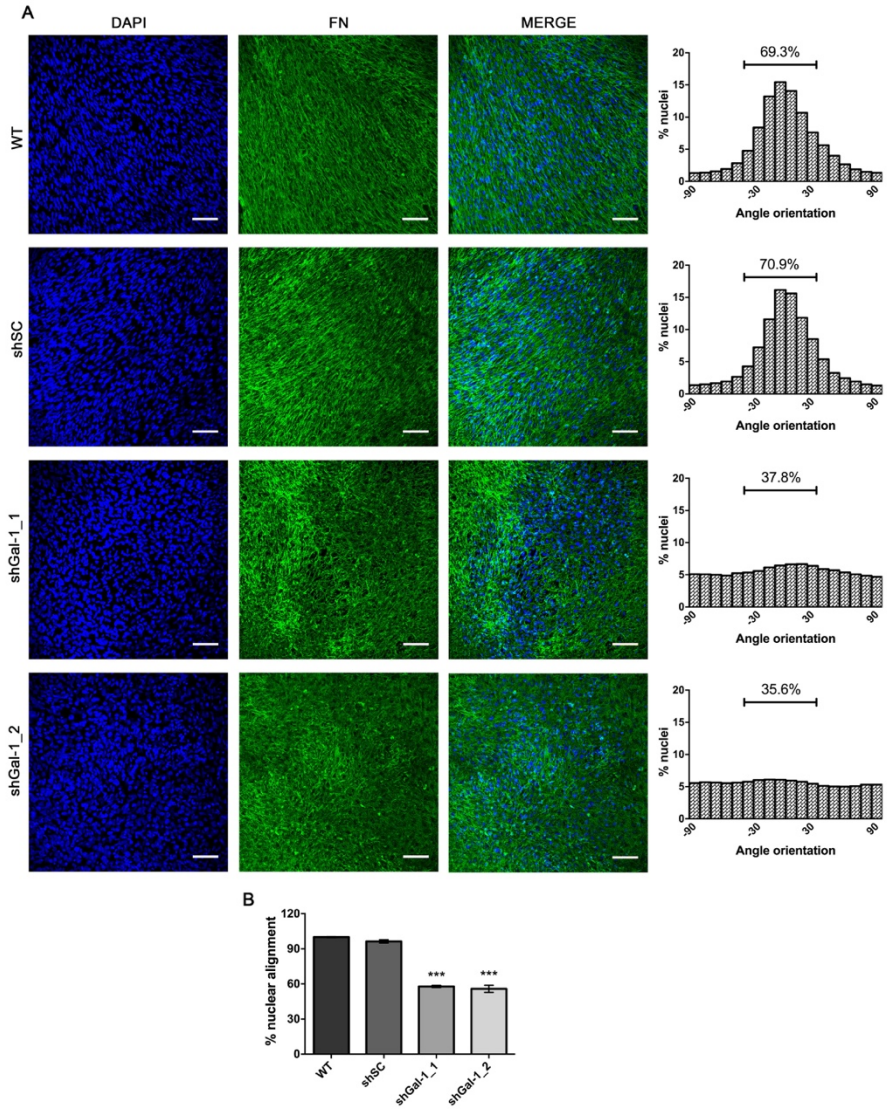

Figure 7. Gal-1 effects on extracellular matrix organization. A) Left, IF staining of secreted fibronectin (green) from WT HPSC (uninfected), shSC (infected with scramble shRNA), and Gal-1 KD (shGal-1_1 and shGal-1_2). DAPI (blue) was used for nuclei staining. Right, percentage of nuclei alignment in which all nuclei with a $\pm 30^{\circ}$ of angle orientation were considered aligned. Representative images are shown. B) Quantification comparing percentage of nuclear alignment between WT, shSC, and HPSC downregulated for Gal-1 (shGal-1_1 and shGal-1_2). Scale bar corresponds to 100μm. Deviation is represented by standard error of the mean

(SEM) of three independent experiments. *p<0.05; **p<0.01; ***p<0.001 relative to WT.

Considering that TGF-β is a well-known factor that exerts an important role in tumor microenvironment modulation and fibroblast activation[215], we next wondered whether the observed Gal-1 effect on ECM structure was depending on TGF-β pathway. To do so, HPSC were treated with TGF-β during the 9 days of the ECM deposition experiment. Interestingly, WT and shSC HPSCs shew the same alignment proportion either in the presence or absence of TGF-β treatment. In contrast, we found that treatment with TGF-β of shGal-1_2 KD results in a strong alignment of ECM, resembling the phenotype of control cells; while none effect was found in sh-Gal-1_1 KD cells, which still generated a disorganized ECM (Fig. 8). Taking in account that shGal-1_1 KD presented a higher decrease of Gal-1 expression (Figs. 2 and 3) and a stronger impairment of fibroblast activation (Figs. 5 and 6), these observed results suggested Gal-1 is able to control fibroblast alignment independently of TGF-β pathway in a Gal-1-dose dependent manner. Indeed, the fact that HPSC *per* se were able to generate an organized ECM with a high degree of alignment that is not further modified by TGF-β treatment indicated that HPSCs already display an *in vitro* highly activated phenotype.

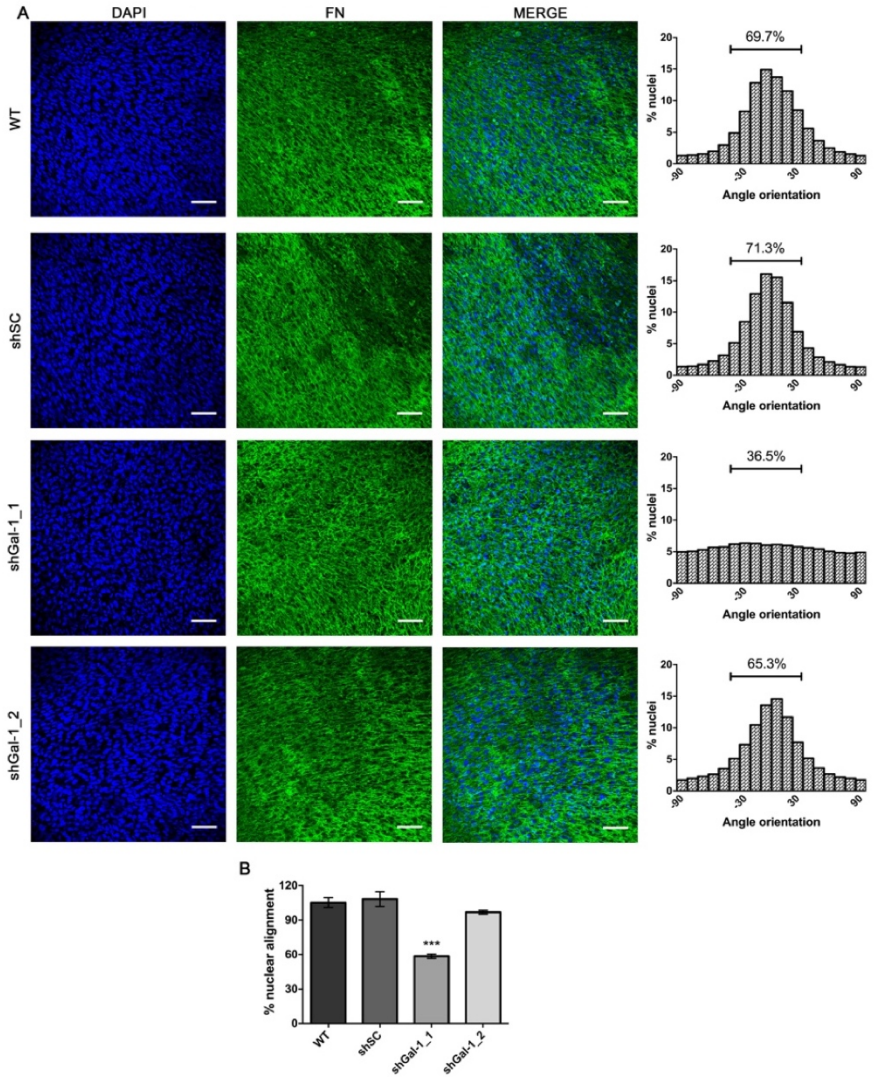

Figure 8. Galectin-1 effects on extracellular matrix organization upon TGF-β treatment. A) Left, IF staining of secreted fibronectin (green) from WT HPSC (uninfected), shSC (infected with scramble shRNA), and Gal-1 KD (shGal-1_1 and shGal-1_2). Cells were treated with TGF-β (5ng/ml) every other day during 9 days. DAPI (blue) was used for nuclei staining. Right, percentage of nuclei alignment in which all nuclei with a ±30° of angle orientation were considered aligned. Representative images are shown. B) Quantification comparing percentage of nuclear alignment between WT, shSC, and HPSC downregulated for Gal-1 (shGal-1_1 and shGal-1_2). Scale bar corresponds to 100μm. Deviation is represented by

standard error of the mean (SEM) of three independent experiments. *p<0.05; **p<0.01; ***p<0.001 relative to WT.

2.2. Deciphering the molecular mechanisms responsible for galectin-1-mediated HPSC activation and functions

2.2.1 Gene expression changes after Gal-1 knockdown in HPSC

Considering that Gal-1 seems to be acting as a master regulator of HPSC activation, favoring ECM fibers alignment, and promoting cell migration and invasion; we decided to explore the molecular mechanisms underlying Gal-1-mediated effects in HPSC. To approach this study, we analyze differences in gene expression between control HPSC (HPSC transfected with si-irrelevant) and HPSC knockdown for Gal-1 (HPSC transfected with siGal-1) using a human whole-transcript microarray (GeneChip® PrimeView™ Human Gene Expression Array). After proper quality control and data normalization, Linear of Models for Microarray (LIMMA) pipeline[216] was used to determine genes differentially expressed between compared conditions (Fig. 9A). Adjusted p-value<0.05 was considered as the threshold to define significant differentially-expressed genes (Table 1S, supplementary data). Interestingly, functional annotation analysis displayed biological functions related to DNA binding and transcription regulation (Fig. 9B, left). According to these results, gene ontology (GO) analysis also showed transcription regulation as one of the most relevant group (Fig. 9B, right), suggesting a role in gene expression regulation for Gal-1 in HPSC.

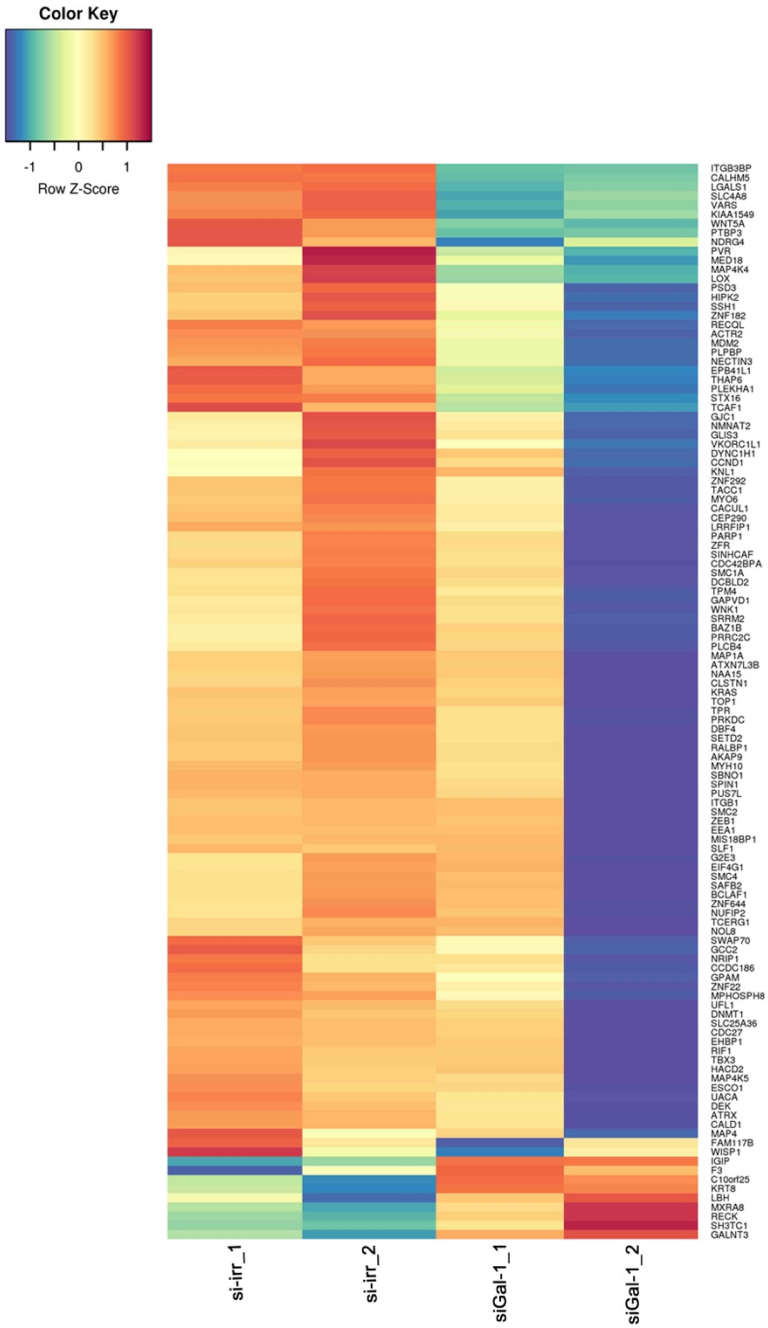

Figure 9A. Gene expression changes driven by Gal-1 knockdown in HPSC. Heatmap of the most differentially expressed genes between HPSC transfected with an irrelevant small interference RNA (si-irr) and HPSC transfected with a

siRNA against *LGALS1* (siGal-1). Linear of Models for Microarray (LIMMA) pipeline was used for data analysis.

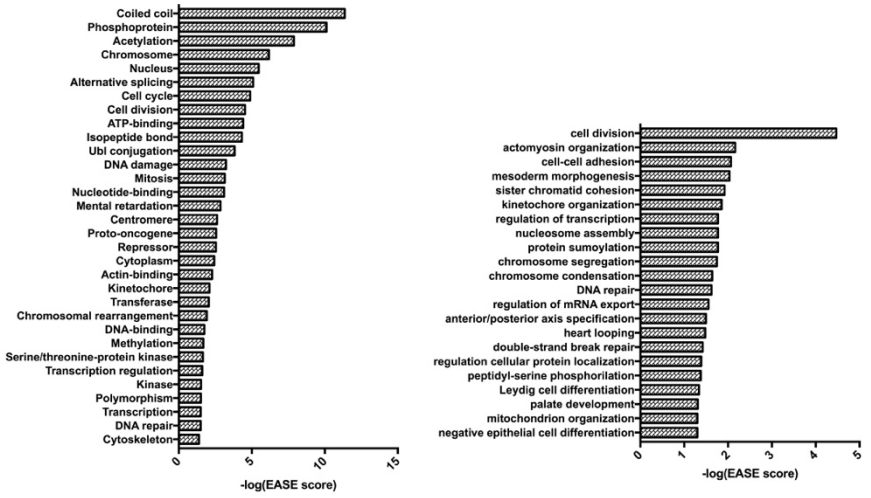

Figure 9B. Microarray functional annotation analysis. Most represented biological processes are shown; functional characterization (left) and gene ontology (right). This analysis was performed using DAVID Database tool.

A set of 86 genes were differentially expressed after Gal-1 KD in HPSC (Table S1, supplementary data), 83 of which were downregulated while only 3 were upregulated in HPSC Gal-1 KD compared to control. Among the mentioned gene list, we decided to focus our attention in *KRAS*, *WNT5A*, and *TACC1* genes given their role in cancer. Downregulation of these genes upon Gal-1 KD was validated at mRNA level by RTqPCR (Fig. 10 A) and protein level by WB analysis (Fig. 10 B).

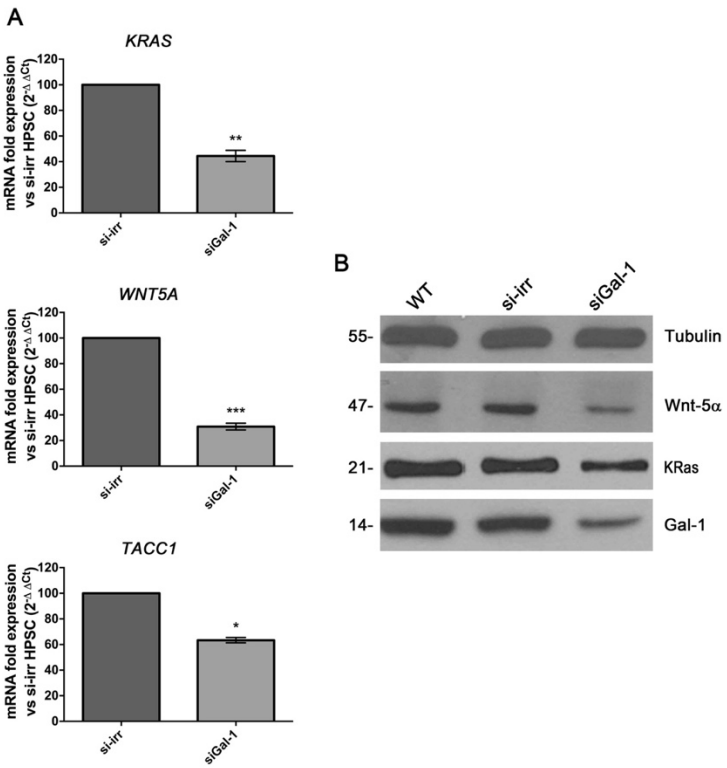

Figure 10. Validation of top differentially expressed genes upon Gal-1 downregulation. A) RTqPCR showing that mRNA levels of *KRAS* (top), *WNT5A* (middle) or *TACC1* (bottom) were reduced upon Gal-1 knockdown in HPSC. B) WB of reduced proteins levels of Wnt-5α and KRas. Tubulin was used as loading control. Deviation is represented by standard error of the mean (SEM) of three independent experiments. *p<0.05; **p<0.01; ***p<0.001 relative to si-irr. Data extracted from Carlos Alberto Orozco Castaño thesis manuscript[211].

2.2.2 Effects of KRas, Wnt-5α or TACC-1 downregulation in HPSC activation and functions

Data from our gene expression microarray analysis and target validation suggested that KRas, Wnt-5α and/or TACC-1 could

be downstream proteins responsible for Gal-1-mediated effects on HPSC, encouraging us to go further in this study. The implication of KRas in pancreatic cancer is widely known since it is mutated in approximately 95% of patients and the mutational activation of this oncogene seems to be prevalent for the generation and maintenance of pancreatic tumors[19]. However little is known about the functionality of KRas in fibroblasts[217–219]. Wnt-5α is a soluble protein, belonging to Wnt signaling family, responsible for activating non-canonical WNT signaling pathways. In cancer, this protein has been described as favoring both oncogenic and tumor-suppressor activities[220]. Specifically in pancreatic cancer, it has been reported that Wnt-5α induces cell apoptosis resistance[221]. Moreover, Wnt-5α has been also described as a regulator of fibroblast proliferation in pulmonary diseases[222]. Finally, transforming acidic coiled-coil protein 1 (TACC1) plays an important role in centrosome and microtubule associated functions[223] and its expression has been linked to morphologic changes associated to a malignant phenotype[224]. Remarkably, functions of these gene are poorly characterized and its role in cancer-associated fibroblasts is unknown. Therefore, in order to gain insights into the putative effects of *KRAS*, *WNT5A* or *TACC1* in HPSC activation and functions we used shRNA methodology and characterize HPSC phenotype after downregulation of the expression of these targets. Suitable downregulation of each gene was corroborated by RTqPCR (Fig. 11 A-C). But confirmation of proper protein levels reduction was only possible for Wnt-5α (Fig. 11 D and E).

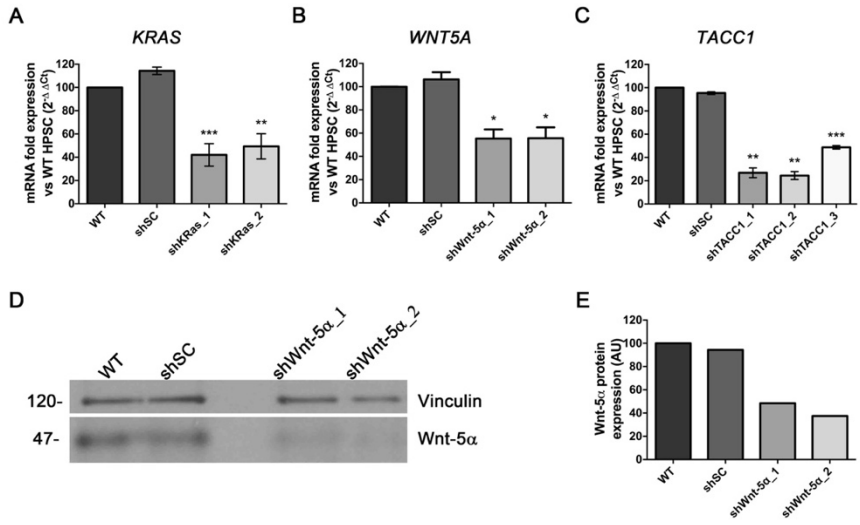

Figure 11. KRas, Wnt-5α and TACC1 downregulation in HPSC. A-C) RTqPCR of mRNA levels of *KRAS* (A), *WNT5A* (B) and *TACC1* (C) from WT HPSC or HPSC infected with a scramble short hairpin RNA (shSC) or a specific shRNA against mRNA of interest (shKRas, shWnt-5α or shTACC1). At least, two shRNA sequences were chosen to study each gene. D) WB presenting protein levels of Wnt-5α after its knockdown in HPSC. Vinculin was used as a loading control. E) Quantification of Wnt-5α protein levels. Deviation is given as standard error of the mean (SEM) of three (A) or two (B and C) independent experiments. *p<0.05; **p<0.01; ***p<0.001 relative to WT.

2.2.2.1 Effects of KRas downregulation in HPSC activation and functions

Decrease of KRas levels in HPSC led to impairment of HPSC activation, shown by a reduction of *ACTA2* (α-SMA) expression at mRNA (Fig. 12 A) and protein levels (Fig 12 D and E), although, no significant differences were observed for the expression of other activation markers like *FAP* and *GFAP* (Fig. 12 B and C).

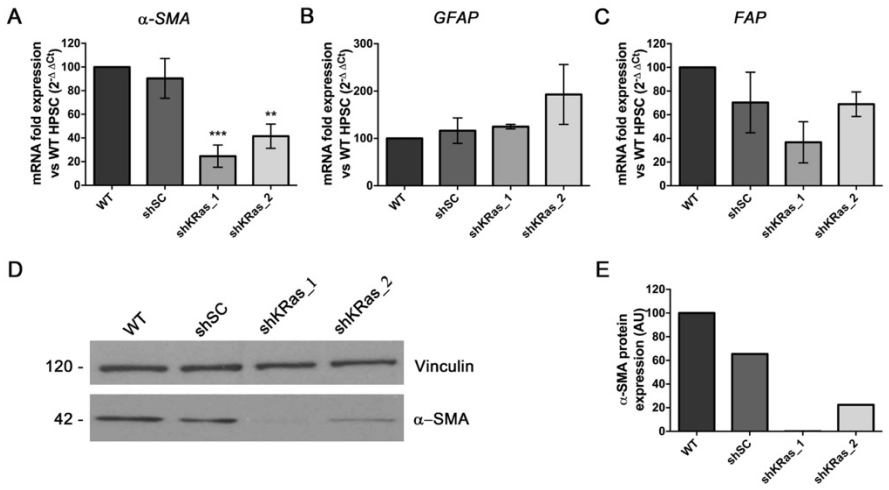

Figure 12. KRas effects on HPSC activation. A-C) RTqPCR comparing mRNA levels fibroblast-activation markers (*ACTA2* (A), *GFAP* (B) and *FAP* (C)) between control HPSC (WT and shSC) and KRas knockdowns (shKRas-1_1 and shKRas-1_2). D) WB of reduced protein levels of α-SMA after KRas knockdown. E) Quantification of α-SMA protein levels in WT, shSC and KRas knockdowns. Deviation is given as standard error of the mean (SEM) of three (A) or two (B and C) independent experiments. *p<0.05; **p<0.01; ***p<0.001 relative to WT.

We also analyzed whether this effect can alter cell morphology. To this aim, we follow the same procedure as explained before by staining actin fibers and determining cell morphology using immunofluorescence microscopy. Interestingly, we observed that downregulation of KRas levels changed HPSC shape to a less spindled morphology compared with control HPSCs (Fig. 13). These data indicate that KRas could exert an effect on HPSC activation, suggesting that Gal-1 may modulate HPSC activation, at least in part, through KRas pathway.

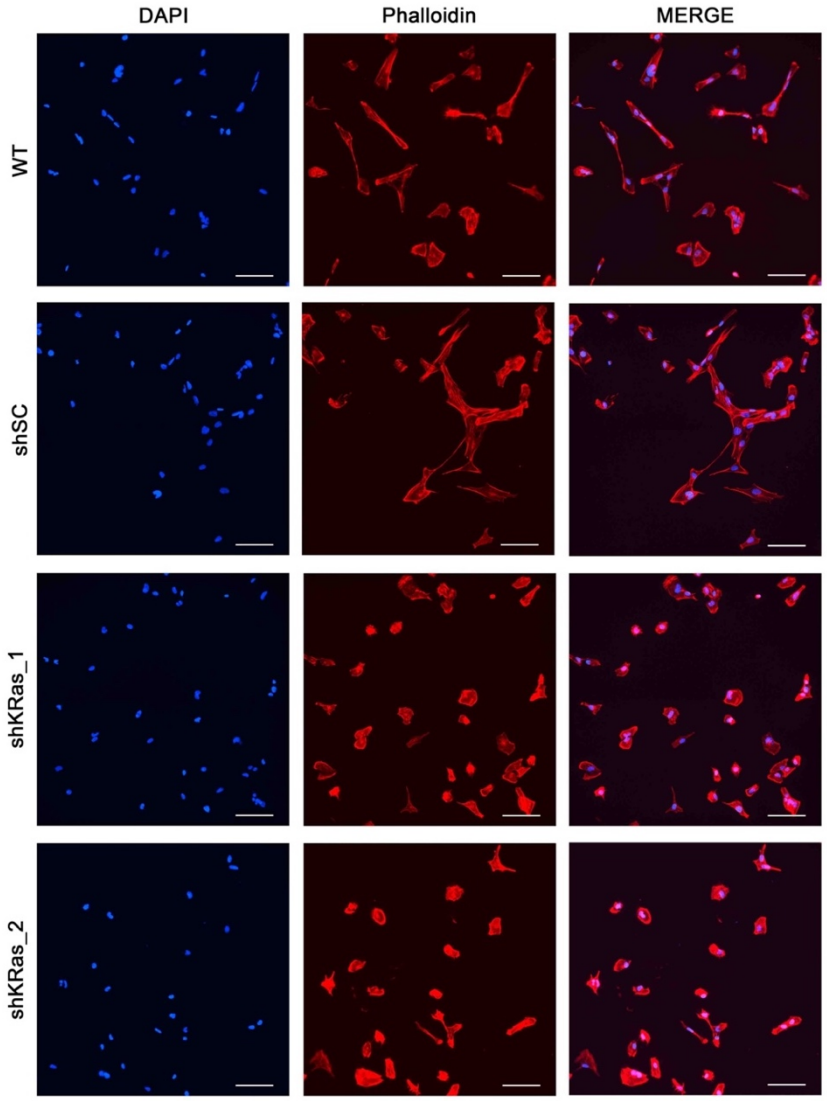

Figure 13. KRas downregulation promotes a less spindled morphology in HPSC. IF of phalloidin staining (red) in WT, shSC, shKRas-1_1 and shKRas-1_2 HPSCs. Scale bar corresponds to 100μm.

Next, the role of KRas in HPSC proliferation, migration and invasion was determined. To assess cell proliferation, MTT assays were performed during 6 days. KRas downregulation in HPSC showed an impaired proliferation compared with controls (Fig. 14 A). To study cell migration after KRas downregulation in HPSC we performed wound-healing experiments. Cells were seeded at total confluence and, at the following day, a scratch was performed generating an empty area to let cell migration. Remaining free area was quantified after 24h: the smaller free area, the greater migratory capacity. Re-covered area was represented for an easier interpretation. We found that shKRas_2 KD was able to significantly reduce cell migration, while shKRas_1 KD did not present significant differences compared to control cells (Fig. 14 B). Concerning invasion studies, cells were seeded into upper chamber after proper Matrigel coating. Once cells were adhered to Matrigel, DMEM 10% FBS was added to the bottom chamber as a chemoattractant. Cell invasion was performed during 36h and the number of invading cells were determined after nuclei DAPI-staining. Similar to the effects found for cell migration, we could only observe a reduction of HPSC invasion capacity after downregulation of KRas in the shKRas_2 KD, but not in the shKRas_1 KD compared to control cells (Fig. 14 C). Altogether, these results indicate that KRas may play a role in HPSC proliferation and likely in migration and invasion. However, different effects found with the shKRas_1 and shKRas_2 KD HPSC suggest that it would be required to test other shRNA sequences to get better conclusions about the involvement of KRAS in HPSC migration and invasion.

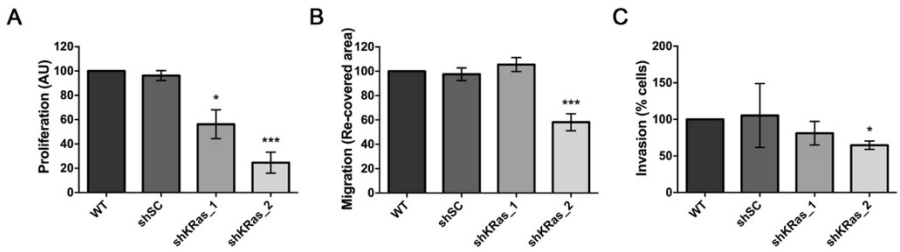

Figure 14. KRas effects on HPSC proliferation, migration and invasion. A) MTT assays showing HPSC proliferation of WT, shSC and KRas KD. B) Quantification of cell migratory capacity WT, shSC and KRas KD. Wound-healing assays were performed and migration capability was assessed after 24h. Re-covered area is represented as 100% (initial free-area) - % remaining free-area after 24h. C) Quantification of invasion ability of WT, shSC and KRas KD using Matrigel-coated Transwells. Percentage (%) of cells that invaded through a Matrigel-coated Transwell chamber during 36h are represented. Deviation is given as standard error of the mean (SEM) of three (A and B) or two (C) independent experiments *p<0.05; **p<0.01; ***p<0.001 relative to WT.

2.2.2.2 Effects of Wnt-5α downregulation in HPSC activation and functions

To test the activation state of HPSC after Wnt-5α downregulation, we determined the expression of α-SMA at mRNA (Fig. 15 A) and at protein levels (Fig. 15 B and C). Clear differences on α-SMA expression were detected between WT HPSC and shSC HPSC presenting, the last one, a reduction of α-SMA expression similar to the α-SMA levels observed in Wnt-5α KD (shWnt-5α_1 and shWnt-5α_2). With these results, despite of low levels of α-SMA after Wnt-5α KD compared with WT HPSC, we could not confirm any contribution of Wnt-5α in HPSC activation. Nevertheless, proliferation, migration and invasion ability were assessed to describe the effects of Wnt-5α on HPSC functions. MTT assays showed that HPSC proliferation significantly increased for shWnt-

5α_2 KD while non-significant differences were observed for shWnt-5α_1 KD proliferation compared to controls (WT and shSC) (Fig. 15 D). To study cell migration, we followed a different strategy in which we used Transwell chambers, after 24h of migration cells were stained with DAPI and nuclei were quantified. Surprisingly, different results were detected when the two different Wnt-5α KD were compared; while shWnt-5α_1 did not exhibited any differences in migratory capacity, shWnt-5α_2 presented an increased migration compared to WT and shSC HPSC (Fig. 15 E). Similar results were obtained in invasion studies, in which shWnt-5α_1 KD did not changed HPSC invasion, while this ability was significantly increased in shWnt-5α_2 KD in comparison with both controls (Fig. 15 F). These results suggested that probably one of the studied shRNA sequences against *WNT5A* (shWnt-5α_2) could have an off-target side effect and therefore producing distinct phenotype. So, unfortunately, non-conclusion could be made about Wnt-5α effects related to HPSC either proliferation, migration or invasion abilities.

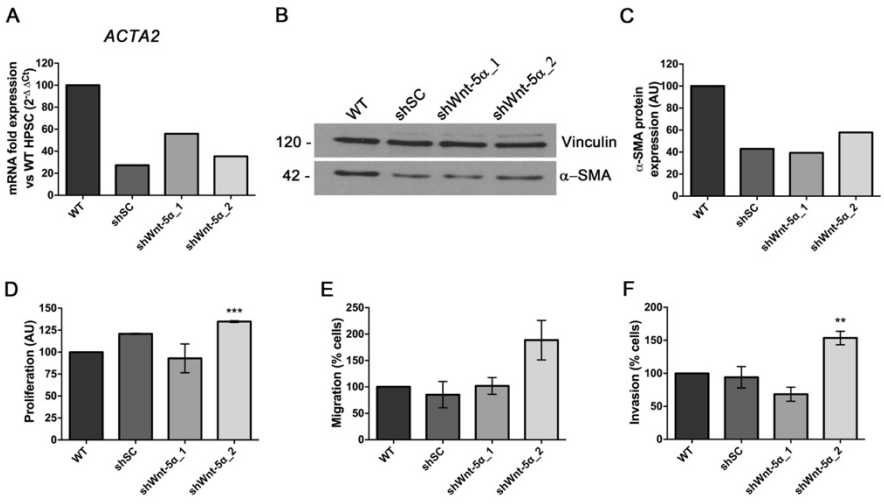

Figure 15. Wnt-5α effects on HPSC activation, proliferation, migration and invasion. A) RTqPCR showing mRNA levels of *ACTA2* in WT, shSC and Wnt-5α KD

(shWnt5α-1_1 and shWnt5α-1_2). B) WB comparing protein levels of α-SMA between control (WT and shSC) and Wnt-5α KD HPSCs. C) Quantification of α-SMA protein levels in control and Wnt-5α KD HPSCs. D) MTT assays showing HPSC proliferation of WT, shSC and Wnt-5α KD. E) Cell migratory capacity of WT, shSC and Wnt-5α KD. Percentage (%) of cells that migrated through a Transwell chamber after 24h are represented. F) Invasion ability of HPSC of WT, shSC and Wnt-5α KD using Matrigel-coated Transwell chambers. Percentage (%) of cells that invaded through a Matrigel-coated Transwell chamber during 36h are represented. Deviation is given as standard error of the mean (SEM) of two (D, E and F) independent experiments *p<0.05; **p<0.01; ***p<0.001 relative to WT.

2.2.2.3 Effects of TACC1 downregulation in HPSC activation and functions

Regarding to HPSC activation, the observed effects of TACC1 downregulation were comparable to those found in Wnt-5α KD studies. Infected cells, shSC and TACC1 KD, presented a reduced α-SMA levels compared with uninfected WT HPSC (Fig. 16 A). And consequently, non-conclusion could be assumed for TACC1 effects in HPSC activation. Similar strategies were performed to assess the effects of TACC1 in HPSC functions. No proliferative defects were observed after the reduction of TACC1 levels in HPSC in MTT assays when compared with shSC. Due to the different phenotype observed between WT and shSC HPSC, we could not assume any difference in HPSC proliferation after TACC1 KD (Fig. 16 B). On the other hand, wound-healing and invasion assays did not exhibit distinct migratory (Fig. 16 C) nor invasive (Fig. 16 D) capabilities between WT, shSC and HPSC downregulated for TACC1. In this case, hexosaminidase activity was measured to determine the invasive capability of TACC1 KD in HPSC. Since non-impaired migration nor invasion was showed upon TACC1 downregulation in HPSC, we concluded that this protein has not any effect on these functions in HPSC.

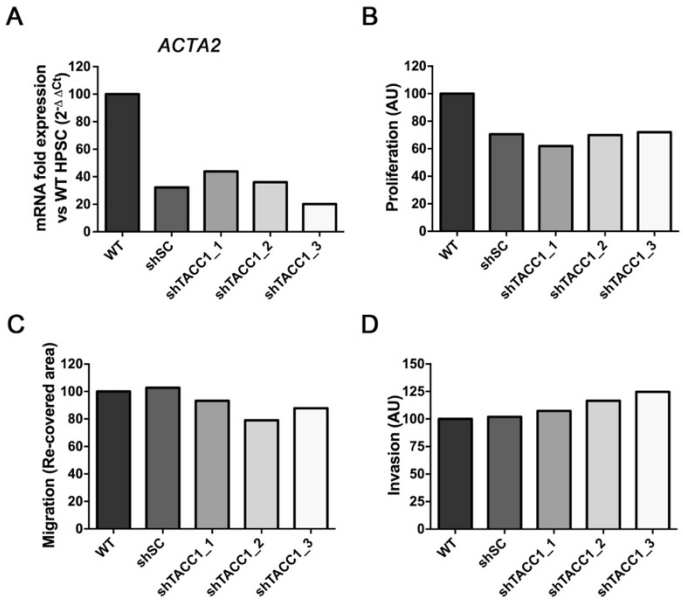

Figure 16. TACC1 effects on HPSC proliferation, migration and invasion. A) RTqPCR comparing mRNA levels of *ACTA2* between WT, shSC and TACC1 KD (shTACC1_1, shTACC1_2 and TACC1_3). B) MTT assays showing HPSC proliferation of WT, shSC and TACC1 KD. C) Cell migratory capacity of WT, shSC and TACC1 KD. Wound-healing assays were performed and migration capability was assessed after 24h. Re-covered area is represented as 100% (initial free-area) - % remaining free-area after 24h. D) Invasion ability of WT, shSC and TACC1 KD using Matrigel-coated Transwell chambers. Hexosaminidase activity was measured at 410 nm after 36h of cell invasion. All data was normalized relative to WT.

In light of these results after knockdown of *KRAS*, *WNT5A* or *TACC1* we can conclude that KRas is involved in HPSC activation and proliferation, and probably also implicated in HPSC migration and invasion suggesting that Gal-1 may induce HPSC activation and the studied biological functions through KRas pathway. However, we have not been able to provide evidences for the contribution of

Wnt-5α nor TACC1 in Gal-1-mediated HPSC activation, proliferation, migration or invasion.

2.3. Nuclear functions of Galectin-1 in human pancreatic stellate cells

Our microarray studies have shown that downregulation of Gal-1 in HPSC results in downregulation of numerous genes, pointing to a role of this protein in regulation of gene expression in pancreatic stromal cells. Moreover, considering the strong expression of Gal-1 found in the nucleus of pancreatic stellate cells in PDA tissue and cell cultures (Fig. 1), we hypothesized that nuclear Gal-1 may be directly involved in regulating gene expression in HPSC. However, as Gal-1 is a secreted protein that can be also extracellularly located, we first analyzed whether extracellular Gal-1 can be also involved in gene expression regulation. In this regard, it has been reported that Gal-1 can bind cell surface glycoligands and trigger intracellular signaling pathways leading to gene expression changes modulating cell functions[225]. Therefore, we explore the involvement of the MAPK/ERK pathway, one of the majors signaling pathways involved in signal transduction to the nucleus and induction of DNA transcription[226], in Gal-1-mediated regulation of gene expression. We found that the treatment with U0126, a selective inhibitor of MAPK/ERK pathway (Fig. 17 A), does not affect *KRAS* mRNA levels, one of the genes found to be regulated in our microarray analysis (Fig. 17 B). As positive control of the experiment, we analyzed the expression of *FOS*, a well-known gene regulated by MAPK/ERK, which was significantly downregulated after U0126 treatment (Fig. 17 C).

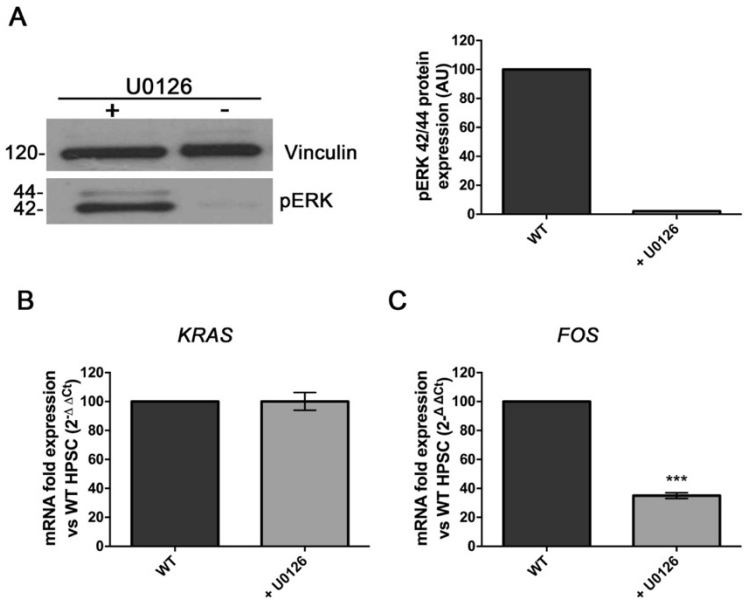

Figure 17. ERK pathway inhibition did not affect KRas expression in HPSC. A) Left, WB showing levels of phosphorylated ERK in HPSC after 2h of UO126 treatment, an inhibitor of ERK pathway. Right, Quantification of p44/42-ERK levels. B) RTqPCR of *KRAS* mRNA levels after UO126 treatment. C) RTqPCR of *C-FOS* mRNA levels as a positive control of UO126 treatment. Deviation is given as standard error of the mean (SEM) of three independent experiments *p<0.05; **p<0.01; ***p<0.001 relative to WT.

Next, we block secreted Gal-1 to prevent any signaling pathway triggered by this lectin. To approach this goal, we treated HPSC with β-lactose, a well-known inhibitor of glycan-mediated Gal-1 interactions, and we analyzed the effects on gene expression by measuring *KRAS* mRNA levels. As shown in figure 18, β-lactose treatment did not change *KRAS* mRNA levels comparing with untreated cells (WT), suggesting that extracellular Gal-1 does not affect the regulation of *KRAS* gene transcription.

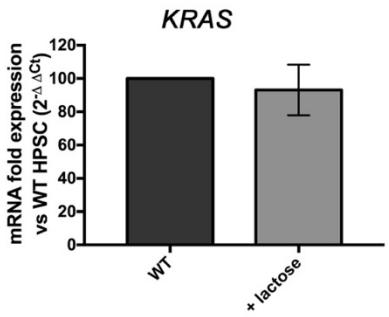

Figure 18. Lactose treatment did not affect *KRAS* mRNA levels in HPSC. HPSC were treated with 100 mM of lactose during 2h and mRNA levels of *KRAS* were assessed by RTqPCR. Deviation is given as standard error of the mean (SEM) of three independent experiments *p<0.05; **p<0.01; ***p<0.001 relative to WT.

These results suggest that extracellular Gal-1 is not responsible for the observed changes in gene expression after Gal-1 downregulation, at least in the case of *KRAS* (used as a proof of concept target), pointing to nuclear Gal-1 as the responsible for controlling gene expression in HPSC. Of note, previous reports have described that nuclear Gal-1 is involved in gene expression regulation by mediating pre-mRNA splicing in HeLa cells[108]. Interestingly, it has been reported Gal-1 interacts with FOXP3 tumor suppressor in breast cancer cells changing genome-wide binding pattern of FOXP3[133]. However, there are no reports regarding Gal-1 nuclear functions in fibroblasts. Thus, we decided to explore the possible roles of nuclear Gal-1 in controlling gene expression in HPSC.

2.3.1 Subcellular localization of galectin-1 in HPSC

To better understand the role of nuclear Gal-1 in HPSC, we performed a subcellular fractionation to determine whether Gal-1 was present in the nucleoplasm, as a nuclear soluble factor, or if it was within the insoluble chromatin fraction. We found that Gal-1 appeared in all subcellular compartments, both cytosol and nucleus, as shown by WB (Fig. 19). Importantly, high levels of Gal-1 were detected in the chromatin bound fraction suggesting a role for this small lectin in controlling gene expression in HPSC.

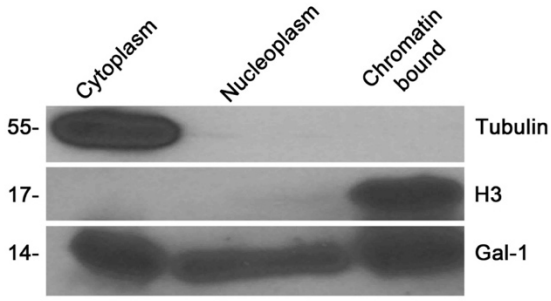

Figure 19. Gal-1 is located in the cytoplasm, in the nucleoplasm and also in the insoluble chromatin fraction in HPSC. Subnuclear fractionation was performed and Gal-1 was detected in all subcellular compartments in HPSC (cytoplasm, nucleoplasm and chromatin bound fractions). Tubulin and histone-3 (H3) were used as controls for a proper subcellular fractionation.

2.3.2 Study of chromatin binding and putative Gal-1-regulated targets in HPSC by Chromatin Immunoprecipitation and DNA sequencing

To gain further insights about the role of Gal-1 in modulating gene expression in HPSC, we decided to explore the capability of Gal-1 to interact with promoters of putative target genes. To this aim, we performed Chromatin Immunoprecipitation and DNA sequencing (ChIP-seq) in HPSC using a Gal-1 antibody. Our objective

with this experiment was to identify, if any, which genes could be regulated by nuclear Gal-1.

Due to there was not an internal positive control of a known gene transcriptionally regulated by Gal-1, before sample sequencing, we checked proper Gal-1 immunoprecipitation (Fig. 20 A). ChIP-seq quality control (FastQC Reports), reads mapping (Bowtie2), and ChIP-seq peak calling (MACS, Model-based Analysis of ChIP-Seq) were performed using Galaxy Platform as previously described (see materials & methods section 5.7.2 ChIP-sequencing and analysis). 7844 peaks were obtained and mapped against reference human genome (hg38, Dec 2013). Then, UCSC Genome Browser database was used for determining 3'UTR, 5'UTR, exon and intron peak distribution. Regarding to promoter regions, we considered as promoters those regions comprised between 1000 base pair (bp) upstream and 1000 bp downstream from transcription start site (TSS), a representation of a gene structure is shown in figure 20 B. Distribution of Gal-1 occupancy along HPSC genome was determined and percentage of found peaks in each region of the genome was represented in figure 20 C.

A set of 874 genes were listed into the promoter category and were selected for further studies as potentially targets regulated by Gal-1. First of all, these genes were analyzed by DAVID functional annotation tool to identify most represented pathways in which they were involved. According to this analysis, most of the genes were implicated in cancer pathways. Moreover, other interesting pathways came up in this analysis, such as Hippo signaling pathway, implicated in cell growth and proliferation; Rap1 signaling pathway which has a dominant role in controlling cell-cell and cell-matrix interactions; and Wnt signaling, a well-known pathway for its contribution in carcinogenesis and its role in cell fate, proliferation and migration (Fig. 20 D).

Next, in order to identify promising candidates that can be transcriptionally regulated by Gal-1 in HPSC, we compared our ChIP-seq gene list (Table S2, supplementary data) with the differentially expressed genes found in our microarray analysis after Gal-1 KD (Table S1, supplementary data and Fig. 9). Interestingly, *KRAS*, *WNK1*, *LRRFIP1* and *TOP1* genes were found in both lists. IGB (Integrated Genome Browser) was used for a better visualization of MACS peaks which allowed us to confirm *in silico* that sequenced reads were correctly mapped in the mentioned gene promoters (Fig. 20 E and F, and Fig S1. supplementary data). Moreover, using UCSC Genome Browser database, we corroborated that *KRAS* and *LRRFIP1* MACS peaks corresponded to actually promoter regions since H3K4Me1, H3K4Me3 and H3K27Ac marks, which are found near promoters and regulatory elements, were also found next to the studied MACS peaks (Fig S1. supplementary data).

To further validate the ability of Gal-1 to bind to *KRAS* and *LRRFIP1* promoters, a ChIP followed by qPCR analysis (ChIP-qPCR) was carried out. Two-fold enrichment of *KRAS* promoter reads was detected in immunoprecipitated (IP) Gal-1 sample compared to control (IgG) (Fig. 20 G), while LRRFIP1 promoter reads were enriched near 1.5 times in Gal-1 IP compared to control (Fig. 20 H). These results confirmed, in both cases, the occupancy of Gal-1 onto *KRAS* and *LRRFIP1* promoters.

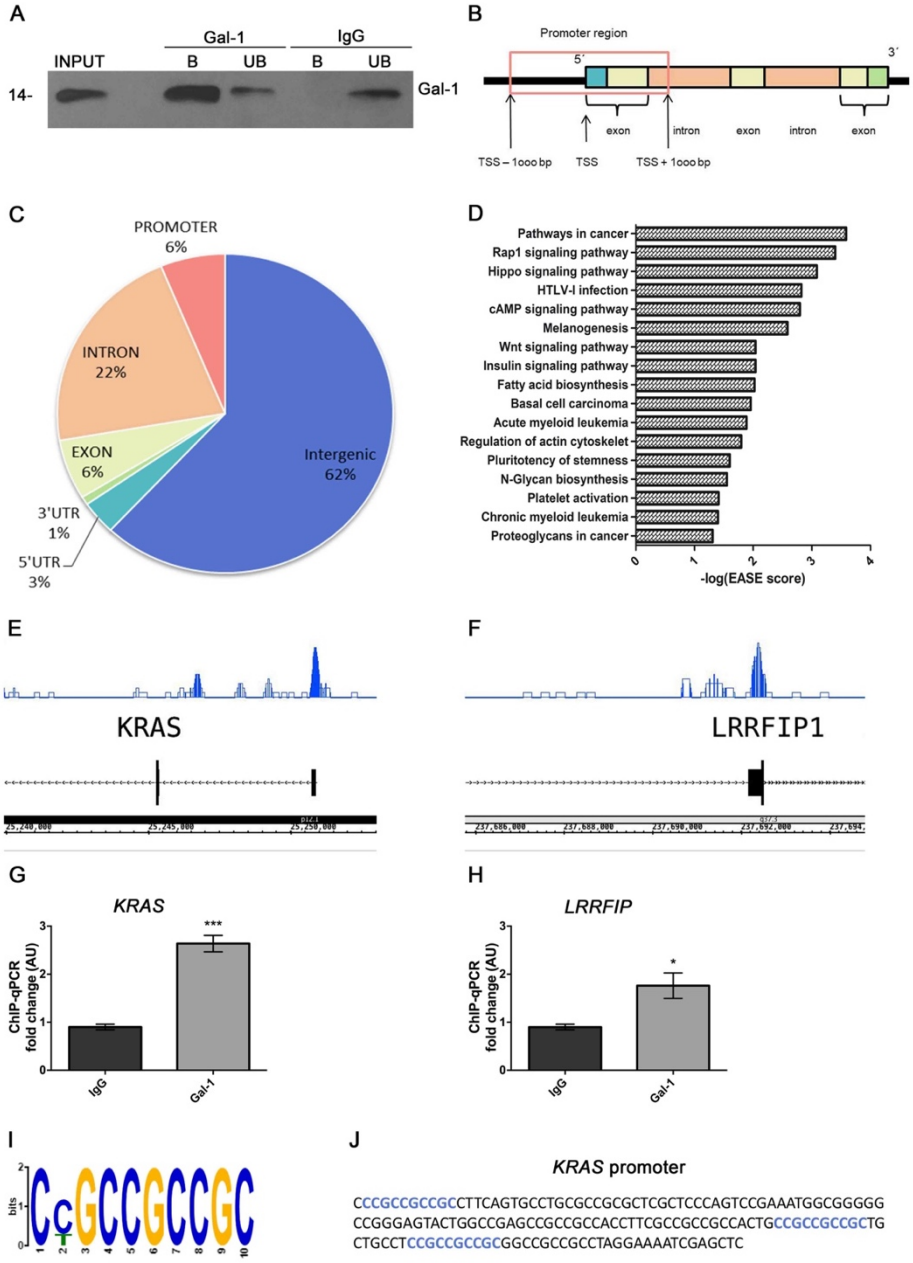

Figure 20. Gal-1 ChIP-seq analysis in HPSC. A) WB showing proper immunoprecipitation of Gal-1. B) Representation of a gene indicating its components: 5'UTR in blue, exons in yellow, introns in orange and 3'UTR in green.

Promoter region is highlighted within a red-box which comprises from 1000 bp upstream to 1000 bp downstream from transcription start site (TSS). C) Distribution of detected MACS peaks along genome (hg38, Dec 2013). D) Analysis of the most representative pathways using DAVID functional annotation tool. Only MACS peaks mapped in promoter regions were included in this analysis. E) MACS peak mapped on *KRAS* promoter region. F) MACS peak mapped on *LRRFIP1* promoter region. G) ChIP-qPCR validation for Gal-1 occupancy at *KRAS* promoter. H) ChIP-qPCR validation for Gal-1 occupancy at *LRRFIP1* promoter. I) Representative binding motif found in Gal-1 ChIP-seq analysis by using The MEME Suite tool. Similar to EGR-recognition site 5'-GCG(T/G)GGGCG-3'. J) Potential EGR1 binding motif was three times found in *KRAS* promoter sequence identified by ChIP-seq. Deviation is represented as standard error of the mean (SEM) of three independent experiments *p<0.05; **p<0.01; ***p<0.001 relative to IgG.

2.3.3 Luciferase reporter assay

It should be noticed that the results shown above only confirmed the physical presence of Gal-1 onto the studied gene promoters. But, these validations did not demonstrate the capacity of Gal-1 to truly regulate gene expression. To further corroborate that Gal-1 binds to specific gene promoters and regulates their expression, we performed a luciferase reporter assay using different cell culture systems.

Besides our microarray and ChIP-seq data, *KRAS* gene was used as a proof-of-concept due to its well-known contribution to pancreatic cancer, its prevalent implication in PDA aggressiveness, and its previously shown effects on HPSC. Hence, we started designing the *KRAS* promoter sequence that should be cloned in pGL3 luciferase reporter vector. Using UCSC Table Browser tool and MACS peak positions in human genome, we recovered all mapped peak sequences and, consequently, identified which region of *KRAS* promoter was recognized by Gal-1. Importantly, it was also described that *KRAS* promoter contains a nuclease hypersensitive polypurine-polypyrimidine element (NHPPE) which is relevant for

transcription regulation[227]. Moreover, it is known that NHPPE is a functionally essential element in *KRAS* promoter since its excision dramatically reduces promoter activity[228]. Considering this information, we decided to include NHPPE motif in conjunction with the *KRAS* promoter region recognized by Gal-1 in ChIP experiments to perform luciferase reporter analysis (Fig. 21 A).

For the first instance, HPSC infected with a scramble RNA sequence (shSC) and HPSC downregulated for Gal-1 (shGal-1_1) were used to assess luciferase reporter activity. shSC and shGal-1_1 KD HPSCs were transfected with pGL3 containing *KRAS* promoter upstream luciferase reporter (*KRAS*_pGL3) together with renilla vector as a transfection control efficacy. Signal resulting from renilla was used for data normalization. As it is shown in figure 21 B, luciferase activity was reduced near three times in shGal-1_1 KD compared with control HPSC (shSC). Indicating that the lack of Gal-1 impaired *KRAS* promoter activity, thus suggesting that Gal-1 may act as a transcription regulator of *KRAS* gene in HPSC. Low levels of Gal-1 in shGal-1_1 HPSC were again corroborated during this experiment (Fig. 21 D and F).

Considering the limitation of low efficiency of plasmid transfection in HPSC, we tested luciferase assay in HEK-293T/17 cells, a fibroblastic cell line easily transfectable, to prove our previous luciferase reporter results in a different fibroblast cell system. Moreover, as HEK-293T/17 cell line does not express Gal-1, it was a good model to analyze the effects of Gal-1 in modulating KRas expression by using an opposite strategy to that of HPSC, that is overexpressing the lectin in HEK-293 instead of performing the Gal-1 knockdown. Indeed, HEK-293T/17 system supposed a suitable method to study whether the complete absence of Gal-1 could diminish even more *KRAS* promoter activity. To do so, HEK-293T/17 cells were transfected with pcDNA_∅ (control) or pcDNA_Gal-1, and

Gal-1 overexpression was corroborated by WB (Fig 21. E and G). 48h after, *KRAS*_pGL3 reporter and renilla vectors were introduced in HEK-293T/17 transfected cells and luciferase activity was assessed after 48h. Unfortunately, no differences were detected between control and Gal-1 overexpressed HEK-293T/17 cells (Fig. 21 C). We speculated that these negative results could be explained because HEK-293 cells have no endogenous Gal-1, so they do not need the presence of this protein for regulating *KRAS* gene expression, and probably HEK-293T/17 cells hold other factors which are in charge of these regulation.

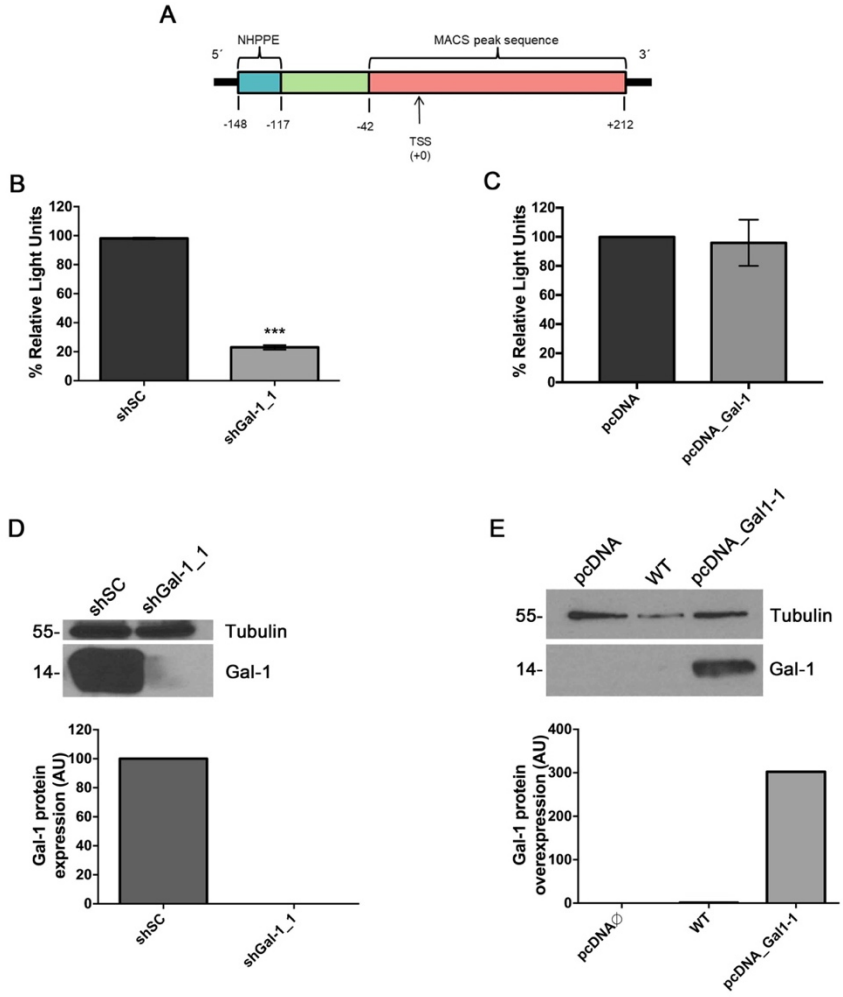

Figure 21. KRas promoter activity was severely diminished after Gal-1 knockdown in HPSC, but no effect was observed in Gal-1 overexpressing HEK-293 cells. A) Representation of *KRAS* promoter used for luciferase reporter assays. Nuclease hypersensitive polypurine-polypyrimidine element (NHPPE) is marked in blue while red box corresponds to the *KRAS* promoter sequence recognized by Gal-1 in ChIP-seq. B) On the top, luciferase assay reporter using shSC and shGal-1_1 HPSC transfected with *KRAS*_pGL3 luciferase reporter and renilla vectors. Luminescence was measured 48h after transfection and renilla was used for signal normalization. At the middle, WB showing low levels of Gal-1 in HPSC shGal-1_1 in comparison to control (shSC). At the bottom, quantification of Gal-1 protein levels in HPSC. C) On top, luciferase assay reporter using HEK-293T/17 transfected with pcDNA_∅ (control) or pcDNA_Gal-1 (Gal-1 overexpression). 48h after pcDNA

transfection, HEK-293T/17 were transfected with KRAS_pGL3 and renilla vectors. After 48h, luminescence was measured and renilla was used for signal normalization. At the middle, WB showing overexpression of Gal-1 in HEK-293T/17 pcDNA_Gal-1_1 transfected cells. At the bottom, quantification of Gal-1 protein levels in WT HEK-293T/17 and HEK-293 pcDNA_∅ or pcDNA_Gal-1 transfected cells. Deviation is given as standard error of the mean (SEM) of three independent experiments *p<0.05; **p<0.01; ***p<0.001 relative to control (shSC or pcDNA_∅).

Altogether, our luciferase reporter data indicate that nuclear Gal-1 seems to directly regulate gene transcription in HPSC, at least for *KRAS* gene.

2.3.4 Galectin-1 as a co-transcription factor

Gal-1 is a small lectin protein that lacks of DNA binding motifs. Therefore, considering its role in gene expression regulation, we supposed that Gal-1 should be acting as a co-transcription factor forming part of a protein complex by recognizing DNA sequences.

Hence, we took an advantage on our ChIP-seq data to search *in silico* potential transcription factors which would interact with Gal-1 to regulate transcription. To do so, sequences of MACS peaks mapped as promoters were analyzed by The MEME Suite tool[229] (http://meme-suite.org/) to find the most representative shared motifs among the identified set of promoters and to identify putative transcription factors that recognize these motifs. One of the most enriched motifs found along ChIP-seq promoter sequences was 5´-GCGGCGGCGG-3' (Fig. 20 I) which could be potentially recognized by early growth response protein 1 (EGR1). Interestingly, this sequence was found three times into *KRAS* promoter (Fig. 20 J) and searching for already published EGR1 ChIP-seq (UCSC Encode

database), a peak was found at *KRAS* promoter (Fig 1S. supplementary data). Meaning that EGR1 is actually able to bind to *KRAS* promoter. Indeed, high nuclear expression of EGR1 was detected in pancreatic stellate cells in human pancreatic cancer tissues (Fig 22. B-D), while only basal levels of EGR1, if so, were detected in healthy pancreas (Fig 22. A). These results, suggested that EGR1 could be a transcription factor for *KRAS* gene at stroma compartment in PDAC.

These findings suggested that Gal-1 and EGR1 could be part of the same transcription complex. For this reason, next step was to corroborate nuclear expression of EGR1 in conjunction with Gal-1 in HPSC. First, we analyzed EGR1 expression in HPSC and we found that both Gal-1 and EGR1 were expressed in HPSC nuclei (Fig. 22 E), suggesting that both proteins might form a complex for regulating gene transcription. To investigate whether Gal-1 and EGR1 are in the same protein complex at the nucleus, immunoprecipitations of both proteins were performed using nuclear HPSC lysates. However, no Gal-1 was detected in EGR1 bounded fraction, neither EGR1 in Gal-1 bounded fraction (Fig. 24). In spite of this observation did not support that Gal-1 interacts with EGR1 to regulate gene expression, further experiments with different experimental conditions and positive controls should be performed before discarding that EGR1 binds to Gal-1 to regulate *KRAS* gene expression.

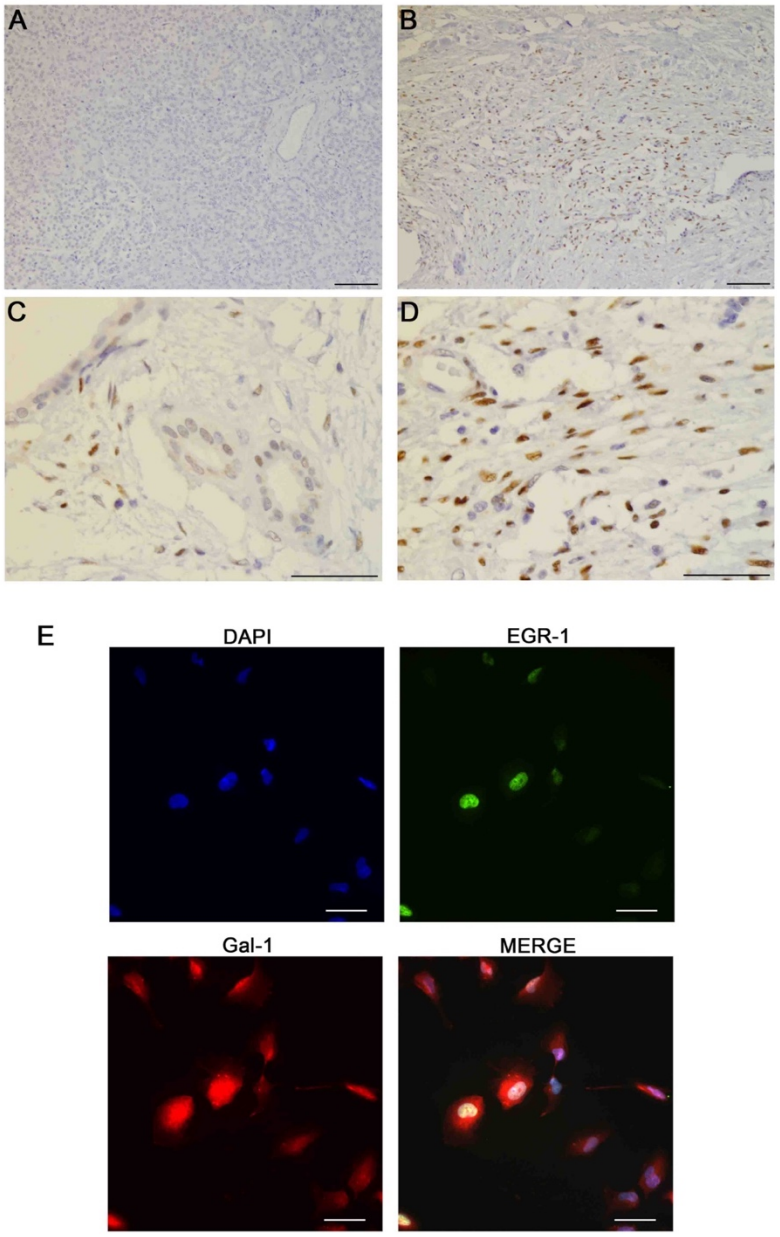

Figure 22. EGR1 is expressed in PDAC stroma and it is strongly detected in pancreatic stellate cell nuclei. A) IHC of EGR1 in a human healthy pancreas. B-D) IHC of EGR1 in human PDAC tissues, more detailed EGR1 expression in PDAC ducts (C) or in PDAC stroma (D). Scale bar corresponds to 100 μm (A and B) and 50 μm

(C and D). E) IF staining of EGR1 (green) and Gal-1 (red) in HPSC. DAPI (blue) staining was used to label nuclei. Scale bar corresponds to 50μm.

To further identify which proteins may be interacting with Gal-1 in the nucleus of HPSC we performed a more exhaustive strategy by immunoprecipitation of HPSC nuclear Gal-1 followed by mass spectrometry (MS) analysis. Two independent IP were performed and proper IP of Gal-1 was assessed by WB (Fig. 23 A). Before MS analysis, immunoprecipitated proteins were digested with Trypsin and LysC enzymes generating known peptide cleavages. Consequently, each peptide composition was identified according to its weight and protein sample content was determined in consonance with previous detected peptides. Irrelevant rabbit antibody (IgG) was used as a negative control and proteins immunoprecipitated with this antibody were also identified and considered as background. Our two mentioned independent experiments resulted in a list of 43 proteins that were identified as putative nuclear Gal-1 interactors in HPSC (Table S3, supplementary data).

Functional annotation analysis was performed using DAVID Database tool, identifying important biological processes related to gene expression regulation (Fig. 23 B) such as chromatin modification by acetylation or methylation, as well as RNA binding and splicing, a function previously reported for Gal-1 in other cell types[108,103]. Interestingly, gene ontology analysis (Fig. 23 C) identified transcription/DNA-templated among the most relevant groups, supporting that nuclear Gal-1 could bind to transcription factors to modulate gene expression.

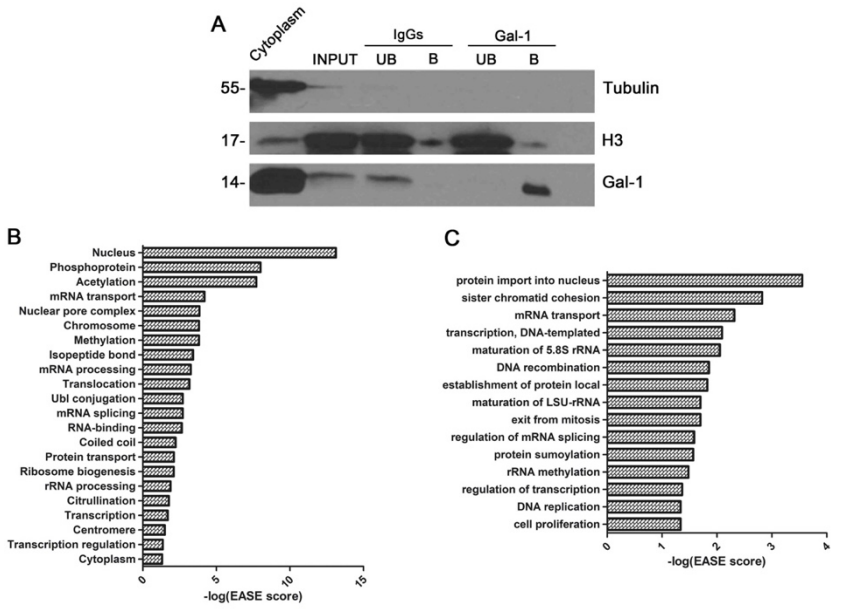

Figure 23. Nuclear Galectin-1 immunoprecipitation and mass spectrometry protein identification. A) WB corroborating proper galectin-1 IP. B and C) Functional annotation analysis using DAVID Database tool. Most represented biological processes are shown; functional characterization (B) and gene ontology (C).

Remarkably, the transcription factor PARP14 was found in the MS list of Gal-1 bound proteins, emerging as a possible nuclear partner through which Gal-1 could exert its ability to modulate gene expression. In order to confirm Gal-1 and PARP14 nuclear binding, nuclear Gal-1 IP was performed followed by WB for PARP14 detection (Fig 24). c-MYC was used as positive control of Gal-1 co-IP since it was found interacting with Gal-1 in published a proteomic study[230,231].

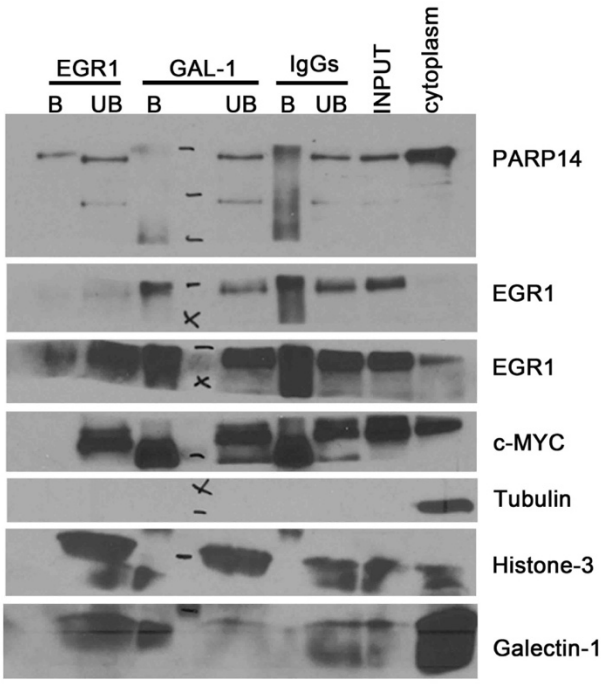

Figure 24. Gal-1 and EGR1 co-immunoprecipitations from nuclear HPSC extracts. WB showing co- immunoprecipitated after nuclear IP of Gal-1 and EGR1 in HPSC. IgGs were used as negative control of non-specific bound proteins. Input corresponds to a sample from HPSC nuclear extract used for performing IP. Histone-3 and tubulin were used as a nuclear and cytoplasm protein controls respectively. UB (unbound), B (bound).

We could not detect any interaction between Gal-1 and PARP14, neither Gal-1 and c-MYC. Therefore, we need further experiments to optimize the experimental conditions to better describe the protein complex through which Gal-1 could be acting as a co-transcription factor to modulate gene expression in HPSC.

DISCUSSION

Pancreatic ductal adenocarcinoma (PDA) is one of the deathliest cancer types, nowadays it represents the fourth leading cause of cancer related deaths, but it is previewed to become the second one by 2030[11]. Despite its low incidence, high mortality index of PDA could be explained because of its symptoms usually do not come up until an advanced stage of the disease, leading to a late diagnosis in which patients frequently already present unresectable metastatic tumors[9,232]. To make matters worse, after decades of large efforts in developing new PDA therapies, current approved-FDA anti-tumoral treatments still resulted inefficient, and a substantial improvement in patient survival has not been reached yet[79]. One of the factors that confers such a resistant phenotype to PDA is its abundant desmoplastic reaction. Given that desmoplastic predominant presence on tumoral tissues, stromal compartment exerts a crucial role in PDA development and maintenance. PSCs, the main component of the PDA stroma, are in constant activation promoting a strong fibrotic deposition acting as a physical barrier and favoring hypovascularization within the tumor, so hampering proper anti-tumoral drug delivery[42,49] (reviewed in section *1.3 The relevance of stroma compartment in PDA*). Cellular and acellular components of the stroma interact with pancreatic stellate cells promoting tumor development, progression and metastasis. Considering the importance of tumor-stroma crosstalk for PDA aggressiveness, new treatments based on tilting stroma signaling favoring an anti-tumoral activity in combination with other drugs could be a promising manner to beat this fatal disease. In this context, it has been proposed that therapy combination by incorporating immune-checkpoint inhibitors has been proposed for patients with an advanced-stage of PDA[37,233].

Interestingly, one of the factors found overexpressed in stromal compartment in PDA is Gal-1, a small lectin defined with a several pleiotropic functions in physiological and pathological

conditions. In this malignancy, PSCs are the main responsible for extracellular Gal-1 secretion. Due to its pleiotropic functions Gal-1 is able to interact with different cellular populations such as tumoral, stellate, immune and endothelial cells, as well as ECM proteins favoring tumor progression and metastasis. Effects of Gal-1 on immune cells have been deeply described, determining Gal-1 as a factor that favors immunosuppressive TME by promoting T cells apoptosis and enhancing Th2 and Treg population as well as affecting other immune cell types such as M2 macrophages and tolerogenic dendritic cells (reviewed in section *1.5.1.3 Modulation of immune system by Gal-1*). Gal-1 has been also described as an angiogenic factor, promoting endothelial cells proliferation and vessel tube formation. Our laboratory, previously described the paracrine effect of Gal-1 in pancreatic cancer cells inducing their proliferation, migration and invasion activities[209]. Moreover, Gal-1 depletion in a *KRAS* driven pancreatic cancer mouse model exhibited an increased survival in comparison with controls that express high stromal Gal-1. Tumors lacking of Gal-1 presented reduced activated stromal compartment and increased immune cell infiltration. In a human setting, orthotopic pancreatic tumors obtained from co-injection of human pancreatic tumoral cells (BxPC-3) and HPSC presented bigger tumor burden compared with orthotopic tumors obtained from injecting only BxPC-3 or co-injecting BxPC-3 with shGal-1 HPSC[209]. These evidences demonstrated stromal Gal-1 as a key factor for PDA progression and aggressiveness; however, little is known about the autocrine and endogenous effect of Gal-1 in activated HPSC. For this reason, we decided to focus our attention on deciphering the role of Gal-1 in HPSC.

3.1 Characterization of the role of Gal-1 effects in HPSC

3.1.1 Expression and localization of Gal-1 in PDA

Firstly, in this work we showed that Gal-1 is strongly expressed in the stromal compartment of human and mouse pancreatic cancer tissues, while only basal levels are found in healthy pancreatic tissues. This observation was in accordance to the previously reported data by Berberat and colleagues who described for the first time the overexpression of Gal-1 in PDA surrounding stroma but not in cancer cells, while Gal-1 levels in normal pancreatic tissues remained negligible. Moreover, in this work, Gal-1 levels were found significantly increased in dedifferentiated PDAs[141]. As described in section *1.5 Galectins in cancer*, overexpression of Gal-1 has been found in cancer cells but also it has been detected (or even limited) to tumor stroma[139,138,142,234], in different cancer cell types (reviewed by Demydenko and Berest[151]). The observed usual expression of Gal-1 in stromal compartment in different cancer malignances suggests a key role of this lectin in remodeling TME towards tumor-friendly niche[127]. In PDA, pancreatic stellate cells (PSCs) have been defined as the main source of Gal-1[196,197], according to these observations, we confirmed Gal-1 overexpression in HPSC, our cell line of work. Interestingly, in addition to cytosolic localization, Gal-1 was also strongly expressed in the nucleus in tumor samples from PDA patients and mouse models as well as in HPSC, suggesting a possible role for Gal-1 in this location.

3.1.2 Effects of Gal-1 knockdown in HPSC activation, proliferation, migration and invasion

Activated PSC (CAFs) secrete several factors that affect cancer and stromal cells, favoring the generation of a proper pro-tumoral niche[235]. Moreover, some of PSC-secreted factors also have an autocrine effect, such as Gal-1 which is overexpressed in aPSC maintaining their own activation through ERK signal transduction pathway and inducing collagen synthesis in a glycan-dependent manner[196]. To better understand the role of Gal-1 in HPSC, this small lectin was downregulated, and different studies were performed to characterize HPSC lacking of Gal-1. Two different strategies were used for knocking down Gal-1 in HPSC, small interference RNA sequences (siRNA) against *LGALS1* allowing transient Gal-1 downregulation or short hairpin RNA shRNA against *LGALS1* to obtain stable Gal-1 KD in HPSC. Interestingly, we have seen that Gal-1 downregulation impaired HPSC activation detected by a reduced expression of different fibroblastic activation markers, such as α-SMA, FAP, GFAP, and COL1A1 promoting a less spindled shape morphology of these cells. Moreover, it was also observed that Gal-1 KD in HPSC reduced their migratory and invasive capacities. Interestingly, recent studies have demonstrated the ability of fibroblasts to migrate and invade in conjunction with cancer cells[75]. Moreover, Xu and colleagues have been shown that PSC have the ability to promote intra- as well as extravasation from blood vessels accompanying pancreatic cancer cells to metastatic sites[76]. Therefore, it is tempting to speculate that Gal-1 could favor pancreatic cancer metastasis by enhancing stellate cells migratory and invasive abilities. Remarkably, in our in vivo studies using K-Ras^{G12V} mouse model and Gal-1 KO mice[209] we have observed a decrease in tumor metastasis after Gal-1 abolishment. Considering that we were using a constitutive KO animal and therefore Gal-1 was depleted in all cellular compartments, reduction of metastasis might

be explained by decreasing the migration and invasion capacities of pancreatic stellate Gal-1 KO cells, hampering their role as "accompanying cells" in these KRas tumors.

3.1.3 Effects of Gal-1 KD in HPSC ECM organization

Cancer associated fibroblasts (CAFs) are able to alter the architecture and physical properties of ECM affecting cell proliferation, migration and invasion[236,237]. Erdogan and colleagues have reported that CAFs generate an aligned fibronectin fibers matrix mediating CAF-cancer cell association and directional migration of prostate cancer cells[214]. This group compared cell derived matrices from normal fibroblasts and CAFs, and showed that former generated a messy matrix in which cancer cells exhibited a random migratory activity, while CAFs were able to generate an anisotropic organization of ECM with aligned fibers that induces a directional migration of cancer cells. This phenotype was moreover confirmed in the invasive regions of human PDA tissue samples[214]. Considering these data, we decided to explore whether Gal-1 hold the ability to modulate ECM organization by HPSC. We have seen that reduction of Gal-1 impaired ECM organization, observed by FN deposition, and HPSC compared to controls. This data indicated that Gal-1 also exerts an effect on the organization of the ECM generated by HPSC, suggesting that this protein also could contribute to ECM-mediated cancer cell migration and invasion. Other studies have demonstrated the contribution of TGF-β, a well-known molecule promoting fibroblast activation[42,214], in this process[238]. Hence, we analyzed the participation of TGF-β in HPSC-generated EMC alignment. Intriguingly, TGF-β only affects ECM alignment in shGal-1_2 KD, rescuing the control phenotype, while shGal-1_1 HPSC

maintained a disorganized matrix. Considering that shGal-1_1 KD presented a bigger reduction in Gal-1 expression compared with shGal-1_2 HPSC, we suggested that TGFβ is able to modify HPSC ECM in a Gal-1 dose dependent manner. Indeed, control HPSC did not present any further effect on ECM alignment upon TGF-β treatment, indicating these cells are already highly activated *in vitro*. We found the observed results in consonance with the ability of Gal-1 to affect HPSC activation, migration and invasion, reinforcing our conviction that Gal-1 favors PDA progression not only affecting pancreatic epithelial tumor cells but also influencing on HPSC pro-tumorigenic activities.

3.2 Deciphering the molecular mechanisms for Gal-1-mediated HPSC functions and activation

Given the relevance of Gal-1 on HPSC activation and functions and considering it is also able to modulate ECM alignment, we decided to determine the mechanisms by which Gal-1 exerts the observed phenotype in HPSC. A microarray analysis was performed comparing differentially-expressed genes between two si-irr and two siGal-1 samples. The analysis of our microarray data displayed 86 dysregulated genes after Gal-1 KD in HPSC. It should be noticed that the two replicates used for siGal-1 were very different, suggesting that Gal-1 downregulation in one of the experiments (siGal-1_1, see Results, Fig. 9A) did not work properly, as the expression pattern was quite similar to si-irr cells. Therefore, as our analyses have been performed using both replicates for statistical reasons, it is plausible that our list of differentially expressed genes is underestimating the effects of Gal-1 KD in HPSC. After microarray

data validation, we focus our attention in *KRAS*, *WNT5A* and *TACC1* genes because of their biological role in cancer and we decided to determine how important could be the expression of these genes for Gal-1-mediated HPSC activation, migration and invasion. Thus, same methodology used for the characterization of Gal-1 KD in HPSC was also followed to describe KRas, Wnt-5α or TACC1 KD in these cells.

We have determined that diminished levels of KRas hampered HPSC cell activation state exhibiting a reduced α-SMA levels and a less spindled cell morphology, two characteristic features of aPCS (reviewed in section *1.3.4 Pancreatic Stellate Cells (PSC)*). However, no differences were observed for the expression of other fibroblastic activating markers such as *FAP* and *GFAP*. KRas downregulation resulted in a significant impaired HPSC proliferation and decreased migration and invasion capabilities, although these two later effects were only observed in shKRas_2 KD. These data indicate that Gal-1 may exerts part of its effects on HPSC via KRas pathway, at least for HPSC activation. The phenotype observed in shKRas_2 migration and invasion suggest that KRas could also be implicated in the induction of these functions by Gal-1 in HPSC, although, additional shRNA against *KRAS* should be tested to confirm these results. Regarding cell proliferation, we have found that HPSC knockdown in HPSC reduces cell growth while Gal-1 KD did not show any deficiency on HPSC proliferation. These results can be explained because the reduction of KRas expression in HPSC was bigger after targeting KRas (shKRas cells) than in HPSC downregulated for Gal-1 (shGal-1 cells), in which KRas reduced levels were a consequence of Gal-1 expression deficiency. Indeed, this data was not surprising considering the well-known mitogenic effects of Raf/MEK/ERK signaling in which KRas is implicated[239].

Regarding to TACC1, we have found that its corresponding KDs did not impaired migration neither invasion in HPSC compared with controls. In contrast, TACC1 effects on HPSC activation and proliferation were difficult to establish. TACC1 KD in HPSC showed reduced levels of α-SMA compared to WT HPSC, however same phenotype was observed in our negative control using HPSC infected with an irrelevant shRNA sequence (shSC), which exhibited similar or even better reduced levels of α-SMA compared with TACC1 KDs. Likewise, shSC as well as TACC1 KDs reduced HPSC proliferation comparing with WT HPSC. Unfortunately, these data did not allow us to make any conclusion about the effects of TACC1 on HPSC activation nor proliferation. Similar phenotype was observed when Wnt-5α KDs were compared to corresponding controls to assess HPSC activation. Wnt-5α KDs showed decreased α-SMA levels compared to untransfected cells, but similar to shSC cells. The similar phenotype observed in Wnt-5α KD, TACC1 KD and shSC HPSC activation studies can be explained in two ways: 1) shSC sequence can affect somehow HPSC activation through an off-target effect. 2) infection procedure and the following infected-HPSC selection can influence on HPSC activation state. In any case, with the observed data, we could not conclude any effect of Wnt-5α nor TACC1 in HPSC activation. Deciphering Wnt-5α effects on HPSC proliferation, migration and invasion were even more challenging, as different effects were detected comparing shWnt-5α_1 and shWnt-5α_2 in the studied HPSC functions. While non-significant differences were detected in shWnt-5α_1 comparing to controls, an increased migration, invasion and proliferation were observed in shWnt-5α_2, reaching the significance in invasion and proliferation assays and exhibiting the opposite expected behavior. Giving these results, we suggest that shWnt-5α_2 could have off-targets affecting other gene (or genes) expression besides Wnt-5α, and thus showing an unexpected and different phenotype in comparison with shWnt-5α_1. In this context, other different shRNA against *WNT5A*

should be tested to better describe the effect of this gene in HPSC migration, invasion and proliferation.

3.3 Nuclear functions of Gal-1 in HPSC

Our microarray data revealed several genes whose expression become altered after Gal-1 downregulation in HPSC. Remarkably, from the total list of altered genes, (>90%) were downregulated when Gal-1 expression was reduced, suggesting a relevant role of this protein in activation of gene expression. Intriguingly, DAVID tool analysis of this gene list displayed regulation of transcription among the most relevant functional groups (Fig. 9B). Moreover, Ingenuity pathway analysis (IPA) showed 26 genes related to gene transcription (Fig. 26). Between them, we found transcriptional factors, which directly affect gene transcription, such as *LRRFIP1* (codifying gene for Leucine-rich repeat flightless-interacting protein 1), *ARTX* (transcriptional regulator ARTX) and *BCLAF1* (Bcl-2-associated transcription factor 1), as well as genes indirectly implicated in gene expression regulation like *KRAS* (v-Ki-ras2 Kirsten rat sarcoma viral oncogene homolog or GTPase KRas)[240] and *ACTR2* (Actin-related protein 2)[241]. These results, together with the strong expression of Gal-1 in PSCs nuclei, suggested that nuclear Gal-1 could have a role in regulating gene transcription in HPSC.

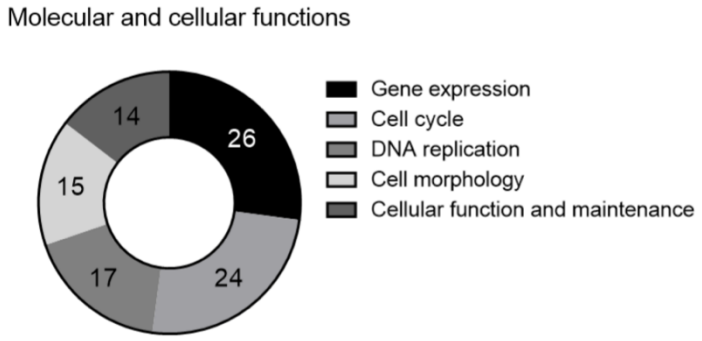

Figure 26. Molecular and cellular functions drived by Gal-1 in HPSC. Most represented molecular and cellular functions after functional annotation of microarray data analysis by Ingenuity software. *Extracted from Carlos Alberto Orozco Castaño thesis manuscript*[211].

However, activation of transcriptional pathways and changes in gene expression can also be consequence of other events taking place in cell membrane or cytoplasm, where Gal-1 is located, making necessary to deeply determine the contribution of nuclear Gal-1 in transcription regulation processes. Gal-1 is able to activate MAPK/ERK pathway, one of the most well-known signaling pathways mediating extracellular signals and transcriptional responses, in a glycan-dependent manner in PSC[196,197]. Moreover, Gal-1 is able to stabilize HRas in the inner part of the cell membrane promoting Erk activation[171]. Therefore, prior to focus in nuclear Gal-1 role in gene expression regulation, we have analyzed the possible contribution of non-nuclear Gal-1 in this event using several approaches. To discard effects of secreted/cytosolic Gal-1 in regulating gene expression, we blocked MAPK/ERK pathway by treating HPSC with U0126, a potent inhibitor of MAPK/ERK signaling that antagonizes AP-1 transcriptional activity[242]. Levels of *KRAS* mRNA, used as a proof of concept target due to its downregulation after Gal-1 KD in our array study, were not affected upon U0126

treatment, indicating that secreted Gal-1 does not exert transcriptionally any effect on *KRAS* expression in HPSC, at least through MAPK/ERK signaling. To further confirm that extracellular Gal-1 does not affect *KRAS* transcription, we blocked extracellular Gal-1-mediated glycan-binding signaling by treating HPSC with lactose. Again, *KRAS* mRNA levels were maintained unaffected after HPSC lactose treatment, confirming that *KRAS* transcription does not depend on secreted Gal-1. It should be noticed that lactose treatment will not only block extracellular Gal-1-glycan bindings, but also other extracellular galectins-glycan interactions, indicating that extracellular galectins are not implicated on transcriptional control of *KRAS* mRNA levels. These results, further suggested that Gal-1 could act as a transcription regulator in HPSC.

3.3.1 Chromatin binding, immunoprecipitation and sequencing and nuclear Gal-1-regulated gene targets in HPSC

Several reports have shown that nuclear galectins can regulate gene expression by several ways. Gal-3 is the most studied member of galectin family regarding its nuclear location and regulation of gene expression. In proliferating fibroblasts, Gal-3 is accumulated in the nucleus[243] and is involved in the splicing and transport of mRNA thought its direct interaction with Gemin4[130,131]. Moreover, it has been described that Gal-3 can also regulate cancer-related gene expression by regulation of transcription. For example, in breast epithelial cancer cells Gal-3 induces cyclin D1 promoter activity by the enhancement and stabilization of nuclear protein-DNA complex formation at the SP1 and cAMP-responsive element (CRE) site of its promoter region[136]. Similarly, in papillary thyroid

cancer cells, nuclear Gal-3 directly interacts with the thyroid-specific TTF-1 transcription factor upregulating its transcriptional activity[135]. Moreover, in human colon cancer cells, Gal-3 can regulate MUC2 mucin expression at the transcriptional level via AP-1 activation through a complex with c-Jun and Fra-1[244]. Thus, Gal-3 can regulate gene expression in several cancer cells acting as an enhancer and modulator of several transcription factors. In the case of nuclear Gal-1, the only mechanism reported for gene expression control is in HeLa cells through interaction with Gemin4 in SMN complexes which are involved in the splicing pathway[103,108]. However, a direct role in DNA transcription by interacting with transcription factors bound to specific gene promoters have not been studied. The observation of Gal-1 in different subnuclear compartments gave us new clues about the possible nuclear functions of this protein in HPSC. Interestingly, Gal-1 was detected in the insoluble chromatin-bound fraction, indicating that our lectin is probably interacting with chromatin in HPSC.

Performing ChIP-seq was the following step to actually confirm that Gal-1 is able to bind DNA sequences. Most of the found peaks were located into intergenic regions and only 6% of them were identified as promoter regions, suggesting Gal-1 is not widely present along genome of HPSC, and that probably only few and specific genes could be directly regulated by Gal-1 in HPSC. Of note, promoter was defined in our ChIP-seq analysis as the region comprised between 1000 bp upstream and 1000 bp downstream of TSS, meaning that those promoters or enhancers located far away from TSS are not considered in this analysis, so consequently, promoter peaks could be underestimated in our data. Functional Annotation tool of DAVID of the found promoter genes highlighted cancer pathways as the most representative pathways regulated by Gal-1 in HPSC. Moreover, pathways implicated in cell growth, cell adhesion and cell fate and migration, such as Hippo, Rap1 and Wnt

signaling, also appeared in this analysis which could explained the observed effect of Gal-1 on HPSC activation and functions presented in this manuscript. Interestingly, we found that Gal-1 recognizes the promoter of *KRAS, LRRFIP1*, *WNK1* and *TOP1* genes, which were also detected in our microarray data. Considering that we validated *KRAS* and *LRRFIP1* gene downregulation after Gal-1 KD (Figs. 10 and 27), we decided to go further with the analysis of these genes as putative targets for Gal-1 transcriptional regulation. LRRFIP1, commonly defined as a transcriptional repressor that also has cytoplasmic functions, is able to promote cancer invasion an metastasis activating both canonical and non-canonical Wnt signaling pathways[245,246]. Ubication of corresponding peaks near to promoter and regulatory elements were confirmed by IGB software visualization and histone methylation and acetylation marks. The occupancy of Gal-1 in *KRAS* and *LRRFIP1* promoters were validated by ChIP-qPCR, confirming the ability of Gal-1 in recognizing the mentioned DNA regions. Of note, these data only demonstrate the capacity of Gal-1 to physically interact with *KRAS* and *LRRFIP1* promoters. To further demonstrate that Gal-1 is able to control gene expression through its (Gal-1) binding to DNA o¡promoter sequences we focus our attention in *KRAS* promoter activation and performed luciferase reporter assays. *KRAS* gene was chosen for this analysis because the effects of its KD in HPSC and given that nuclear Gal-1 is able to modulate *KRAS* mRNA levels and to bind to its (*KRAS*) promoter in our ChIP experiments. We have found that Gal-1 is required for *KRAS* expression in HPSC, as HPSC downregulated for Gal-1 exhibited a significant reduction on luciferase reporter compared with its control (shSC). However, we have not seen any change in *KRAS* promoter activity in luciferase reporter assays using the other way around strategy, by overexpressing Gal-1 in a fibroblastic cell line that do not express this protein, HEK-293 cells. These later results can be explained because maybe HEK-293 do not need Gal-1 for gene transcription regulation and that perhaps other

factors (probably other galectins) participate in this function, at least in the case of *KRAS* expression.

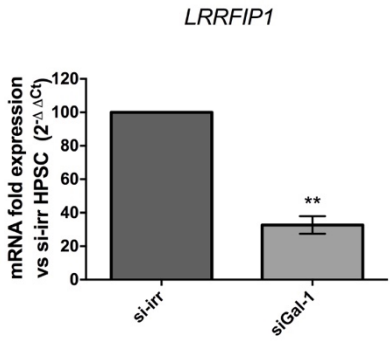

Figure 27. Validation of *LRRFIP1* differentially expressed gene upon Gal-1 downregulation. RTqPCR showing that mRNA levels of *LRRFIP1* was reduced upon Gal-1 knockdown in HPSC. Deviation is represented by standard error of the mean (SEM) of three independent experiments. *p<0.05; **p<0.01; ***p<0.001 relative to si-irr. *Extracted from Carlos Alberto Orozco Castaño thesis manuscript.*

Our data from ChIP analysis and luciferase analysis indicate a transcriptional role for nuclear Gal-1 in HPSC. However, since Gal-1 lacks of DNA binding motifs, this function requires its binding to other proteins to act as a co-transcription factor regulating gene transcription through its binding to other proteins. ChIP-seq experiment not only gave us the chance to determine which genes could be regulated by Gal-1, but also which are the DNA sequences that Gal-1 is actually recognizing in along HPSC genome, and consequently we could identify those transcription factors that recognize found DNA binding motifs. One of the most enriched promoter sequences recognized by Gal-1 was 5'-GCGGCGGCGG-3' which resembles to the EGR site DNA binding sequence 5'-GCG(T/G)GGGCG-3'. Interestingly, this EGR-like DNA binding motif is present in *KRAS* promoter sequence three times and moreover,

public ChIP-seq data in UCSC database revealed EGR1 occupancy on *KRAS* promoter in different cell lines (GM12878, H1-hESC and K562) indicating that EGR1 could act as a transcription factor regulating *KRAS* gene expression. Although EGR1 has been mainly defined as a tumor suppressor[247], EGR1-mediated pro-tumoral functions have been described for this transcriptional regulator in prostate cancer[248]. Interestingly, EGR1 has been linked to promoting myofibroblast phenotype in pulmonary fibrosis[249] and it was found overexpressed in PanINs and PDA tisssues[250]. Indeed, it has been reported that silencing Gal-3 overexpression in melanoma cells resulted in an enhanced binding of EGR1 at VE-cadhering and IL-8 promoters, decreasing its transcription, and consequently, reducing vascular tube formation. Linking Gal-3 and EGR1 in gene transcription regulation[251]. We found that EGR1 expression pattern was similar to the one observed for Gal-1 in healthy and pancreatic cancer tissues, that is insignificant levels of this transcription factor were detected in healthy human pancreatic tissue, while strong expression of this protein was found in stromal compartment. Moreover, double immunofluorescence of EGR1 and Gal-1 allowed us to observe that both proteins are localized in the nucleus of HPSC. Unlike Gal-1, EGR1 expression was limited to the nucleus of stromal fibroblasts and a mild detection of this protein was also seen in ductal cells, both in the cytoplasm and nucleus. Considering all observed data, we hypothesized that Gal-1 and EGR1 could form part of the same protein complex and that together, probably in conjunction with other proteins, transcriptionally regulate *KRAS* expression in HPSC. To better confirm this hypothesis, we performed both Gal-1 and EGR1 co-IPs using nuclear HPSC protein extracts. Unfortunately, we could not find an interaction between EGR1 and Gal-1, however interaction with c-Myc, used as a positive control for Gal-1 co-IP, was neither observed indicating that Gal-1 and EGR1 interaction cannot be ruled out. Further experiments in our lab using different IP conditions or alternative experimental

approaches will be necessary to investigate the possible interaction between Gal-1 and EGR1 in HPSC.

We have also analyzed putative nuclear Gal-1 interactions by detecting proteins bound to this lectin in HPSC nuclear extracts using co-immunoprecipitation and MS analysis. From two independent IPs, 44 proteins were identified by co-IP/MS proteomics after applying exclusion criteria for specific positive interactions. Interestingly, PARP14, a member of the poly ADP-ribose polymerases (PARP) family which participates in transcriptional gene regulation[252], was found in co-IP Gal-1 samples. Unfortunately, we were not able to validate this target using Gal-1 co-IP experiments followed by WB to detect PARP14. However, similarly to that previously mentioned in EGR1 data, the positive control c-Myc was neither detected bound to Gal-1, indicating that the experimental conditions for nuclear Gal-1 protein-protein complexes require further set up. Interestingly, functional annotation analysis of the list of nuclear Gal-1 associated-proteins identified by MS in HPSC showed up DNA acetylation and methylation as some of the most represented biological functions of nuclear Gal-1 in HPSC, and gene ontology (GO) analysis also determined transcription/DNA template as a significant detected molecular function, reinforcing our conviction about the lectin ability to modulate gene expression at DNA transcriptional level. Moreover, GO analysis also displayed regulation of mRNA splicing as one of the major functions (10^{th} top position), indicating that nuclear Gal-1 may also play a role in HPSC pre-mRNA splicing, as previously reported in HeLa cells. More investigations will be required to determine whether nuclear Gal-1 may also regulate gene expression in HPSC by modulating RNA splicing.

To sum up, our work demonstrated that Gal-1, which is highly expressed in PSC, modulates HPSC activation, migration and invasion as well as HPSC ability to generate aligned extracellular matrices. We observed that, at least, part of these effects mediated by Gal-1 could take place though KRas pathway, specially HPSC activation. Regarding to the nuclear functions of Gal-1 in HPSC, we showed, for the first time, that this protein is able to bind to different DNA promoter genes and, in the case of *KRAS*, transcriptionally regulate its expression by stimulating its promoter activity which describes a new function for Gal-1 as a co-transcriptional factor in HPSC. Further approaches should be performed to better decipher the mechanism and protein complexes by which nuclear Gal-1 could be exerting its functions in HPSC and to determine how essential is the localization of this lectin in HPSC for the observed pro-tumoral activities.

CONCLUSIONS

“Apart from pure results and reflections of the data obtained, I visualize a thesis as a whole interpersonal artwork. The frustration, the countless trials to move forward, the obsession to decipher what’s behind of the shadows… are also part of these experience”

David Cabrerizo Granados

1. Our results after *in vitro* downregulation of Gal-1 using shRNA indicate that this protein promotes cell migration and invasion in HPSC. In contrast, it does not affect HPSC proliferation.

2. Gal-1 is involved in HPSC activation because, after downregulating Gal-1, these cells showed decreased levels of activation markers like α-SMA, GFAP, FAP and COL1A1. Moreover, HPSC with reduced levels of Gal-1 display morphological changes, showing a less-spindle phenotype.

3. *In vitro* downregulation of Gal-1 in HPSC using shRNA impairs ECM organization and fiber alignment, indicating that Gal-1 triggers changes in ECM composition and organization towards a more activated phenotype. Moreover, Gal-1 controls ECM organization and fibroblast's fiber alignment in a dose dependent manner independently of TGF-β.

4. Comparative analysis of gene expression in HPSC control and after Gal-1 downregulation using a whole-transcript microarray identifies 86 differentially expressed genes, of which 83 were downregulated and 3 were upregulated in Gal-1 KD versus control HPSC. DAVID annotation tool displayed regulation of transcription among the most relevant functional groups. KRAS, WNT5A and TACC1 were selected from our microarray list and validated by RTqPCR as putative target genes responsible for Gal-1 mediated effects in HPSC.

5. Functional studies using shRNA for these specific genes shows that KRas can be, at least in part, responsible for Ga´-1 mediated effects in HPSC migration, invasion and activation.

6. KRas gene expression was not altered after blockade of the of the MAPK/ERK pathway using the MEK inhibitor U0126 or after

inhibition of extracellular Gal-1-glycan interactions using lactose, indicating that changes in gene expression after Gal-1 downregulation in HPSC are not mediated by extracellular or cytosolic protein signaling by likely mediated by nuclear Gal-1.

7. Nuclear Gal-1 is found in the chromatin bound fraction in HPSC. Chromatin immunoprecipitation experiments demonstrate that Gal-1 is able to specifically bind 874 DNA promoter sequences, most of them involved in cancer pathways (DAVID Database tool), such as *KRAS* and *LRRFIP1*.

8. Using luciferase reporter assays, we demonstrate that nuclear Gal-1 directly promotes KRAS transcription by recognizing its promoter in HPSC. However, as Gal-1 has no DNA binding motifs, this regulation requires the formation of a protein complex with transcription factors.

9. *In silico* studies suggest that Gal-1 can bind *KRAS* promoter though its interaction with EGR1 transcription factor. Accordingly, KRas promoter contains numerous EGR1 binding motifs, EGR1 is highly expressed in PDA stromal compartment (while it is barely found in normal counterparts) and Gal-1 and EGR1 colocalize in HPSC nuclei.

10. Proteomic studies using Gal-1 co-immunoprecipitation and mass spectrometry analysis identifies 44 putative nuclear interactions for this lectin in HPSC. Functional annotation and Gene Ontology analysis using DAVID Database tool, unveils biological processes related to gene expression regulation (i.e. chromatin modification by acetylation or methylation), as well as genes related to transcription/DNA-templated among the most relevant clusters, supporting that nuclear Gal-1 can play a key role in DNA transcriptional regulation to modulate gene expression in HPSC.

MATERIALS & METHODS

6.1 Cell lines and culture conditions

Human Pancreatic Stellate Cells (HPSC) have been our principal system of work in this project, and were kindly given by Dra. Hwang (Department of Surgical Oncology, The University of Texas MD Anderson Cancer Center, Houston, USA). These cells were isolated from the PDA of a patient who had undergone primary surgical resection without previous treatment and were immortalized by lentiviral infection with human telomerase (hTERT) or SV40 large T antigen (TAg)[253]. HEK-293T/17 cell line[254], obtained from Cancer Cell Line Repository (IMIM, Barcelona), were used for lentivirus generation and for *in vitro* luciferase reporter assays. All cells were cultured in a cell incubator at 37ºC and CO_2 5%, and their maintenance was performed using DMEM (Gibco) medium supplemented with FBS 10%, L-Glutamine 2mM, sodium pyruvate 1mM, penicillin 100U/ml, streptomycin 100μg/ml. For lentivirus generation and cell infection, cell culture was performed in BioSafety Level 2 Room (BSL-2, P2).

6.2 Immunohistochemistry (IHC)

Formalin-fixed pancreatic tissues were embedded in paraffin and resulting blocks were microsectioned in 5μm slides. Slides were heated at 60ºC during 30min, and deparaffined following a sequential set of solvents from xylene, though alcohols until water. Then, they were incubated in citrate buffer 0.01M pH 6 at 120ºC during 15min in a pressure cooker for antigen retrieval. Endogenous peroxidase activity was quenched using H_2O_2 3% for 10min, and blocking was performed by incubating samples with PBS BSA 1% for 1h. Primary antibodies (see section *6.21 Antibody table*) were properly diluted in PBS BSA 1% and incubated overnight (O/N) at

4ºC. The following day, secondary antibodies (Envision+ reagent anti-rabbit HRP conjugated (DAKO) or LSAB + System HRP for primary goat antibodies (DAKO)) were incubated for 1h at room temperature (RT). Antibody reaction was developed using 3,3'-diaminobenzidine (DAB) as substrate. Finally, tissue slides were counterstained with hematoxylin, dehydrated and mounted with DPX. Images were taken using Olympus BX16 microscope.

6.3 Immunofluorescence (IF)

Proximately, 40000 HPSC per well (about 50% of confluence) were plated on sterile coverslips in 24-well plates. The following day, cells were fixed with 400µl of paraformaldehyde (PFA) 4% at RT during 15min. After washing with PBS, fixation was quenched during 15min at RT by adding NH_4Cl 0.1M (diluted in PBS). Then, cells were incubated with permeabilization and blocking solution (Triton X-100 0.3%, BSA 1%, diluted in PBS) during 1h at RT. Primary antibody incubation (see section *6.21 Antibody table*) was performed O/N at 4ºC. After washing with PBS-BSA 1%, cells were incubated during 1h at RT with proper secondary antibody (anti-rabbit Alexa® 488 or anti-goat Alexa® 555; ThermoFisher Scientific) diluted 1:300. Primary and secondary antibodies were diluted using permeabilization and blocking solution. Then, cells were washed with PBS and incubated during 5min at RT with DAPI diluted 1:20000 in PBS. Finally, slides were mounted using Fluoromount-G® (SouthernBiotech). Fluorescent pictures were taken under proper emission filters using NIKON Eclipse N*i* microscope. For ECM IF (see section *5.11 Extracellular Matrix (ECM) alignment analysis*), total confluent HPSC were fixed with PFA 4% during 10min, and quenched with NH_4Cl 50mM for 5min. Then, same IF protocol steps were followed as described.

6.4 small interference RNA (siRNA) transfection*

For transient Gal-1 downregulation, HPSC were plated in 6-well plates and transfected when cell confluence was about 50%. Cells were transfected with a pool of siRNA sequences against *LGALS1* (SMARTpool®, Dharmacon) or with a non-targeting Irrelevant siRNApool (SMARTpool®, Dharmacon) used as a control. For each well, siRNAs were used at 50nM (final concentration), diluted with OptiMem (Gibco) and mixed with 10μl of Lipofectamine 2000™ transfection reagent (Invitrogen). This mixture was incubated for 30min at RT for complexes formation; meanwhile, cells were washed with PBS and incubated with OptiMem. Finally, transfection mixture was added to each well (1ml of final volume) and cells were incubated at 37ºC and CO_2 5% for 6h. After transfection, cell medium was removed and fresh DMEM 10% medium was added for cell recovery. After 48h, proper Gal-1 KD as well as the expression levels of other molecules of interest were checked at mRNA and protein levels by using RTqPCR (see section *6.6 RNA extraction and Reverse Transcription and Real Time quantitative Polymerase Chain Reaction (RTqPCR)*) and WB (see section *6.7 Cell lysis and Western Blot (WB)*) strategies.

6.5 Lentivirus generation and HPSC infection with short hairpin RNA (shRNA)

HEK293T/17 cells were plated at 90% of confluence in 6-well plates and transfected with 3 vectors for lentivirus generation (pMDLg/pRRE (0.3μg/ml), pRSV (0.1μg/ml), pVSV-G (0.1μg/ml)) mixed with a pLKO.1-puro vector (1μg/ml) carring the shRNA of interest: *LGALS1* shRNA (MISSION® *RNAi*), *KRAS* shRNA (MISSION® *RNAi*), *WNT5A* shRNA (MISSION® *RNAi*), *TACC1* shRNA (MISSION®

RNAi) or the non-targeting scramble shRNA (Sigma, SHC002) used as a control. Previous to transfection, vectors were mixed and incubated 30min at RT with 190μl of sterile NaCl 150mM and 10μl of PEI (1 mg/ml) for complexes formation; then, these mixtures were added to HEK293T/17 cells incubated with 2ml of DMEM FBS 10% at 37ºC and CO_2 5%. The following day, HEK293T/17 medium was changed for 2ml of fresh DMEM FBS 10%. 48 h after transfection, conditioned media (CM) from HEK293T/17 containing generated lentivirus were collected, filtered with 0.45μm filters (Millipore) and mixed with polybrene, at 8μg/ml final concentration, to increase transduction efficiency. For cell infection, HPSC were plated at 50% confluence in 6-well plates and incubated with collected lentiviral CM during 6h at 37ºC and CO_2 5%, then, media was changed for fresh DMEM FBS 10% allowing cell recovery. These steps were performed twice to improve HPSC infection efficiency. Infected HPSC were selected and expanded with DMEM FBS 10% supplemented with Puromycin (0.75μg/ml) during one week. Finally, proper KDs were determined by RTqPCR and WB strategies.

6.6 RNA extraction, Reverse Transcription and Real Time quantitative Polymerase Chain Reaction (RTqPCR)

RNA was purified using Gene Elute™ Mammalian Total RNA Miniprep Kit (Sigma) following manufacturer's instructions. After RNA quantification using NanoDrop ND-1000 Spectrophotometer (NanoDrop Technologies), 1μg of isolated RNA was retrotranscribed with RevertAid First Strand cDNA Synthesis Kit (ThermoFisher Scientific). SYBR® Select Master Mix (Applied Biosystems), proper pair of primers (Sigma, used at 0.5μM final concentration each one), and 33ng of cDNA were mixed in a 10μl volume RTqPCR reaction. Primers were designed using PrimerQuest tool (Integrated DNA

Technologies, IDT), Primer Blast (NCBI) was used for determining the specificity *in silico* of each pair of primers and Multiple Primer Analyzer (ThermoFisher) for checking possible formation of self- and/or cross-primer dimers. Human *HPRT* and *PUM1* were used as endogenous controls for RTqPCR normalization. All primers as well as their utility were listed in a table at section *6.22 Primers*. Analysis was performed quantifying gene fold expression relative to endogenous controls and relative to WT sample using $2^{-\Delta\Delta CT}$ method (devised by Livak and Schmittgen[255,256]) using QUANSTUDIO12K (Applied Biosystems).

6.7 Cell lysis and Western Blot (WB)

Cells were lysed using RIPA Buffer (Tris-HCl pH 7.5 50mM, NaCl 150mM, EDTA 1mM, Triton X-100 0.1%, SDS 0.1%, sodium deoxycholate 1%) supplemented with cOmplete™, EDTA-free protease inhibitor cocktail (Sigma), NaF 5mM, and sodium orthovanadate for protease and phosphatase enzymes inhibition. After proper homogenization using a syringe, cell lysates were centrifuged at 13000rpm at 4ºC during 10min. Supernatants were collected and quantified with DC™ Protein Assay Kit (BioRad). Before electrophoresis, Laemmli Buffer 4X (Tris-HCl pH 6.8 62.5mM, SDS 2%, glycerol 40%, 2-βmercaptoethanol 5%, bromophenol blue 0.01%) was added to samples at a 1X final concentration. Then, samples were boiled at 98ºC during 10min. 20μg of each protein sample were loaded to a 6-15% poliacrylamide gel and electrophoresis was performed at 120V during 1-1.5h. Proteins were transferred to a nitrocellulose (Amershan Protan 0.45μm pore size, GE Healthcare Life Sciences) or Polyvinylidene Difluoride (PVDF) membranes by applying 300mA during 2h at 4ºC. Proper protein transference was corroborated by Ponceau staining

(Ponceau S 0.1% (w/v), acetic acid 5% (v/v)) and then membranes were blocked for 1h at RT with powder milk 10% (w/v) diluted in TBS Tween-20 0.1% (TBS-T). For protein detection, blocked membranes were incubated O/N on a shaker at 4ºC with primary antibodies of interest (see section *6.21 Antibody table*), previously diluted with TBS-T BSA 1%, Azide 0.02%. After washing with TBS-T, membranes were incubated for 1h at RT with corresponding secondary antibodies (goat anti-rabbit (0.25 g/L), rabbit anti-mouse (1.3 g/L), rabbit anti-goat (0.55 mg/L), or rabbit anti-rat (1.3 g/L) immunoglobulins conjugated to HRP; DAKO). All secondary antibodies were used 1:2000 diluted in TBS-T. Once membranes were washed, chemiluminescence signal was detected with Pierce™ ECL Western Blotting Substrate (ThermoFisher Scientific). WB densitometry quantification was performed using ImageJ and data was normalized relative to load control (tubulin or vinculin).

6.8 Cell proliferation: MTT assay

For cell proliferation, 3-(4,5-Dimethylthiazol-2-yl)-2,5-Diphenyltetrazolium Bromide (MTT, Sigma) colorimetric assay was performed. 1000 HPSC per well were seeded in quintuplicates in 96-well plates, and were grown with DMEM FBS 2%. The experiment was performed during 6 days, in which cell proliferation was determined every day. To measure cell proliferation, cell medium was removed and 200µl of MTT at 1mg/ml diluted in DMEM FBS 0% were added per well. After 3h of incubation at 37ºC and CO_2 5%, medium was removed and formazan precipitates were solubilized by mixing with 100µl of isopropanol:DMSO (4:1). Finally, absorbance was measured at 570nm using TECAN luminometer and resulting data was normalized versus (vs) day 1 and represented relative to WT.

6.9 Cell migration

6.9.1 Wound healing (WH)

To analyze cell migration, in KRas and TACC1 studies, 80000 HPSC were plated in triplicates in 24-well plates with DMEM FBS 10%. Once cells reached 100% confluence, a scratch was performed using a micropipette tip. Cells were washed with DMEM FBS 0% and incubated at 37ºC and CO_2 5% with DMEM FBS 0.5% to avoid cell proliferation during the assay. Cell migratory effect was determined after 24h. For proper analysis, pictures were taken at 0h (when the scratch was performed), and at 24h as well. Then, free areas were measured using ImageJ software, data was normalized vs 0h and represented relative to WT.

6.9.2 Transwell chamber

In the case of Wnt-5α studies, migration assays were performed using 24-well Transwell® chamber with 8μm Polycarbonate Membrane (Corning). 10000 cells were resuspended in DMEM FBS 0%, plated in duplicates on the top chamber and incubated at 37ºC and CO_2 5% during 4h. Once cells were attached to the upper part of the membrane, 400μl of DMEM FBS 10% were added to the bottom chamber, which will favor cell migration throw membrane acting as a chemoattractant. After 24h of incubation at 37ºC and CO_2 5%, the number of migrating cells that reached the bottom part of membrane was analyzed. Cells were fixed with PFA 4% during 15min at RT, washed with PBS and stained with DAPI (diluted 1:20000 in PBS) for 5min. Membranes were mounted in slides using Fluoromount-G®. 5 pictures per well were taken under proper emission filters using Olympus BX61. Finally, nuclei were counted using ImageJ and data was normalized relative to WT.

6.10 Cell invasion

24-well Transwell chamber were also used to study cell invasion in KRas and Wnt-5α studies. To mimic a matrix layer, the upper chamber was coated with 50µl of Matrigel™ Matrix (Corning), previously diluted 20 times in sterile PBS. After let Matrigel dry at RT during 3h, 10000 cells were resuspended in DMEM FBS 0%, plated in duplicates on top of matrix and incubated at 37ºC and CO_2 5% during 4h. Once cells were attached to matrix layer, 400µl of DMEM FBS 10% were added to the bottom of the chamber, which will favor cell invasion throw matrix acting as a chemoattractant. After 36 h incubation at 37ºC and CO_2 5%, the number of invading cells that reached the bottom part of membrane was analyzed. Cells were fixed with PFA 4% during 15 min at RT, washed with PBS and stained with DAPI (diluted 1:20000 in PBS) during 5min. Membranes were mounted in slides using Fluoromount-G®. 5 pictures per well were taken under proper emission filters using Olympus BX61. Finally, nuclei were counted using ImageJ and data was normalized relative to WT. For TACC1 KDs invasion analysis, Matrigel-coated 96-well 8µm membrane Transwells (Corning) were used. In this case, 30µl of Matrigel were used for matrix generation and 5000 cells per well were plated. As described, DMEM FBS 10% (100µl) was added to the bottom chamber and invasive capability was analyzed after 36h. For this analysis, invading cells were detached by incubating with 100µl of dissociation solution (Cultex) for 1h. Then, collected cells were incubated with hexosaminidase enzymatic substrate during 4h at 37ºC and CO_2 5%. Finally, 160µl of hexosaminidase developing solution were added and absorbance was measured at 410nm using TECAN spectrophotometer. Obtained data was represented relative to WT.

6.11 Extracellular Matrix (ECM) alignment analysis

For ECM generation, HPSC were plated at maximum confluence in 24-well plates and incubated during 9 days to let them generate ECM deposition. Before plating cells, sterile coverslips needed to be pre-treated for a better matrix anchoring. Sterile coverslips were placed into the plate and rinse once with PBS, then they were incubated with gelatin solution (Sigma) 0.2% diluted in sterile PBS for 1h at 37ºC. After removing remaining gelatin and washing with PBS, coverslips were treated with filtered glutaraldehyde (Sigma) 1% (diluted in PBS) during 30 min at RT. PBS washings were performed before treating coverslips with filtered ethanolamine 1M (diluted in distillated water) for 30 min at RT. Coverslips were again washed with PBS and proper pH was corroborated by the red-colored DMEM FBS 10% medium when it was added. Then 250000 HPSC per well were plated in duplicates. Each other day, during 9 days, cell medium was replaced for fresh DMEM FBS 10% containing acid ascorbic at 50μg/ml, which promotes ECM deposition without affecting cell activation. Cells and generated ECM were fixed and immunofluorescence was performed (see section *6.3 Immunofluorescence (IF)*) for ECM and nuclei alignment observation and analysis. Finally, 5 pictures of each well were taken using confocal TCS SP5 microscope (Leica), and nuclei alignment were analyzed using ImageJ software as described by Franco-Barraza *et al.*[257] For TGFβ studies, this experiment was performed as described, but cells were treated with acid ascorbic at 50μg/ml together with human TGF-β1 (PeproTech) at 5ng/ml.

6.12 Microarray analysis*

Differences in gene expression after Gal-1 KD in HPSC were determined by performing microarray analysis. Samples were amplified, labeled and hybridized to GeneChIP® PrimeView™ Human Gene Expression Array (Affymetrix) and differentially-expressed genes between two HPSC controls (si-irr_1 and si-irr_2) compared with two HPSC KDs for Gal-1 (siGal-1_1 and siGal-1_2) were identified by following Linear Models of Microarray Analysis (LIMMA) pipeline. Finally, genes with p-value<0.01 were selected as significant.

*Very briefly explanation about microarray performance and analysis extracted from Carlos Alberto Orozco Castaño thesis manuscript.

6.13 Extracellular Gal-1 blockage

6.13.1 MAPK/ERK pathway inhibition with U0126

To inhibit MAPK/ERK pathway, 40000 HPSC per well were seeded in duplicates in 24-well plates. U0126 (Cell Signaling), a highly selective inhibitor of MEK1/2 kinases, was added at 10μM to each well and cells were incubated at 37ºC and CO_2 5% during 2h. Then, RNA extraction was performed and *KRAS* as well as *FOS* mRNA levels, used as positive control, were determined by RTqPCR (see section *6.6 RNA extraction, Reverse Transcription and Real Time quantitative Polymerase Chain Reaction (RTqPCR)*). Protein levels of phosphorylated ERK (p44/42-ERK) were detected by WB (see secion *6.7 Cell lysis and Western Blot (WB)*) to check proper blockage of MAPK/ERK pathway.

6.13.2 Carbohydrate-binding impairment by lactose treatment

Extracellular carbohydrate-bindings mediated by secreted galectins were blocked by treating cells with β-lactose 100mM (Sigma). As described above 40000 HPSC per well were seeded in duplicates in 24-well plates. β-lactose at 100mM final concentration was added to each well and cells were incubated at 37ºC and CO_2 5% during 2h. Finally, RNA extraction was performed and *KRAS* mRNA levels were determined by RTqPCR (see section *6.6 RNA extraction, Reverse Transcription and Real Time quantitative Polymerase Chain Reaction (RTqPCR)*).

6.14 Subcellular fractionation

HPSC were plated near 90% confluence in 100mm dishes. The following day, after washing with PBS, 300µl of buffer A (HEPES-KOH pH 7.8 10mM, $MgCl_2$ 1.5mM, KCl 10mM; supplemented with protease inhibitors cocktail, NaF 5mM, and sodium orthovanadate) were added and cells were scrapped and collected into a microcentrifuge tube. After chilling out in ice for 10mins, 1/30 volume of Triton X-100 10% was added and the mixture was vortex for 20s. Cytoplasmic proteins, solubilized in supernatant fraction (SN), were obtained after centrifuge at 11000rpm for 1min at 4ºC. Pellet (nuclei) was washed with buffer A, resuspended in 100µl of buffer C (HEPES-KOH pH 7.8 20mM, glycerol 25%, NaCl 420mM, $MgCl_2$ 1.5mM, EDTA 0.2mM; supplemented with protease inhibitors cocktail, NaF 5mM and sodium orthovanadate) and kept in rotation at 4ºC during 20min. After centrifuge at 13000rpm for 15min at 4Cº, nucleoplasmic soluble proteins (SN) and insoluble chromatin bound fraction (pellet) were obtained. Pellet was washed with buffer C,

resuspended in 100µl of SDS 2% buffer (SDS 2%, Tris-HCl pH 7.5 20mM, glycerol 10%), boiled at 95ºc for 3min and well-homogenized with a syringe. Finally, Gal-1 localization was determined by WB (see section *6.7 Cell lysis and Western Blot (WB)*). Tubulin and histone 3 (H3) were used as cytoplasmic and chromatin bound protein controls respectively.

6.15 Chomatin Immunoprecipitation and sequencing (ChIP-seq)

6.15.1 Chomatin Immunoprecipitation (ChIP)

$2 \cdot 10^6$ of HPSC were seeded in 150mm dishes and kept growing for 2 days in DMEM FBS 10% at 37ºC and CO_2 5%; one plate was used for counting cells and each immunoprecipitation (IP) was performed with $2 \cdot 10^6$ lysed nuclei. For cell fixation, cells were incubated with formaldehyde solution 37% (Merck) at final concentration of 1% during 10min at RT. Quenching was performed by 5min incubation at RT with glycine at final concentration of 0.125M. After washing with PBS, cells were scraped with 5ml of PBS supplemented with protein inhibitor cocktail. Then, samples were centrifuged for 5min at 800 G at 4ºC, and Cell Lysis Buffer (CLB; PIPES 5mM, KCl 85mM, NP-40 0.5%, Tris-HCl pH 8.1 1mM; supplemeted with protease inhibitors cocktail) was added to pelleted cells which were vortexed every 5min during 15min for proper cell lysis. 500µl of CLB was enough for lysing 10^7 of cells. Nuclei were collected after centrifuge for 5min at 800G at 4ºC and lysed by adding Nulcear Lysis Buffer (NLB; Tris-HCl pH 8.1 50mM, EDTA pH 8 10mM, SDS 1%; supplemeted with protease inhibitors cocktail); 1ml of NLB was used per 10^7 nuclei. DNA was sonicated performing 10 pulses of 10s at 40% of amplitude using BRANSON biorruptor. Proper sonication

(200-500bp DNA fragments) was checked and insoluble material was removed by spinning samples at 12000 G during 10min at 4ºC. Before performing IP, sonicated DNA was 10 times diluted with Dilution Buffer (Tris-HCl pH 8.1 16.7mM, NaCl 167mM, EDTA pH 8 1.2mM, Triton X-100 1%, SDS 0.01%; supplemented with protease inhibitors cocktail). Preclearing was performed by incubating each 10ml of diluted samples during 1h and rotating at 4ºC with 1μg of anti-rabbit irrelevant IgGs and 10μl of Agarose Protein-A Beads (Sigma), previously blocked with TBS-BSA 0.5% for 1h and rotating at 4ºC. After discarding beads, 200μl of sample (10% of IP volume) were taken as INPUT, and 2ml of sample were used for each IP incubated with 5μg of Gal-1 antibody kindly given by Dr. Gabius (Institut für Physiologische Chemie, Tierärztliche Fakultät, Ludwig-Maximilians-Universität, Munich, Germany) or with 5μg of irrelevant anti-rabbit IgGs, used as an unspecific binding control. Samples were incubated with proper antibodies O/N rotating at 4ºC. The following day, 30μl of blocked beads were added to each IP and kept rotating at 4ºC during 3-4h. Unbound (UB) faction was collected after centrifuging IPs during 5min at 1800rpm at 4ºC. Pelleted beads were washed three times with Low Washing Buffer (Tris-HCl pH 8.1 20mM, NaCl 150mM, EDTA pH 8 2mM, Triton X-100 1%, SDS 0.1%), three times with High Washing Buffer (Tris-HCl pH 8.1 20mM, NaCl 500mM, EDTA pH 8 2mM, Triton X-100 1%, SDS 0.1%) and two times with LiCl Washing Buffer (Tris-HCl pH 8.1 10mM, LiCl 0.25M, EDTA pH 8 1mM, deoxycholate 1%, NP-40 1%). Then, immunoprecipitated DNA and protein complexes where eluted by adding 100μl of freshly prepared Elution Buffer (Na_2CO_3 0.1M, SDS 1% diluted in distillated water) to each sample and incubating them for 1h in a shaker at 800rpm and at 37ºC. Beads were discarded after centrifuge samples during 3min at 2000rpm. Supernatants were collected and both, INPUT and IPs, were decrosslinked by adding NaCl to a 200mM final concentration and by incubating O/N at 65ºC in a shaker at 800rpm. The following day,

10µl of EDTA pH 8 0.5M, 20µl of Tris-HCl pH 6.5 1M and 2µl of proteinase K, recombinant, PCR grade (19 mg/ml; Sigma) were added to each sample (indicated volumes were calculated for 100µl sample volume). Finally, DNA was purified using QIAquick® PCR Purification kit (QIAGEN). Samples were eluted in 20µl for ChIP-seq experiments or in 50µl for ChIP-qPCR validation assays.

6.15.2 Sequencing and analysis

For Sequencing, samples were eluted with 20µl using Nuclease-free water. High sensitivity quality control (Qubit), DNA libraries (Bioanalyzer, Agilent Technologies) and DNA sequencing (Sanger) were performed by Genomics Unit (Centre of Genomic Regulation (CRG), PRBB, Barcelona).

We analyzed our ChIP-seq data using a free online platform: The Galaxy Project, https://usegalaxy.org/, which includes several tools for analyzing high throughput data. Firstly, proper quality of immunoprecipitated DNA reads was determined by Fast Quality Control Report (FastQC) tool and therefore, those reads with >30 score were considered for the analysis. Then, reads were mapped with Bowtie2 tool using Homo Sapiens b38 (hg38) as a reference genome. MACS peak calling was also performed using The Galaxy platform in which aligned reads from Gal-1 IP were used as ChIP-seq Tag File while aligned reads from IgG IP were used as ChIP-seq control File, a 10^{-5} p-value cutoff was applied for peak detection, and an upper MFOLD range of 32 was determined to build the model and select proper regions with a high-confidence enrichment ratio against background (ChIP-seq control File). Peak distribution along the genome was determined by using 3'UTR, 5'UTR, exon and intron mapped regions from UCSC Genome Browser database. Promoter

regions where considered as those regions confined between 1000 bp upstream and 1000 bp downstream from TSS. On the other hand, DNA sequences corresponding to MACS peaks located at promoter regions were analyzed using The MEME Suite tool[229] (http://meme-suite.org/) to identify the most representative DNA motifs and their corresponding transcription factors.

6.16 ChIP-qPCR validation

ChIP experiments were performed as described in section *6.15.1 Chomatin Immunoprecipitation (ChIP)*; in this case, samples were eluted with 50 μl of Nuclease-free water. Quantification of immunoprecipitated DNA corresponding to *KRAS* and *LRRFIP1* promoters was performed in 10μl of reaction volume using SYBR® Select Master Mix and proper pair of primers named as KRAS or LRRFIP1 promoter (see section *6.22 Primers*). For *LRRFIP1* validation, primers were used at 0.5mM final concentration (each one) and DMSO 2% was added to reaction mix to improve primer annealing; for *KRAS* validation primers were used at 0.25mM final concentration (each one) and DMSO 2% was added to reaction. In both cases, extended annealing and elongation steps (30s each one) were needed for proper analysis using LightClycler. Finally, data was quantified relative to INPUT (10%) and the results were represented as fold enrichment relative to IgG sample (control).

6.17 *KRAS* promoter cloning in pGL3-Basic reporter vector

To perform luciferase assay KRas promoter was cloned in pGL3-Basic luciferase reporter vector (Promega). During this process

it was necessary to amplify *KRAS* promoter sequence using pGEM®-T Easy Vector System (Promega) and then to clone it in pGL3 luciferase reporter vector (kindly given by Antonio García de Herreros laboratory, PRBB, Barcelona) following a restriction enzyme directed strategy.

6.17.1 *KRAS* promoter amplification and pGEM-T cloning

Genomic DNA was extracted from HPSC using GeneElute™ Mammalian Genomic DNA MiniPrep Kit following manufacturer's instructions. NHPPE_KRAS pair of primers (see section *5.17 Primers*) were used to amplify *KRAS* promoter (including NHPPE region). PCR product was isolated by agarose gel electrophoresis (35min at 120V) and purified using GFX™ PCR DNA and Gel Band Purification Kit (GE HealthCare). To have better amount of PCR product, amplified *KRAS* promoter was cloned in pGEM-T Easy Vector following manufacturer's instructions. 3:1 insert:vector ratio was needed to achieve proper ligation reaction, incubated O/N at 4ºC. XL1-Blue Escherichia Coli competent cells were transformed with all ligation product following the heat shock transformation protocol[258]. And vector isolation and purification from transformed bacteria was performed using Wizard® Plus SV Minipreps DNA purification System Kit (Promega) following manufacturer's instructions.

6.17.2 Restriction enzyme directed cloning in pGL3 reporter vector

A directed restriction enzyme approach was necessary for proper cloning of *KRAS* promoter in pGL3-Basic vector. *KRAS* promoter sequence was flanked between HindIII and XhoI restriction enzyme sites through DNA amplification using

HindIII_KRAS FW and XhoI_KRAS RV primers (see section *6.22 Primers*) using 250 ng of pGEM-T vector containing *KRAS* promoter as DNA template (*see section 6.16.1 KRAS promoter amplification and pGEM-T cloning*). To favor an efficient restriction enzyme digestion, resulting PCR product (KRAS promoter flanked by enzyme restriction sites) was cloned in pGEM-T Easy Vector System, 3:1 insert:vector ratio was used for ligation reaction, incubated O/N at 4ºC. After XL1-Blue bacteria transformation using all ligation product, vector was isolated and purified as described. 1μg of pGEM-T vector containing *KRAS* promoter flanked by HindIII and XhoI restriction sites was digested with 1μl of Hind III (New England BioLabs) at 37ºC during 1h in 50μl of reaction volume. After purifying digested vector, resulting product was digested with 1μl XhoI enzyme (New England BioLabs) during 2.5h at 37ºC in 50μl of reaction volume, and purified again. Parallelly, 1μg of pGL3-basic vector was digested and purified in same conditions. Ligation was performed using 1μl of T4 DNA Ligase (New England BioLabs) in 20μl of reaction volume by incubating 3:1 insert:vector ratio O/N at 4ºC. After transforming bacteria with all ligation product, *KRAS*_pGL3 reporter was isolated and proper *KRAS* promoter sequence was confirmed by sequencing.

6.18 Luciferase assay

To further demonstrate Galectin-1 contributes in controlling *KRAS* gene expression, luciferase assay was performed. For this experiment, two different cell systems were used: HPSC (shSC and shGal-1_1) as well as HEK-293 cells transfected with pcDNA_∅ or pcDNA_LGALS1.

6.18.1 HPSC

HPSC were plated in triplicates in 24-well plates at 50% confluence (40000 cells per well). Next day, transfection was performed by mixing 38μl of sterile NaCl 150mM, 100ng of *KRAS*_pGL3 reporter, 6ng renilla (pTK-renilla, kindly given by Mireia Duñach laboratory, UAB, Barcelona) and 1.06μl PEI (1 μg/μl) per well. Mixture was incubated during 30min at RT and added to each well. HPSC were previously washed with PBS and incubated with 500μl OptiMem. Transfection was performed for 6h at 37ºC and CO_2 5%, then medium wash replaced by fresh DMEM FBS 10%. Luciferase activity was measured 48h after transfection using Dual-Luciferase® Reporter (DLR) Assay System (Promega). Cells were lysed and incubated during 30min at RT with 50μl of Passive Lysis Buffer. For DLR measurement, 20μl of lysed cells were incubated with 20μl of Luciferase Assay Reagent II (LAR II). After pre-measurement delay of 3s, a 9s measurement was performed to determine luciferase activity. Then, 20μl of Stop&Glo® Reagent were added and equally measured to determine renilla signal using a luminometer. Luciferase signal was normalized relative to renilla and results were represented relative to shSC HPSC (control).

6.18.2 HEK-293T/17 cells: Gal-1 overexpression and luciferase assay

293 were plated at confluence 50 % in 6-well plates, cells were transfected with 1μg of pcDNA 3.1 containing *LGALS1* gene sequence (pcDNA_Gal-1) or with pcDNA 3.1 empty vector as a control (pcDNA_∅). Previously, pcDNA_Gal-1 or pcDNA_∅ were mixed with 190μl NaCl 150mM and 10μl PEI (1 μg/μl) and incubated

during 30min at RT and this mixture was added to HEK-293T/17 cells incubated with DMEM FBS 10%. Transfection media was changed the following day for new fresh DMEM FBS 10% and 48h after transfection, proper Gal-1 overexpression was confirmed by WB. HEK-293T/17 cells (pcDNA_∅ and pcDNA_Gal-1) were plated in triplicates in 24-well plates at 50% confluence and transfected, as explained above, with 100μg of *KRAS*_pGL3 reporter and 6ng of renilla vector, for proper assay normalization. Luciferase activity was measured, as described, 48h after transfection using DLR assay. Luciferase signal was normalized relative to renilla and results were represented relative to shSC HPSC (control).

6.19 Co-Immunoprecipitation (Co-IP)

HPSC were plate at high confluence (80%) in 150mm dishes. After washing with PBS, cells were scrapped with PBS supplemented with protease inhibitor cocktail and centrifuge at 800 G 5mins. Pellet was lysed with 1ml of Soft Lysis Buffer (Tris-HCl pH 8.0 50 mM, EDTA 10 mM, glycerol 10%, Nonidet P-40 0.1%; supplemented with protease inhibitor cocktail, NaF 5mM, sodium orthovanadate) and incubate 15min at 4ºC in rotation. Then, lysates were centrifuge at 3000 rpm 15min at 4ºC for nuclei collection. Supernatant, corresponding to cytoplasmic proteins, was collected and quantified with DC™ Protein Assay Kit (BioRad); at least 1 mg of protein per IP was required for mass spectrometry analysis. Meanwhile, pelleted nuclei were lysed with 1ml of High Lysis Buffer (HEPES pH 7.4 20mM, NaCl 0.35M, Glycerol 10%, $MgCl_2$ 1mM, Triton X-100 0.5%, DTT 1mM; supplemented with protease inhibitor cocktail, NaF 5mM, sodium orthovanadate). For proper homogenization, samples were sonicated by 2 pulses of 10s each at 20% amplification. Nuclear membranes and cell debris were discarded by centrifugation at

15000 G 4ºC during 10min. Next, Balance Buffer (HEPES pH 7.4 20mM, $MgCl_2$ 1mM, KCl 10mM) was added to reach NaCl 300mM final concentration for performing co-IP. 50µl of nuclear protein was taken as INPUT and 1ml of nuclear samples were incubated O/N and rotating at 4ºC with 5µg of anti-Galectin1 antibody or 5µg of anti-rabbit irrelevant IgGs, used as a negative control. The following day, 30µl of agarose protein-A beads were added to each sample and incubated 3-4 h rotating at 4ºC. Beads were previously blocked with TBS BSA 1% O/N at 4ºC. Unbound fraction (UB) was collected after centrifuging samples during 5min at 2000 rpm and 4ºC. Bound-Beads fractions were washed with Washing Buffer (HEPES pH 7.4 20mM, NaCl 0.3M, Glycerol 8.62%, $MgCl_2$ 1mM, Triton X-100 0.4%, KCl 1.6mM, supplemented with protease inhibitor cocktail, NaF 5mM, sodium orthovanadate). For WB co-IP detection, beads were incubated with 30µl of Laemmly Buffer (2X) during 10 min at 98 ºC. Then, samples were centrifuge during 1 min at 15000 G and bound fraction (B) was collected for WB analysis (see section *5.7 Cell lysis and Western Blot (WB)*). Regarding mass spectrometry, Bound-Beads fractions were washed twice with PBS. Then, *In-solution digestion in beads protocol*, explained in the following section, was performed.

6.20 In-solution digestion in beads

Bound-Beads fractions from nuclear co-IP were washed three times with ammonium bicarbonate (ABC) 200 mM. Beads were resuspended in 100µl of urea 6M, and a reduction step was performed by adding 3µl DTT 10mM (diluted in ABC) and incubating at 37ºC during 1h and shaking at 600rpm. Then, 3µl of iodoacetamide 20mM (diluted in ABC) were added to each sample and incubated 30min at RT in darkness for proper alkylation.

Samples were diluted by adding ABC until reaching urea 2M final concentration. Then, samples were incubated O/N with 1μg of endoprotease Lysine C at 37ºC and shaking at 600rpm. Next day, urea concentration was diluted at 1M with ABC and samples were incubated over day (at least, 8h) with 1μg of trypsine at 37ºC and shaking at 600rpm. Supernatants containing peptides were collected after centrifuging beads at 13000 rpm during 3min. Formic acid was added at 10% final concentration and samples were kept at -20ºC until mass spectrometry analysis. Volumes and indicated amounts were used considering 10μg of nuclear protein were co-immunoprecipitated. Simultaneously, 15μg of E.Coli protein were used as proper digestion control.

6.21 Antibodies and using conditions

Antibody	Host	Dilution	Reference number	Use
Galectin-1	Rabbit	1:1000	Abcam	WB, IF
Galectin-1	Rabbit	5 μg/IP	Dr. Gabius lab[259]	IP, ChIP
Galectin-1	Goat	1:1000	R&D	Double IF
GAPDH	Mouse	1:1000	Abcam	WB
αSMA	Mouse	1:1000	Sigma	WB
GFAP	Mouse	1:1000	Sigma	WB
Fibronectin	Mouse	1:10000	Sigma	WB
Alexa Fluor™ 568 Phalloidin	_	1:200	ThermoFisher Scientific	IF
Wnt-5α	Rat	2μl/ml	R&D	WB
Fibronectin	Rabbit	1:1000	DAKO	IF
Tubulin	Mouse	1:10000	Sigma	WB
Histone-3	Rabbit	1:10000	Abcam	WB
Vinculin	Mouse	1:1000	Santa Cruz	WB
EGR1	Rabbit	1:50	Cell Signaling	IHC
EGR1	Rabbit	1:800	Cell Signaling	IF
EGR1	Rabbit	1:50	Cell Signaling	IP
EGR1	Rabbit	1:1000	Cell Signaling	WB
c-Myc	Rabbit	1:1000	Abcam	WB
PARP-14	Rabbit	1:1000	Sigma	WB

6.22 Primers

Name	Sequence 5'-3'	Utility
HPRT FW	GGCCAGACTTTGTTGGATTTG	Housekeeping
HPRT RV	TGCGCTCATCTTAGGCTTTGT	Housekeeping
PUM FW	CGGTCGTCCTGAGGATAAAA	Housekeeping
PUM RV	CGTACCTGAGGCGGTGAGTAA	Housekeeping
GAL1 FW	CAGCAACCTGAATCTCAAACC	Expression levels
GAL1 RV	GCACAGGTTGTTGCTGTCTTT	Expression levels
ACTA2 (αSMA) FW	TCCTCCCTTGAGAAGAGTTACG	Expression levels
ACTA2 (αSMA) RV	AGCATAGAGGTCCTTCCTGATG	Expression levels
GFAP FW	ATGCATGAAGCCGAAGAGTG	Expression levels
GFAP RV	AGGTCAAGGACTGCAACTGG	Expression levels
FAP FW	TCAGCTATGATGCCATTTCG	Expression levels
FAP RV	ATTTATGGCCTCCCACTTGC	Expression levels
COL1A1 FW	ACGAAGAGACATCCCACCAATC	Expression levels
COL1A1 RV	TCACGTCATCGCACAACA	Expression levels
KRAS FW	GGCTTTCTTTGTGTATTTGCCAT A	Expression levels
KRAS RV	CTGTTCTAGAAGGCAAATCACA TTTATT	Expression levels
WNT5A FW	CACTGTGGATAACACCTCTGTT TTTG	Expression levels
WNT5A RV	CGGCTCATGGCGTTCAC	Expression levels
TACC1 FW	CAAGGAGTCCTGTGATCCATCA	Expression levels
TACC1 RV	ACATTTTTCAACCACTTCTGCTA CA	Expression levels
LRRFIP1 FW	GAAGTCAAGGAGGCCCTGAAG	Expression levels
LRRFIP1 RV	GGGTGTCGGAAGTCTCTCCAT	Expression levels
KRAS promoter FW	GTGCTCGGAGCTCGATTTTCCT	ChIP validation
KRAS promoter RV	GGAGGGGTGGTCCGCT	ChIP validation
LRRFIP1promoter FW2	GAGCCCGGCAGGATGAC	ChIP validation
LRRFIP1promoter3 RV	CGATCTCCCGGCTTTGA	ChIP validation
NHPPE_KRAS FW	CGCTCCGGGTCAGAATTG	Promoter amplification
NHPPE_KRAS RV	GGGGACCCCTCCTTCATTCA	Promoter amplification
HindIII_KRas FW	GGTGGTAAGCTTCGCTCCGGG TCAGAATTG	Cloning
XhoI_KRas RV	GGTGGTCTCGAGGGGGACCCC TAATTCATTCA	Cloning
FOS FW	TCCAGCATGGGCTCGC	Expression levels
FOS RV	ACAACGCCAGCCCTGG	Expression levels

6.23 Statistical analysis

Values are represented as the mean of three (or two) independent experiments and normalized relative to its corresponding control, error bars correspond to the standard error of the mean (±SEM). Statistical analysis was performed using GraphPad Prim 5 and p values were determined by the t-Student test. Those experiments represented without error bars correspond to a representative expreriment.

SUPPLEMENTARY DATA

Table 1S. Differentially expressed genes after Gal-1 KD in HPSC

Symbol	Name	logFC	adj. p-value	FC
WNK1	WNK lysine deficient protein kinase 1	-1,39	0	0,38
THAP6	THAP domain-containing protein 6	-1,08	0,00001	0,47
CCND1	cyclin D1	-1,06	0,00002	0,48
ESCO1	establishment of cohesion 1 homolog 1	-1	0,00012	0,5
DCBLD2	discoidin, CUB and LCCL domain-containing protein 2	-0,99	0,00013	0,5
TOP1	topoisomerase (DNA) I	-0,96	0,00024	0,51
NECTIN3	nectin-3 or poliovirus receptor-related protein 3	-0,95	0,00029	0,52
PUS7L	pseudouridylate synthase 7 homolog	-0,95	0,00029	0,52
PTBP3	polypyrimidine tract-binding protein 3 or regulator of differentiation 1	-0,94	0,00034	0,52
ACTR2	ARP2 actin-related protein 2 homolog	-0,94	0,00036	0,52
PRRC2C	BAT2 domain containing 1	-0,93	0,00045	0,53
CALHM5	calcium homeostasis modulator protein 5	-0,92	0,00052	0,53
SETD2	cistone-lysine N-methyltransferase	-0,9	0,00075	0,53
WISP1	WNT1 inducible signaling pathway protein 1	-0,9	0,0008	0,54
CEP290	centrosomal protein 290kDa	-0,88	0,00119	0,54
NUFIP2	nuclear fragile X mental retardation protein interacting protein 2	-0,88	0,00134	0,54
SAFB2	scaffold attachment factor B2	-0,87	0,00144	0,55
LGALS1	Lectin, galactoside-binding, soluble, 1	-0,87	0,00154	0,55
ZFR	zinc finger RNA-binding protein	-0,86	0,00203	0,55
ITGB3BP	integrin beta 3 binding protein (beta3-endonexin)	-0,85	0,00203	0,55
CCDC186	coiled-coil domain-containing protein 186	-0,85	0,00203	0,55
NOL8	nucleolar protein 8	-0,85	0,00204	0,55
SRRM2	serine/arginine repetitive matrix 2	-0,84	0,00235	0,56
EPB41L1	erythrocyte membrane protein band 4.1-like 1	-0,84	0,00257	0,56
KIAA1549	UPF0606 protein KIAA1549	-0,84	0,00271	0,56
MIS18BP1	mis18-binding protein 1	-0,83	0,003	0,56

Symbol	Name	logFC	adj. p-value	FC
AKAP9	A kinase (PRKA) anchor protein (yotiao) 9	-0,82	0,00343	0,56
ZNF22	zinc finger protein 22 (KOX 15)	-0,82	0,00376	0,57
FAM117B	family with sequence similarity 117, member B	-0,82	0,00376	0,57
MAP4K5	protein-serine/threonine kinase gene	-0,82	0,00376	0,57
CALD1	caldesmon 1	-0,81	0,00376	0,57
TACC1	transforming acidic coiled-coil containing protein 1	-0,81	0,00376	0,57
MYO6	myosin VI	-0,81	0,00393	0,57
ATRX	putative DNA dependent ATPase and helicase	-0,81	0,00413	0,57
SMC1A	structural maintenance of chromosome 1-like 1 protein	-0,81	0,00416	0,57
SLF1	SMC5-SMC6 complex localization factor protein 1	-0,8	0,00445	0,57
SPIN1	spindlin-1	-0,79	0,00524	0,58
EIF4G1	eukaryotic translation initiation factor 4 gamma, 1	-0,79	0,00611	0,58
PLEKHA1	pleckstrin homology domain containing, family A (phosphoinositide binding specific) member 1	-0,79	0,00611	0,58
PRKDC	Protein kinase, DNA-activated, catalytic polypeptide	-0,78	0,00694	0,58
LOX	full-length cDNA clone LOX, lysyl oxidase	-0,78	0,00694	0,58
DEK	DEK oncogene	-0,78	0,00756	0,58
SMC4	Structural maintenance of chromosomes 4	-0,77	0,00882	0,59
NAA15	N-alpha-acetyltransferase 15, NatA auxiliary subunit	-0,77	0,00882	0,59
G2E3	G2/M phase-specific E3 ubiquitin-protein ligase	-0,77	0,00882	0,59
KNL1	kinetochore scaffold 1	-0,77	0,00882	0,59
MPHOSPH8	M-phase phosphoprotein 8	-0,76	0,00882	0,59
NRIP1	nuclear receptor interacting protein 1	-0,76	0,00882	0,59
TPR	translocated promoter region (to activated MET oncogene)	-0,76	0,00982	0,59
GPAM	Glycerol-3-phosphate acyltransferase 1, mitochondrial	-0,75	0,01176	0,59

Symbol	Name	logFC	adj. p-value	FC
NMNAT2	nicotinamide nucleotide adenylyltransferase 2	-0,75	0,01197	0,59
GAPVD1	GTPase activating protein and VPS9 domains 1	-0,75	0,01197	0,59
WNT5A	wingless-type MMTV integration site family, member 5A	-0,75	0,01217	0,6
CLSTN1	calsyntenin 1	-0,74	0,01427	0,6
VKORC1L1	Vitamin K epoxide reductase complex subunit 1-like protein 1	-0,74	0,01462	0,6
LRRFIP1	Leucine rich repeat (in FLII) interacting protein 1	-0,73	0,01595	0,6
TPM4	tropomyosin 4	-0,73	0,01595	0,6
SMC2	Structural maintenance of chromosomes protein 2 chromosome-associated protein E mRNA	-0,73	0,01746	0,6
CDC27	Cell division cycle 27 homolog	-0,72	0,02023	0,61
BCLAF1	BCL2-associated transcription factor 1	-0,71	0,02322	0,61
PARP1	Poly (ADP-ribose) polymerase 1	-0,71	0,02358	0,61
HACD2	very-long-chain (3R)-3-hydroxyacyl-CoA dehydratase 2	-0,71	0,02358	0,61
GJC1	gap junction protein, gamma 1	-0,7	0,02742	0,61
MYH10	gyosin, heavy chain 10, non-muscle	-0,7	0,02833	0,61
VARS	valyl-tRNA synthetase	-0,7	0,02869	0,62
RECQL	truncated helicase isoform	-0,7	0,02955	0,62
MAP4K4	mitogen-activated protein kinase kinase kinase kinase 4	-0,7	0,03037	0,62
EEA1	early endosome antigen 1	-0,69	0,03237	0,62
MED18	mediator complex subunit 18	-0,69	0,03321	0,62
BAZ1B	bromodomain adjacent to zinc finger domain, 1B	-0,69	0,03379	0,62
SLC4A8	solute carrier family 4, sodium bicarbonate cotransporter, member 8	-0,69	0,03491	0,62
SBNO1	protein strawberry notch homolog 1	-0,69	0,03491	0,62
NDRG4	NDRG family member 4	-0,69	0,03491	0,62
SLC25A36	solute carrier family 25, member 36	-0,68	0,03681	0,62
ATXN7L3B	ataxin-7-like protein 3B	-0,68	0,03723	0,62
HIPK2	protein kinase HIPK2	-0,68	0,03882	0,62
CDC42BPA	serine/threonine protein kinase PK428	-0,68	0,04122	0,63

Symbol	Name	logFC	adj. p-value	FC
KRAS	V-Ki-ras2 Kirsten rat sarcoma viral oncogene homolog	-0,68	0,04163	0,63
GLIS3	zinc finger protein GLIS3	-0,67	0,04305	0,63
TBX3	T-box transcription factor TBX3	-0,67	0,04328	0,63
DBF4	DBF4 homolog	-0,67	0,04717	0,63
MAP1A	microtubule-associated protein 1A	-0,67	0,04717	0,63
PSD3	PH and SEC7 domain-containing protein 3	-0,67	0,04823	0,63
MXRA8	matrix-remodelling associated 8	0,69	0,03549	1,61
RECK	reversion-inducing-cysteine-rich protein with kazal motifs	0,75	0,01202	1,68
GALNT3	UDP-N-acetyl-alpha-D-galactosamine:polypeptide N-acetylgalactosaminyltransferase 3	0,81	0,00412	1,75

Table 2S. ChIP-seq promoter gene list

Gene	Score	Gene	Score	Gene	Score
ARHGAP39	720,27	BMS1P22	130,99	LOC101929574	106,37
FLJ36000	528,67	GATA5	130,99	LOC400002	105,82
RNA5S2	393,30	MSX1	130,99	TMEM56	105,72
LOC100288778	380,44	ADPGK-AS1	130,32	ZDHHC2	105,06
NDRG1	372,31	HIPK3	129,41	CALM1	104,63
CT47A7	335,55	SRPRB	127,65	ERG	104,00
DUSP5P1	316,66	PASK	125,60	BRSK2	103,96
CT47A2	297,77	LOC105376772	124,99	ZBTB7A	103,53
MIR1302-11	265,29	TTPA	124,64	SPTBN1	103,31
RNA5S5	260,69	PLOD2	123,80	MIR941-3	103,24
DRD5P2	255,95	SYT15	123,74	ARIH1	103,09
WASH3P	251,90	P2RY12	123,61	IRF2BP1	103,04
CT47A1	250,59	UBE2QL1	123,27	SDHAP2	102,24
LOC100507639	246,71	GPAT4	122,85	GAB2	102,21
RNA5S13	241,60	PLEKHF2	122,38	ULK2	102,21
CT47A11	225,05	PTPRT	122,04	USP43	102,21
CT47A9	218,36	EDEM1	120,82	VSX1	102,21
AMZ1	210,98	OPCML	120,59	APC2	101,63
CT47A5	209,55	RB1CC1	119,84	CHST1	101,49
LOC101060524	206,67	RNF170	119,84	SLC2A11	101,43
HNCAT21	201,17	COLEC12	119,75	CANT1	100,48
RNA5S17	196,46	CPEB1-AS1	119,06	HECTD4	100,36
CT47A3	189,39	PACS1	118,16	RCN1	100,18
KCNB1	188,68	TTLL9	117,92	MIR6071	99,83
CT47A6	186,55	MIR6726	116,50	FAM129B	98,55
NTRK3	185,06	PHF3	116,50	LINC01467	98,37
SLC18A3	168,39	GPC1	115,71	ABHD18	98,33
TCEB3C	167,67	ORAI1	115,56	C1QL4	98,33
ACVRL1	163,58	PPP1R9B	115,13	GATAD2A	98,33
ZDHHC22	162,79	C1GALT1	114,93	MAN1A2	98,33
HYAL1	160,47	KHDRBS3	114,92	PALM2-AKAP2	98,33
WASH5P	160,34	HR	114,07	TMEM171	98,33
BHLHE23	154,81	CPAMD8	112,35	TP53I11	98,33
CYFIP2	153,86	PUS7	112,10	PLEKHF1	98,22
BSG	150,09	UBE2L3	111,89	KRTAP2-2	98,02
SELENOO	149,43	PCMTD2	111,53	KRTAP2-4	98,02
SCHLAP1	147,04	FAM230C	111,05	HENMT1	97,96
LINC01925	147,02	RNF135	109,84	CROCCP2	97,77
AGTPBP1	144,01	NSG1	109,76	ARCN1	97,58
BOLA2	143,60	FASN	109,44	KLRG2	97,13
ELOA3B	142,12	LOC107161159	108,75	CDH4	97,10
BOLA2-SMG1P6	141,94	TLX3	108,55	CHSY1	96,80
MPPE1	134,97	LINC01160	108,24	CD47	96,74

Gene	Score	Gene	Score	Gene	Score
NR6A1	96,28	TMEM178A	87,93	FOXE1	81,22
CENPVL1	96,11	PIEZO2	87,70	CNIH2	81,20
CEP170B	95,83	RRAS2	87,65	NPTXR	81,16
LINC00472	95,39	TAF5	87,26	EXOC6	81,13
DPY19L2P3	95,20	SLC16A6	87,18	CNTN4	81,01
DYNC1H1	94,89	RAB6B	87,00	GRIK3	81,01
KCTD15	94,79	ADGRL1	86,60	SNORA70	80,79
DENND3	94,50	AFG3L2	86,46	RNF180	80,41
LINC01003	94,48	SAMD15	86,37	VDAC1	80,34
PTBP1	94,27	CREBBP	86,35	PLEKHD1	80,28
STAC2	94,21	HTR4	86,08	PGM5P4-AS1	80,17
ANXA4	93,87	MAFB	85,92	SMA4	80,09
COTL1	93,56	RASL11B	85,70	LINC01667	80,07
PRELID3B	92,82	GATM	85,63	ADGRA1	79,93
SBF2	92,20	GOLGA2P10	85,43	RTN1	79,80
TAZ	91,90	ABR	85,36	SPON1	79,80
INSR	91,88	BLVRA	85,36	CRIP2	79,75
SLC35G5	91,50	ANKS1B	85,15	EXTL3	79,68
TRAPPC5	91,20	LINC00869	85,15	HS3ST3A1	79,58
PAX8-AS1	90,99	LINC01138	85,15	EGR2	79,10
NFKBIZ	90,81	LOC727751	85,15	SEMA7A	79,10
LYNX1	90,56	SLC24A3	85,15	SPTAN1	79,08
ABCC3	90,31	TMEM189-UBE2V1	85,15	FRMD3	78,64
DUSP28	90,01	ZNF318	85,15	TAF4B	78,64
LINC01647	89,74	USP22	85,14	SLC2A13	78,49
N4BP2L1	89,74	TAF1	84,82	CHST15	78,41
PLIN2	89,74	SLCO4A1	84,62	MRPS34	78,41
SOWAHD	89,58	GLDN	84,43	NSFL1C	78,32
C10orf11	89,56	TMEM132E	84,39	MAPRE1	78,10
SYNDIG1	89,14	FAM170A	84,22	ANKRD20A1	78,00
TRAM1	88,88	ANKRD13A	84,13	CTAG2	78,00
EPC2	88,86	OSBPL6	84,01	DOCK9	78,00
CCND3	88,75	DND1	83,00	FAM120B	78,00
ZNF362	88,74	PPP1R16B	82,56	FRMD8	78,00
INPP5A	88,63	RNPS1	82,27	GZF1	78,00
P4HA2	88,63	KRTAP2-3	82,20	HUS1B	78,00
MPST	88,39	SLC16A3	82,01	TH2LCRR	78,00
CTAG1A	88,33	CADM1	81,90	THEM6	78,00
SCO2	88,16	VEGFA	81,62	PARD6B	77,96
CORO7	88,01	VWC2	81,56	CT47B1	77,92
ERAS	88,01	LRBA	81,43	NCOA5	77,81
FNBP1	88,01	POLR2L	81,43	FNDC3B	77,78
LOC105369879	87,93	SBSPON	81,26	BOC	77,74

Gene	Score	Gene	Score	Gene	Score
ZNF571-AS1	77,61	RIMS2	75,09	LHFPL2	71,93
NCLN	77,52	UCN	74,97	SLC6A1	71,93
ADAMTS19-AS1	77,30	LPAR1	74,92	TSPAN11	71,93
CORO1C	77,30	DEGS1	74,87	MIR215	71,89
PDE1C	77,30	KLC1	74,77	AMMECR1L	71,68
PPP1R3F	77,30	FGF12-AS3	74,66	SCRN1	71,68
DOCK3	77,20	KANK4	74,65	SMARCB1	71,68
DLG5-AS1	77,09	SDK2	74,64	WNT9A	71,51
ABCA5	77,08	ANKRD36C	74,54	ZBTB16	71,44
RIN3	77,08	SLC35G1	74,54	RNF157	71,42
ASAP2	76,99	BLACE	74,43	TGIF2	71,38
TMEFF1	76,98	CDR2L	74,41	TMEM52	71,19
WHAMMP3	76,98	MTURN	74,37	WDR17	71,19
METRN	76,87	SIMC1	74,33	SUV39H2	71,13
CPSF4	76,67	LOC101927502	74,27	CGNL1	70,95
GPRIN3	76,67	BAALC-AS2	74,21	LZTS3	70,92
WWC2-AS2	76,64	ZNF517	74,13	TRIM7	70,88
LOC105374366	76,44	KRAS	74,12	MIR7108	70,79
PROKR1	76,43	CTNNBIP1	74,10	VASN	70,71
GRK2	76,39	MIR6087	74,10	OLFM2	70,64
TMEM179B	76,38	SNTA1	73,85	LINC00094	70,52
GRIN3A	76,22	FRA10AC1	73,73	GPR83	70,47
JAM3	76,22	STX3	73,58	LKAAEAR1	70,35
DNAI2	76,21	CTHRC1	73,36	LARGE2	70,34
D2HGDH	75,90	ZMAT3	73,15	GPX4	70,32
ARHGEF4	75,80	ITGB3	73,00	MIR1302-3	70,30
DDX25	75,80	ZFAND5	73,00	DVL1	70,23
FAM127B	75,53	DAPK1	72,95	TXNDC11	70,15
LOC729732	75,46	TYSND1	72,95	LINC01554	70,14
ANKRD10	75,38	KIF2C	72,90	UBE2G1	70,14
AKT1	75,37	GJA3	72,81	HN1L	70,10
BZW1	75,37	TAF10	72,81	TTC9B	69,83
CTSD	75,37	ATOH8	72,73	PRTG	69,77
DOCK1	75,37	FAM57A	72,72	SLC35C1	69,77
ENDOD1	75,37	XPNPEP1	72,72	WEE1	69,72
HLF	75,37	HPS6	72,69	MIR4650-2	69,67
RPS17	75,37	SAMD1	72,69	PHLDA3	69,66
RUNX1T1	75,37	MCAT	72,55	RNA5-8S5	69,59
UCK2	75,37	FLJ16779	72,41	CCSER1	69,54
HM13-AS1	75,36	DGKZ	72,33	NR3C1	69,54
HMGA1	75,18	PDE4A	72,18	RP9	69,46
ZC3H12C	75,16	CEBPB	72,12	DCUN1D2	69,43
ADORA2B	75,10	PGAM5	72,02	LRRC24	69,42
KDSR	75,09	FNBP4	71,95	PYGO1	69,32

Gene	Score	Gene	Score	Gene	Score
CACNA1C-AS2	69,27	ARL6IP4	67,74	SLC1A4	66,31
RIMKLA	69,27	NELFB	67,71	ADCY1	66,11
SLC45A3	69,27	GALNT12	67,67	DHRS11	66,11
ZNF316	69,27	RNA28S5	67,61	RGMB-AS1	66,11
AMER3	69,24	LANCL2	67,56	TAP2	66,11
NOTCH2NL	69,22	LINC01671	67,56	LINC00672	66,02
MIR320E	69,19	CEBPA-AS1	67,53	KRTAP2-1	66,01
ATP9B	69,09	KIF21A	67,42	CDHR2	65,98
DLX4	69,09	C1orf229	67,35	MGAT4A	65,91
FGD5-AS1	69,08	CREG1	67,35	TARM1	65,91
GLIPR2	69,08	FABP5	67,35	THBD	65,91
GRSF1	69,08	LDLRAP1	67,35	CDCA4	65,80
MAN2A2	69,08	GSPT1	67,32	MCRIP2	65,76
ZDHHC18	69,08	CAMKK1	67,21	BACH1	65,71
NOTCH2	68,85	BNIP3	67,20	LINC01363	65,71
SOX12	68,85	DUSP16	67,20	ME1	65,71
MGRN1	68,73	PVT1	67,20	PKD1P6-NPIPP1	65,71
SLC2A8	68,64	SLC39A14	67,20	RPRML	65,71
SLC25A37	68,56	CHL1-AS2	67,14	SH2D4A	65,71
SOCS1	68,48	FAM150A	67,14	CD164	65,51
ASPG	68,42	NRIP3	67,14	HS3ST2	65,51
VGLL3	68,42	PANK1	67,14	INPP5E	65,51
ARHGEF6	68,35	PPP2R2D	67,14	LRRFIP1	65,51
ACTL10	68,34	HES6	67,10	RNF175	65,51
ADCY5	68,34	LOC101927666	67,10	KATNBL1	65,43
AKAP7	68,34	COL4A2	66,93	STAT5B	65,27
LOC105371328	68,34	EN2	66,93	MIR31HG	65,12
LY6E	68,34	GSG1L	66,93	SYDE2	65,12
PLXNB1	68,34	LOC102724511	66,93	GKAP1	65,03
PYCR1	68,34	NXPH4	66,93	ARV1	64,92
SAMD4A	68,34	TOMM40	66,93	HEY2	64,92
ACSBG2	68,31	ZNF341	66,83	PLEC	64,92
RNU5A-1	68,31	SGPP1	66,80	PROB1	64,92
MMP23A	68,24	GLRB	66,72	YPEL2	64,92
RAI14	68,20	PFN2	66,72	FADD	64,73
PFN1	68,05	ZNF860	66,72	LOC101927815	64,73
NOMO1	68,04	NETO2	66,69	PLCL2	64,73
PDIA3	67,99	FARP1	66,52	PLLP	64,73
RASA3	67,99	CDIP1	66,51	RALYL	64,73
TOP1	67,96	MOXD1	66,51	IQCH-AS1	64,71
LBX1	67,77	LYPLA1	66,46	BEX2	64,54
LOC642361	67,77	UBE2Q1	66,38	DSC3	64,54
SYNJ2	67,77	ACTN3	66,31	GLP1R	64,54
ZPBP2	67,77	KIAA1024	66,31	LOC100505938	64,54

Gene	Score	Gene	Score	Gene	Score
LTBP2	64,54	MIR429	63,79	SLC39A13	61,58
RARB	64,54	SRGAP1	63,79	CDC20B	61,49
SLC27A2	64,54	UCHL1-AS1	63,79	CALM3	61,45
RBPMS2	64,43	HGSNAT	63,76	CLCN2	61,44
APOOL	64,35	ECI1	63,63	DOCK5	61,44
C17orf107	64,35	RNF216	63,61	GMDS	61,44
ELOB	64,35	MMP17	63,54	MIR1302-9	61,44
LEPROTL1	64,35	NACC2	63,53	PLEKHG5	61,44
PHLDA2	64,35	PLCG1	63,53	LOC100130849	61,37
RNF165	64,35	SLC43A2	63,53	SURF4	61,37
RPL36	64,35	SREBF1	63,53	SYCE1	61,34
RUNX1	64,35	CCDC57	63,42	ERAP1	61,30
TCF3	64,35	HIVEP2	63,42	MTMR12	61,29
TTLL3	64,35	KCTD1	63,42	CSNK1G2	60,96
ARSB	64,34	LOC339166	63,42	TANGO2	60,93
B4GALNT2	64,18	SH3RF3-AS1	63,42	LOC375196	60,90
FRG1BP	64,18	GPR68	63,39	DFFB	60,75
MTHFD1L	64,18	FOXK2	63,35	LOC101927588	60,75
CTXN1	64,16	PBX4	63,26	MIR8085	60,75
FLT1	64,16	TUBB2A	63,26	NDUFAF6	60,75
FNDC4	64,16	ZBTB7C	63,20	LTB4R	60,66
FZD2	64,16	ANGEL2	63,15	LYN	60,62
HNRNPDL	64,16	FLII	63,12	ZXDC	60,58
IQSEC3	64,16	COL4A3	63,05	CHD7	60,56
MEGF6	64,16	FZD8	63,05	KLHL42	60,56
MTUS1	64,16	LMO1	63,05	FAM53A	60,53
NNT	64,16	BMP7	62,99	GOLGA2P7	60,53
PAWR	64,16	TBX21	62,90	LOC100133669	60,53
RGMB	64,16	NUDT14	62,68	BOLL	60,37
ST8SIA5	64,02	ZXDA	62,61	ZFAND4	60,37
UBAC1	64,02	OGFRL1	62,50	PRKCI	60,33
KCNQ1OT1	63,97	PPP1R36	62,48	GABBR2	60,20
MAP3K14	63,97	UBXN2A	62,47	NINL	60,06
NBEA	63,97	EVA1C	62,41	SLC16A10	60,06
NPFFR1	63,97	ZNF532	62,41	XYLT1	60,04
NT5DC3	63,97	MIR6720	62,14	MCF2L2	59,89
PTPRS	63,97	CPSF1	62,10	ISPD	59,84
RUNX2	63,97	PIK3CA	62,08	FGF4	59,83
SCLY	63,97	MADD	62,07	PPP1CA	59,78
TMEM80	63,97	RNF24	62,04	CIZ1	59,69
MIR6740	63,92	POLR3C	61,88	MIR1972-1	59,66
TP53INP2	63,82	ARID1A	61,82	RASSF2	59,62
DNAJC6	63,79	EBF3	61,72	NOMO2	59,46
HOXD9	63,79	YWHAG	61,72	NOMO3	59,46

Gene	Score	Gene	Score	Gene	Score
PIM3	59,40	ARFRP1	58,00	PPM1A	55,76
LOC729652	59,25	MIR3187	57,94	FOXN3	55,75
EXOC3	59,21	MTA2	57,91	KLHL21	55,72
ARNTL2	59,05	ACSL1	57,84	ARHGAP27	55,69
BOK-AS1	59,05	C3orf67	57,70	DDX51	55,69
CEBPD	59,05	ERN1	57,70	HERC2	55,69
CHD5	59,05	PTPRU	57,70	OSBP	55,69
DKFZP434L187	59,05	KLF15	57,68	MARCH2	55,68
ELOA2	59,05	CACNA1F	57,67	PPP1R3G	55,67
FECH	59,05	MXD4	57,67	FAM160B1	55,54
GJB6	59,05	SART1	57,67	APPL2	55,53
GUSBP3	59,05	C14orf177	57,57	INA	55,53
KMT2B	59,05	LOC389906	57,57	RRP1B	55,43
LINC00623	59,05	NIPAL2	57,57	CT47A10	55,42
LINC01194	59,05	TRIB1	57,52	CTBP1	55,35
LOC101928565	59,05	TMEM245	57,48	DOC2B	55,34
LY6K	59,05	MLST8	57,47	EZR-AS1	55,34
MRGPRX3	59,05	TPBGL	57,46	SORBS3	55,27
NPY4R	59,05	LOC105376671	57,43	LMX1B	55,23
POTEH	59,05	MIR6819	57,26	LOC644794	55,23
SLC4A11	59,05	DNHD1	57,09	PRR23B	55,23
SMA5	59,05	HES5	57,09	NBPF1	55,18
SMIM10L1	59,05	PRR23A	57,09	KCTD18	55,16
SNRK	59,05	PGD	57,03	RMI2	55,07
SPRN	59,05	SHCBP1L	56,94	TSPAN10	55,07
TBC1D30	59,05	KMT5B	56,89	GRHL1	54,97
VANGL1	59,05	PPP1R9A	56,85	MYO1E	54,97
WDR5	59,05	KIAA1841	56,73	PAXIP1-AS1	54,97
WNK1	59,05	PHF20L1	56,54	TSPY26P	54,81
C1orf159	58,96	CRNDE	56,50	BMP2	54,79
SLC13A3	58,91	TBX20	56,50	HES4	54,79
FAM98C	58,84	TESC-AS1	56,50	PATL1	54,79
SPEG	58,84	KCNK3	56,43	PXMP2	54,79
FOXC2-AS1	58,76	ASAP1	56,40	RNF126	54,79
CDC42EP1	58,74	CXADRP3	56,30	LOC202181	54,74
CDH22	58,55	OLFML2A	56,16	MGAT5B	54,60
SLTM	58,52	B4GALT2	56,11	SERPINA3	54,48
NLRP7	58,45	DNAJC11	56,11	FDX1	54,46
SHB	58,42	LINC01792	56,11	FOXA2	54,42
PARP12	58,33	ELP5	55,93	GGTA1P	54,34
PITPNC1	58,11	HNRNPAB	55,92	CTPS1	54,09
NCOA6	58,10	PKD1P1	55,90	GIT1	54,09
C9orf69	58,01	ATP2B1-AS1	55,86	GTF2I	54,09
STK3	58,01	PRSS23	55,82	NPTX1	54,09

Gene	Score	Gene	Score	Gene	Score
SOCS6	54,09	EBF4	51,29	KLHL30	50,16
TMEM44	54,09	FAM106CP	51,29	LINC00508	50,16
WDR53	54,09	RHOB	51,29	LOC100131532	50,16
ZNF395	54,09	SLC7A2	51,29	LOC101928386	50,16
RTN4RL1	54,06	CBFA2T2	51,10	LOC101929151	50,16
FZD1	53,89	FANK1	51,10	LOC103091866	50,16
ZBTB8A	53,89	MAN1C1	51,05	MEX3B	50,16
GPM6B	53,75	TBC1D12	51,04	MIR7844	50,16
GUSBP11	53,72	KIAA1958	50,88	NTSR1	50,16
GFOD1	53,71	PRPH	50,75	NUDT18	50,16
TRIO	53,54	FRAT1	50,71	OCM2	50,16
VAMP2	53,53	HBZ	50,71	OR2H1	50,16
PPM1M	53,32	SLC25A33	50,68	OSBPL5	50,16
TMEM170B	53,30	CHRD	50,56	PDIA6	50,16
POU3F1	53,17	LINC00461	50,47	PKP2	50,16
DRD5	53,01	SETD3	50,34	PLXNC1	50,16
HPN-AS1	53,01	CDT1	50,25	PTMS	50,16
RGS17	53,01	FAM83C	50,25	RASGEF1A	50,16
SLC6A8	53,01	LOC101930370	50,25	SRRM1	50,16
CABLES1	52,98	ANKRD6	50,16	ST3GAL5	50,16
LINC01214	52,67	CCNY	50,16	STYXL1	50,16
MATN2	52,64	CT62	50,16	VENTX	50,16
P4HB	52,64	DNAAF2	50,16	WNK2	50,16
PKIG	52,61	DRAM1	50,16	ZFX	50,16
LDLRAD4	52,54	FOXJ1	50,16	NLRP2	50,09
CD19	52,42	FOXO6	50,16	KIF17	50,06
NR2F6	52,26	GATS	50,16	TMCC3	50,06
COASY	51,95	GBX2	50,16	TNK2	50,02
OR5AC2	51,30	GRPEL2	50,16		
CADM2	51,29	IGFBP4	50,16		

Table 3S. Identified nuclear Gal-1 partners by MS

UniProt	Gene Symbol	Name
P84103	SRSF3	serine and arginine rich splicing factor 3
Q9NUC0	SERTAD4	SERTA domain containing 4
P55735	SEC13	SEC13 homolog, nuclear pore and COPII coat complex component
Q14974	KPNB1	karyopherin subunit beta 1
P11388	TOP2A	topoisomerase (DNA) II alpha
O00534	VWA5A	von Willebrand factor A domain containing 5A
Q8N3X1	FNBP4	formin binding protein 4
Q9Y230	RUVBL2	RuvB like AAA ATPase 2
P78527	PRKDC	protein kinase, DNA-activated, catalytic polypeptide
P84101	SERF2	small EDRK-rich factor 2
P84243	H3F3A	H3 histone family member 3A
Q96PK6	RBM14	RNA binding motif protein 14
Q14498	RBM39	RNA binding motif protein 39
O95373	IPO7	importin 7
P28340	POLD1	DNA polymerase delta 1, catalytic subunit
Q8WXH0	SYNE2	spectrin repeat containing nuclear envelope protein 2
Q92539	LPIN2	lipin 2
Q8WU68	U2AF1L4	U2 small nuclear RNA auxiliary factor 1 like 4
Q9H307	PNN	pinin, desmosome associated protein
P09382	LGALS1	galectin 1
P57740	NUP107	nucleoporin 107
Q460N5	PARP14	poly(ADP-ribose) polymerase family member 14
Q6ZU35	KIAA1211	KIAA1211
Q05481	znf91	zinc finger protein 91
Q9GZS1	POLR1E	RNA polymerase I subunit E
Q96SB3	PPP1R9B	protein phosphatase 1 regulatory subunit 9B
O94885	SASH1	SAM and SH3 domain containing 1
Q5BKZ1	ZNF326	zinc finger protein 326
O60318	MCM3AP	minichromosome maintenance complex component 3 associated protein
Q96FS4	SIPA1	signal-induced proliferation-associated 1
Q8IY81	FTSJ3	FtsJ homolog 3
Q86V48	LUZP1	leucine zipper protein 1
O00541	PES1	pescadillo ribosomal biogenesis factor 1
O95983	MBD3	methyl-CpG binding domain protein 3
O00567	NOP56	NOP56 ribonucleoprotein

UniProt	Gene Symbol	Name
P22087	FBL	fibrillarin
O60216	RAD21	RAD21 cohesin complex component
P16401	HIST1H1B	histone cluster 1 H1 family member b
P50748	KNTC1	kinetochore associated 1
Q14764	MVP	major vault protein
P43243	MATR3	matrin 3
Q15649	ZNHIT3	zinc finger HIT-type containing 3
Q5VWX1	KHDRBS2	KH RNA binding domain containing, signal transduction associated 2

A

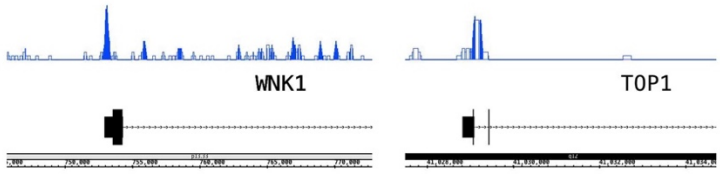
WNK1
TOP1

B

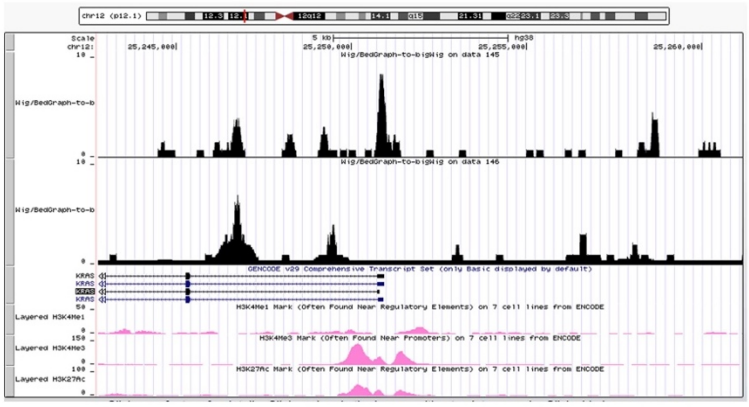
GENCODE v29 Comprehensive Transcript Set (only Basic displayed by default)
H3K4Me1 Mark (Often Found Near Regulatory Elements) on 7 cell lines from ENCODE
H3K4Me3 Mark (Often Found Near Promoters) on 7 cell lines from ENCODE
H3K27Ac Mark (Often Found Near Regulatory Elements) on 7 cell lines from ENCODE

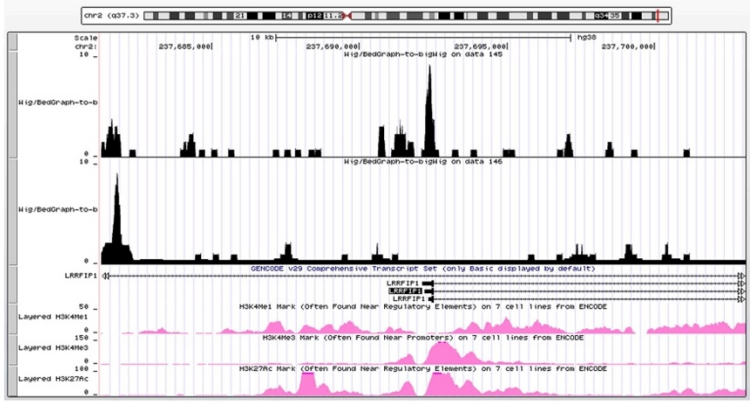
GENCODE v29 Comprehensive Transcript Set (only Basic displayed by default)
H3K4Me1 Mark (Often Found Near Regulatory Elements) on 7 cell lines from ENCODE
H3K4Me3 Mark (Often Found Near Promoters) on 7 cell lines from ENCODE
H3K27Ac Mark (Often Found Near Regulatory Elements) on 7 cell lines from ENCODE

C

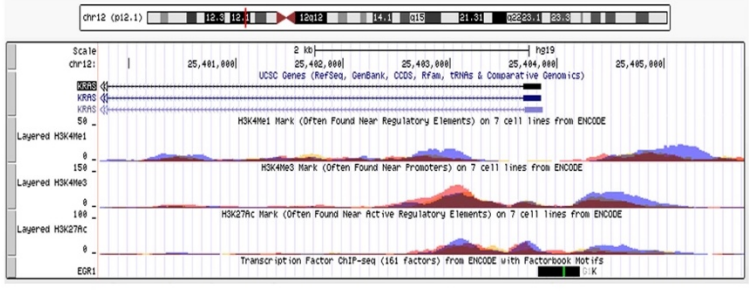
UCSC Genes (RefSeq, GenBank, CCDS, Rfam, tRNAs & Comparative Genomics)
H3K4Me1 Mark (Often Found Near Regulatory Elements) on 7 cell lines from ENCODE
H3K4Me3 Mark (Often Found Near Promoters) on 7 cell lines from ENCODE
H3K27Ac Mark (Often Found Near Active Regulatory Elements) on 7 cell lines from ENCODE
Transcription Factor ChIP-seq (161 factors) from ENCODE with Factorbook Motifs

Figure 1S. MACS peaks analysis. A) MACS peaks of mapped on *WNK1* and *TOP1* promoter regions. B) H3K4Me1, H3K4Me3 and H3K27Ac marks were used as controls of promoter regulatory elements for *KRAS* (top) and *LRRFIP1* (bottom) promoters. C) MACS peak on *KRAS* promoter from an EGR1 ChIP seq. Coloured regions indicate H3K4Me1, H3K4Me3 and H3K27Ac regions of promoter regulatory elements.

ABBREVIATIONS

aa	amino acid
ABC	ammonium bicarbonate
Ac	acetylation
ACTR2	actin-related protein 2
ADM	acinar-to-ductal metaplasia
APC	adenomatous polyposis coli protein
ARX	homeobox protein ARX
ARTX	transcriptional regulator ARTX
α-SMA	smooth muscle actin alpha
BCLAF1	Bcl-2-associated transcription factor 1
bFGF	basic fibronectin growth factor
BMDC	bone marrow-derived cells
Bp	base pair
BRCA2	breast cancer type 2 susceptibility protein homolog
BRN4	brain-4
BSA	bovine serum albumin
BSL-2	biosafety level 2 room
c-MYC	myelocymatosis viral oncogene
CA19-9	carbohydrate antigen 19-9
CAC	centro-acinar cells
CAF	carcinoma associated fibroblast
CAR-T	chimeric antigen receptor T cells
CD	cluster of differentiation
CDKN2A	cyclin-dependent kinase inhibitor 2A
CEA	carcinoembryonic antigen
ChIP	chromatin immunoprecipitation
CINC1	cytokine-induced neutrophil chemoattractant-1
CLB	cell lysis buffer
CM	conditioned medium
COL1A1	collagen alpha-1(I) chain
CP	chronic pancreatitis
CPA1	carboxypeptidase A1
CRD	carbohydrate recognition domain
CSC	cancer stem cell
CT	computer tomography
CTGF	connective tissue growth factor
CTLA4	cytotoxic T-lymphocyte associated protein 4
CXCL2	C-X-C motif chemokine 2
CXCR4	C-X-C chemokine receptor type 4
DAPI	5',6-diamidino-2-phenylindole
DAVID	database for annotation, visualization and integrated discovery
DMEM	Dulbecco's Modified Eagle's Medium
DNA	deoxyribonucleic acid
E	embryonic day
EC	endothelial cells
ECM	extracellular matrix

EGF	epidermal growth factor
EGFR	epidermal growth factor receptor
EGR1	early growth response protein 1
Ela	elastase
ELISA	enzyme-linked immunosorbent assay
EMT	epidermal-to-mesenchymal transition
ERBB2	receptor tyrosine-protein kinase erbB-2
ERK	extracellular signal-regulated kinase
EUS	endoscopic ultrasonography
FAP	fibroblast activating protein
FBS	fetal bovine serum
FCS	fetal calf serum
FDA	food and drug administration
FGF	fibroblast growth factor
FN	fibronectin
FOLFIRINOX	folinic acid, 5-fluorouracil [5-FU], irinotecan, and oxaliplatin
FOS	proto-oncogene c-Fos
FOXP3	forkhead box protein 3
FW	forward
Gal-1	galectin-1
GEM	gemcitabine
GFAP	glial fibrillary acidic protein
GO	gene ontology
GTP	guanosine triphosphate
HA	hyaluronic acid
HEK-293	human embryonic kidney 293 cells
HES1	hairy and enhancer of split 1
Hh	hedgehog
HIF-1α	hypoxia inducible factor 1α
HNF1b	hepatocyte nuclear factor 1-beta
HNF6	hepatocyte nuclear factor 6
HPSC	human pancreatic stellate cells
HRas	Harvey rat sarcoma viral oncogene homolog
HRP	horseradish peroxidase
hTERT	human telomerase reverse transcriptase
IF	immunofluorescence
IFN	interferon
IFP	interstitial fluid pressure
IGB	integrated genome browser
IgG	immunoglobulin G
IHC	immunohistochemistry
IL	interleukin
IP	immunoprecipitation
IPMN	intraductal papillary mucinous neoplasm
LRRFIP1	leucine-rich repeat flightless-interacting protein 1
JAK	janus kinases

KD	knockdown
KPC	*LSL-Kras$^{G12D/+}$;LSL-Trp53$^{R172H/+}$;Pdx-1-Cre* mice
KO	knockout
KRas	Kirsten rat sarcoma viral oncogene homolog
LacNAc	N-acetyllactosamine
LEF1	lymphoid enhancer-binding factor 1
LIMMA	linear of models for microarray
Mac-2BP	Mac-2 binding protein
MACS	model-based analisys of chip-seq
MAFB	transcription factor MafB
MAPK	mitogen-activated protein kinases
MEME	Multiple Em for Motif Elicitation
MCN	mucinous cystic neoplasm
MCP1	monocyte chemoattractant protein 1
MDM2	E3 ubiquitin-protein ligase Mdm2
MDSC	myeloid-derived suppressor cells
Me	methylation
MHC	major histocompatibility complex
MIC1	macrophage inhibitory cytokine 1
MIST1	muscle, intestine and stomach expression 1
MMP	matrix metalloproteinases
mRNA	messenger ribonucleic acid
MRI	magnetic resonance imaging
MS	mass spectrometry
MTT	3-(5,5-dimethylthiazol-2-yl)-2,5-diphenyltetrazolium bromide
NAB	nanoparticle albumin-bound
NEUROG3	neurogenin-3
NF-kβ	nuclear factor kappa β
NHPPE	nuclease hypersensitive polypurine-polypyrimidine element
NK	natural killer cells
NKX6.1	homeobox protein Nkx-6.1
NLB	nuclear lysis buffer
NR5A2	nuclear receptor subfamily 5 group A member 2
NRP1	neuropilin 1
O/N	overnight
OPN	osteopontin
OptiMEM	Opti-minimal essential medium
PARP14	poly [ADP-ribose] polymerase 14
PanIN	pancreatic intraepithelial neoplasia
PanNET	pancreatic neuroendocrine tumors
PBS	phosphate buffered saline
PC	pancreatic cancer
PCR	polymerase chain reaction
PD1	programmed cell death protein 1
PDA	pancreatic ductal adenocarcinoma
PDGF	plateled-derived growth factor

PDL1	programmed cell death protein ligand 1
PDX1	pancreatic and duodenal homeobox 1
PEG	polyethylene glycol
PEI	polyethylenimine
PFA	paraformaldehyde
PFS	progression-free-survival
PI3K	phosphoinositide 3 kinase
PP cell	pancreatic polypeptide cell
Pro-24	protocadherin-24
PRSS	serine protease 1 (trypsin 1)
PSC	pancreatic stellate cells
PTF1A	pancreas transcription factor 1a
PyMT	polyoma virus middle T
RBP-J_L	recombining binding protein suppressor of hairless-like protein
RNA	ribonucleic acid
ROS	reactive oxygen species
RT	room temperature
RTqPCR	real time quantitative PCR
RV	reverse
SCA	serous cystadenomas
SDS	sodium dodecyl sulfate
SEM	standard error of the mean
Seq	sequencing
SHH	sonic hedgehog
shRNA	small hairpin RNA
siRNA	small interference RNA
SMAD4	mothers against decapentaplegic homolog 5
SMN	survival motor neuron
snRNP	small nuclear ribonucleoproteins
Sox9	sry-box 9
SPARC	secreted protein acidic and rich in cysteine
SPN	solid-pseudopapillary neoplasms
SV40	simian vacuolating virus 40
TACC1	transforming acidic coiled-coil-containing protein 1
TAg	T antigen
TAM	tumor associated macrophages
TAN	tumor associated neutrophils
TBS	tris buffered saline
TBS-T	TBS Tween 20
TCR	T cell receptor
TF	transcription factor
TGF	transforming growth factor
Th	T helper
TIL	tumor infiltrated lymphocytes
TIM	T cell immunoglobulin mucin
TIMP	tissue inhibitor of metalloproteinases

TME	tumor microenvironment
TNF	tumor necrosis factor
TOP1	DNA topoisomerase 1
Treg	T regulatory
TP53	cellular tumor antigen p53
tPA	tissue plasminogen activator
TTF-I	thyroid-specific transcription factor
TSS	transcription start site
UCSC	university of California Santa Cruz
UTR	untranslated region
VEGF	vascular endothelial growth factor
VEGFR	vascular endothelial growth factor receptor
vSMC	vascular smooth muscle cells
WB	western blot
WNK	serine/threonine-protein kinase WNK (with no lysine)
WNT	wingless proto-oncogene integration
WT	wild type

REFERENCES

1. Treuting, P. M., Dintzis, S. M. & Montine, K. S. *Comparative Anatomy and Histology*. (Mica Haley, 2018).

2. Dolenšek, J., Rupnik, M. S. & Stožer, A. Structural similarities and differences between the human and the mouse pancreas. *Islets* (2015). doi:10.1080/19382014.2015.1024405

3. Larsen, H. L. & Grapin-Botton, A. The molecular and morphogenetic basis of pancreas organogenesis. *Seminars in Cell and Developmental Biology* **66,** 51–68 (2017).

4. Sakhneny, L., Khalifa-Malka, L. & Landsman, L. Pancreas organogenesis: Approaches to elucidate the role of epithelial-mesenchymal interactions. *Semin. Cell Dev. Biol.* (2018). doi:10.1016/j.semcdb.2018.08.012

5. Benitez, C. M., Goodyer, W. R. & Kim, S. K. Deconstructing pancreas developmental biology. *Cold Spring Harb. Perspect. Biol.* **4,** 1–17 (2012).

6. Cano, D. A., Soria, B., Martín, F. & Rojas, A. Transcriptional control of mammalian pancreas organogenesis. *Cellular and Molecular Life Sciences* **71,** 2383–2402 (2014).

7. Bardeesy, N. & DePinho, R. A. Pancreatic cancer biology and genetics. *Nat. Rev. Cancer* **2,** 897–909 (2002).

8. Lennon, A. M. & Wolfgang, C. Cystic Neoplasms of the Pancreas. *J. Gastrointest. Surg.* (2013). doi:10.1007/s11605-012-2072-6

9. Zhang, Q. *et al.* Pancreatic Cancer Epidemiology, Detection, and Management. *Gastroenterology Research and Practice* **2016,** (2016).

10. Bollen, T. L. & Wessels, F. J. Radiological workup of cystic neoplasms of the pancreas. *Visc. Med.* **34,** 182–190 (2018).

11. Rahib, L. *et al.* Projecting cancer incidence and deaths to 2030: The unexpected burden of thyroid, liver, and pancreas cancers in the united states. *Cancer Research* (2014). doi:10.1158/0008-5472.CAN-14-0155

12. Siegel, R. L., Miller, K. D. & Jemal, A. Cancer Statistics, 2019. *CA. Cancer J. Clin.* **69,** 7–34 (2019).

13. American Cancer Society. Cancer Facts & Figures 2019. *Am. Cancer Soc.* (2019).

14. Ilic, M. & Ilic, I. Epidemiology of pancreatic cancer. *World Journal of Gastroenterology* (2016). doi:10.3748/wjg.v22.i44.9694

15. Yadav, D. & Lowenfels, A. B. The epidemiology of pancreatitis and pancreatic cancer. *Gastroenterology* **144,** 1252–1261 (2013).

16. Binkley, C. E. *et al.* The molecular basis of pancreatic fibrosis: Common stromal gene expression in chronic pancreatitis and pancreatic adenocarcinoma. *Pancreas* (2004). doi:10.1097/00006676-200411000-00003

17. T. M. Gress, J. P. Neoptolemos, N. R. Lemoine, F. X. R. *Exocrine pancreas cancer*. *The European Pancreatic Cancer-Research Cooperative* (2004).

18. Hezel, A. F., Kimmelman, A. C., Stanger, B. Z., Bardeesy, N. & Depinho, R. A. Genetics and biology of pancreatic ductal adenocarcinoma. *Genes Dev. 201218–1249* **20,** 1218–1249 (2006).

19. Makohon-Moore, A. & Iacobuzio-Donahue, C. A. Pancreatic cancer biology and genetics from an evolutionary perspective. *Nat. Rev. Cancer* **16,** 553–565 (2016).

20. Morris, J. P., Wang, S. C. & Hebrok, M. KRAS, Hedgehog, Wnt and the twisted developmental biology of pancreatic ductal adenocarcinoma. *Nature Reviews Cancer* (2010). doi:10.1038/nrc2899

21. Bailey, J. M. *et al.* Sonic hedgehog promotes desmoplasia in pancreatic cancer. *Clin. Cancer Res.* (2008). doi:10.1158/1078-0432.CCR-08-0291

22. Mccleary-Wheeler, A. L., Mcwilliams, R. & Fernandez-Zapico, M. E. Aberrant signaling pathways in pancreatic cancer: A two compartment view. *Mol. Carcinog.* (2012). doi:10.1002/mc.20827

23. Kleeff, J. *et al.* Pancreatic cancer. *Nat. Rev. Dis. Prim.* **2,** 1–23 (2016).

24. Hernández-Muñoz, I., Skoudy, A., Real, F. X. & Navarro, P. Pancreatic ductal adenocarcinoma: Cellular origin, signaling pathways and stroma contribution. *Pancreatology* **8,** 462–469 (2008).

25. Wagner, M., Luhrs, H., Kloppel, G., Adler, G. & Schmid, R. M. Malignant transformation of duct-like cells originating from acini in transforming growth factor transgenic mice. *Gastroenterology* (1998). doi:10.1016/S0016-5085(98)70098-8

26. Means, A. L. *et al.* Pancreatic epithelial plasticity mediated by acinar cell transdifferentiation and generation of nestin-positive intermediates. *Development* (2005). doi:10.1242/dev.01925

27. Ferreira, R. M. M. *et al.* Duct- and Acinar-Derived Pancreatic Ductal Adenocarcinomas Show Distinct Tumor Progression and Marker Expression. *Cell Rep.* (2017). doi:10.1016/j.celrep.2017.09.093

28. Yoshida, T. & Hanahan, D. Murine pancreatic ductal adenocarcinoma produced by in vitro transduction of polyoma middle T oncogene into the islets of Langerhans. *Am J Pathol* (1994).

29. Stanger, B. Z. *et al.* Pten constrains centroacinar cell expansion and malignant transformation in the pancreas. *Cancer Cell* (2005). doi:10.1016/j.ccr.2005.07.015

30. Passegué, E., Wagner, E. F. & Weissman, I. L. JunB deficiency leads to a myeloproliferative disorder arising from hematopoietic stem cells. *Cell* (2004). doi:10.1016/j.cell.2004.10.010

31. Bender Kim, C. F. *et al.* Identification of bronchioalveolar stem cells in normal lung and lung cancer. *Cell* (2005). doi:10.1016/j.cell.2005.03.032

32. Maitland, N. J. & Collins, A. A tumour stem cell hypothesis for the origins of prostate cancer. *BJU International* (2005).

doi:10.1111/j.1464-410X.2005.05744.x

33. Blau, H. M., Brazelton, T. R. & Weimann, J. M. The evolving concept of a stem cell: Entity or function? *Cell* (2001). doi:10.1016/S0092-8674(01)00409-3

34. Sharma, A. *et al.* The homeodomain protein IDX-1 increases after an early burst of proliferation during pancreatic regeneration. *Diabetes* (1999). doi:10.2337/diabetes.48.3.507

35. Conroy, T. *et al.* FOLFIRINOX versus Gemcitabine for Metastatic Pancreatic Cancer. *N. Engl. J. Med.* (2011). doi:10.1056/NEJMoa1011923

36. Von Hoff, D. D. *et al.* Increased Survival in Pancreatic Cancer with nab-Paclitaxel plus Gemcitabine. *N. Engl. J. Med.* (2013). doi:10.1056/NEJMoa1304369

37. Garrido-Laguna, I. & Hidalgo, M. Pancreatic cancer: From state-of-the-art treatments to promising novel therapies. *Nature Reviews Clinical Oncology* **12,** (2015).

38. Son, S. H. *et al.* The technical feasibility of an image-guided intensity-modulated radiotherapy (IG-IMRT) to perform a hypofractionated schedule in terms of toxicity and local control for patients with locally advanced or recurrent pancreatic cancer. *Radiat. Oncol.* (2012). doi:10.1186/1748-717X-7-203

39. Pietras, K. & Östman, A. Hallmarks of cancer: Interactions with the tumor stroma. *Exp. Cell Res.* **316,** 1324–1331 (2010).

40. Lin, H. J. & Lin, J. Seed-in-soil: Pancreatic cancer influenced by tumor microenvironment. *Cancers (Basel).* **9,** 1–13 (2017).

41. Chu, G. C., Kimmelman, A. C., Hezel, A. F. & DePinho, R. A. Stromal biology of pancreatic cancer. *J. Cell. Biochem.* **101,** 887–907 (2007).

42. Weniger, M., Honselmann, K. C. & Liss, A. S. The extracellular matrix and pancreatic cancer: A complex relationship. *Cancers (Basel).* **10,** (2018).

43. Özdemir, B. C. *et al.* Depletion of carcinoma-associated

fibroblasts and fibrosis induces immunosuppression and accelerates pancreas cancer with reduced survival. *Cancer Cell* **25,** (2014).

44. Rhim, A. D. *et al.* Stromal elements act to restrain, rather than support, pancreatic ductal adenocarcinoma. *Cancer Cell* (2014). doi:10.1016/j.ccr.2014.04.021

45. Veenstra, V. L., Garcia-Garijo, A., Van Laarhoven, H. W. & Bijlsma, M. F. Extracellular influences: Molecular subclasses and the microenvironment in pancreatic cancer. *Cancers (Basel).* **10,** 1–26 (2018).

46. Pothula, S. P. *et al.* Key role of pancreatic stellate cells in pancreatic cancer. *Cancer Lett.* **381,** 194–200 (2015).

47. Medici, D. & Nawshad, A. Type I collagen promotes epithelial-mesenchymal transition through ILK-dependent activation of NF-κB and LEF-1. *Matrix Biol.* (2010). doi:10.1016/j.matbio.2009.12.003

48. Vaquero, E. C. *et al.* Extracellular matrix proteins protect pancreatic cancer cells from death via mitochondrial and nonmitochondrial pathways. *Gastroenterology* (2003). doi:10.1016/S0016-5085(03)01203-4

49. Michl, P. & Gress, T. M. Improving drug delivery to pancreatic cancer: breaching the stromal fortress by targeting hyaluronic acid. *Gut* **61,** 1377–1379 (2012).

50. Subarsky, P. & Hill, R. P. The hypoxic tumour microenvironment and metastatic progression. *Clinical and Experimental Metastasis* (2003). doi:10.1023/A:1022939318102

51. Commisso, C. *et al.* Macropinocytosis of protein is an amino acid supply route in Ras-transformed cells. *Nature* (2013). doi:10.1038/nature12138

52. Kamphorst, J. J. *et al.* Human pancreatic cancer tumors are nutrient poor and tumor cells actively scavenge extracellular protein. *Cancer Res.* (2015). doi:10.1158/0008-5472.CAN-14-2211

53. Zhao, H. *et al.* Tumor microenvironment derived exosomes

pleiotropically modulate cancer cell metabolism. *Elife* (2016). doi:10.7554/eLife.10250

54. Sousa, C. M. *et al.* Pancreatic stellate cells support tumour metabolism through autophagic alanine secretion. *Nature* (2016). doi:10.1038/nature19084

55. Johnsen, A. K., Templeton, D. J., Sy, M.-S. & Harding, C. V. Deficiency of Transporter for Antigen Presentation (TAP) in Tumor Cells Allows Evasion of Immune Surveillance and Increases Tumorigenesis. *J. Immunol.* (1999).

56. Gabitass, R. F., Annels, N. E., Stocken, D. D., Pandha, H. A. & Middleton, G. W. Elevated myeloid-derived suppressor cells in pancreatic, esophageal and gastric cancer are an independent prognostic factor and are associated with significant elevation of the Th2 cytokine interleukin-13. *Cancer Immunol. Immunother.* (2011). doi:10.1007/s00262-011-1028-0

57. Kurahara, H. *et al.* Significance of M2-polarized tumor-associated macrophage in pancreatic cancer. *J. Surg. Res.* (2011). doi:10.1016/j.jss.2009.05.026

58. Vizio, B. *et al.* Potential plasticity of T regulatory cells in pancreatic carcinoma in relation to disease progression and outcome. *Exp. Ther. Med.* (2012). doi:10.3892/etm.2012.553

59. Song, X., Liu, J., Lu, Y., Jin, H. & Huang, D. Overexpression of B7-H1 correlates with malignant cell proliferation in pancreatic cancer. *Oncol. Rep.* (2014). doi:10.3892/or.2013.2955

60. Bengsch, F., Knoblock, D. M., Liu, A., McAllister, F. & Beatty, G. L. CTLA-4/CD80 pathway regulates T cell infiltration into pancreatic cancer. *Cancer Immunol. Immunother.* (2017). doi:10.1007/s00262-017-2053-4

61. Boone, B. A. *et al.* The receptor for advanced glycation end products (RAGE) enhances autophagy and neutrophil extracellular traps in pancreatic cancer. *Cancer Gene Ther.* (2015). doi:10.1038/cgt.2015.21

62. Martinez-Bosch, N., Vinaixa, J. & Navarro, P. Immune evasion

in pancreatic cancer: From mechanisms to therapy. *Cancers (Basel).* **10,** 1–16 (2018).

63. Cirri, P. & Chiarugi, P. Cancer associated fibroblasts: the dark side of the coin. *Cancer Res* **1,** 482–97 (2011).

64. Hwang, R. F. *et al.* Cancer-associated stromal fibroblasts promote pancreatic tumor progression. *Cancer Res.* **68,** 918–926 (2008).

65. Nielsen, M. F. B., Mortensen, M. B. & Detlefsen, S. Key players in pancreatic cancer-stroma interaction: Cancer-associated fibroblasts, endothelial and inflammatory cells. *World J. Gastroenterol.* **22,** 2678–2700 (2016).

66. Öhlund, D., Elyada, E. & Tuveson, D. Fibroblast heterogeneity in the cancer wound. *J. Exp. Med.* (2014). doi:10.1084/jem.20140692

67. Moir, J. A. G., Mann, J. & White, S. A. The role of pancreatic stellate cells in pancreatic cancer. *Surg. Oncol.* **24,** 232–238 (2015).

68. Erkan, M. *et al.* StellaTUM: current consensus and discussion on pancreatic stellate cell research. *Gut* (2012). doi:10.1136/gutjnl-2011-301220

69. Phillips, P. A. *et al.* Rat pancreatic stellate cells secrete matrix metalloproteinases: Implications for extracellular matrix turnover. *Gut* (2003). doi:10.1136/gut.52.2.275

70. Kl□ppel, G., Detlefsen, S. & Feyerabend, B. Fibrosis of the pancreas: the initial tissue damage and the resulting pattern. *Virchows Arch.* (2003). doi:10.1007/s00428-004-1021-5

71. Dvorak, H. F. Tumors: wound that do not heal. Similarities between Tumors Stroma Generation and Wound Healing. *N. Engl. J. Med.* (1986). doi:10.1056/NEJM198612253152606

72. Apte, M. V. *et al.* Desmoplastic reaction in pancreatic cancer: Role of pancreatic stellate cells. *Pancreas* **29,** 179–187 (2004).

73. Apte, M. V., Pirola, R. C. & Wilson, J. S. Pancreatic stellate cells: A starring role in normal and diseased pancreas. *Frontiers in Physiology* (2012). doi:10.3389/fphys.2012.00344

74. Omary, M. B., Lugea, A., Lowe, A. W. & Pandol, S. J. The pancreatic stellate cell: A star on the rise in pancreatic diseases. *J. Clin. Invest.* **117,** 50–59 (2007).

75. Alba-Castellón, L. *et al.* Snail1-dependent activation of cancer-associated fibroblast controls epithelial tumor cell invasion and metastasis. *Cancer Res.* (2016). doi:10.1158/0008-5472.CAN-16-0176

76. Xu, Z. *et al.* Role of pancreatic stellate cells in pancreatic cancer metastasis. *Am. J. Pathol.* (2010). doi:10.2353/ajpath.2010.090899

77. Neesse, A., Algül, H., Tuveson, D. A. & Gress, T. M. Stromal biology and therapy in pancreatic cancer: A changing paradigm. *Gut* (2015). doi:10.1136/gutjnl-2015-309304

78. Kota, J., Hancock, J., Kwon, J. & Korc, M. Pancreatic cancer: Stroma and its current and emerging targeted therapies. *Cancer Lett.* **391,** 38–49 (2017).

79. Kanat, O. & Ertas, H. Shattering the castle walls: Anti-stromal therapy for pancreatic cancer. *World J. Gastrointest. Oncol.* **10,** 202–210 (2018).

80. Olive, K. P. *et al.* Inhibition of Hedgehog Signaling Enhances Delivery of Chemotherapy in a Mouse Model of Pancreatic Cancer. *Science* **324,** 1457–1461 (2009).

81. Sherman, M. H. *et al.* Vitamin D receptor-mediated stromal reprogramming suppresses pancreatitis and enhances pancreatic cancer therapy. *Cell* **159,** 80–93 (2014).

82. Kozono, S. *et al.* Pirfenidone inhibits pancreatic cancer desmoplasia by regulating stellate cells. *Cancer Res.* (2013). doi:10.1158/0008-5472.CAN-12-3180

83. Masamune, A. *et al.* The angiotensin II type i receptor blocker olmesartan inhibits the growth of pancreatic cancer by targeting stellate cell activities in mice. *Scand. J. Gastroenterol.* (2013). doi:10.3109/00365521.2013.777776

84. Provenzano, P. P. & Hingorani, S. R. Hyaluronan, fluid pressure, and stromal resistance in pancreas cancer. *British Journal of Cancer* (2013). doi:10.1038/bjc.2012.569

85. Provenzano, P. P. *et al.* Enzymatic Targeting of the Stroma Ablates Physical Barriers to Treatment of Pancreatic Ductal Adenocarcinoma. *Cancer Cell* **21,** 418–429 (2012).

86. Thompson, C. B. *et al.* Enzymatic Depletion of Tumor Hyaluronan Induces Antitumor Responses in Preclinical Animal Models. *Mol. Cancer Ther.* (2010). doi:10.1158/1535-7163.MCT-10-0470

87. Jacobetz, M. A. *et al.* Hyaluronan impairs vascular function and drug delivery in a mouse model of pancreatic cancer. *Gut* (2013). doi:10.1136/gutjnl-2012-302529

88. Hingorani, S. R. *et al.* Phase Ib study of PEGylated recombinant human hyaluronidase and gemcitabine in patients with advanced pancreatic cancer. *Clin. Cancer Res.* (2016). doi:10.1158/1078-0432.CCR-15-2010

89. Li, S. *et al.* Angiogenesis in pancreatic cancer: current research status and clinical implications. *Angiogenesis* (2018). doi:10.1007/s10456-018-9645-2

90. Martínez-Bosch, N. *et al.* The pancreatic niche inhibits the effectiveness of sunitinib treatment of pancreatic cancer. *Oncotarget* **7,** (2016).

91. Cooper, D. N. W. & Barondes, S. H. God must love galectins; he made so many of them. *Glycobiology* (1999). doi:10.1093/glycob/9.10.979

92. Barondes, S. H. *et al.* Galectins: A family of animal β-galactoside-binding lectins. *Cell* (1994). doi:10.1016/0092-8674(94)90498-7

93. Varki, A. *et al.* Essentials of glycobiology, third edition. – *Cold Spring Harb. Cold Spring Harb. Lab. Press* (2017). doi:10.1016/S0962-8924(00)01855-9

94. Brewer, C. F., Miceli, M. C. & Baum, L. G. Clusters, bundles, arrays and lattices: Novel mechanisms for lectin-saccharide-mediated cellular interactions. *Current Opinion in Structural Biology* (2002). doi:10.1016/S0959-440X(02)00364-0

95. Johannes, L., Jacob, R. & Leffler, H. Galectins at a glance. *J. Cell Sci.* (2018). doi:10.1242/jcs.208884

96. Yang, R. Y., Rabinovich, G. A. & Liu, F. T. Galectins: Structure, function and therapeutic potential. *Expert Rev. Mol. Med.* (2008). doi:10.1017/S1462399408000719

97. Elola, M. T., Wolfenstein-Todel, C., Troncoso, M. F., Vasta, G. R. & Rabinovich, G. A. Galectins: Matricellular glycan-binding proteins linking cell adhesion, migration, and survival. *Cellular and Molecular Life Sciences* (2007). doi:10.1007/s00018-007-7044-8

98. Ahmad, N. *et al.* Galectin-3 Precipitates as a Pentamer with Synthetic Multivalent Carbohydrates and Forms Heterogeneous Cross-linked Complexes. *J. Biol. Chem.* (2004). doi:10.1074/jbc.M312834200

99. Hughes, R. C. Galectins as modulators of cell adhesion. *Biochimie* (2001). doi:10.1016/S0300-9084(01)01289-5

100. Chou, F. C., Chen, H. Y., Kuo, C. C. & Sytwu, H. K. Role of galectins in tumors and in clinical immunotherapy. *International Journal of Molecular Sciences* (2018). doi:10.3390/ijms19020430

101. Hughes, R. C. Secretion of the galectin family of mammalian carbohydrate-binding proteins. *Biochimica et Biophysica Acta - General Subjects* (1999). doi:10.1016/S0304-4165(99)00177-4

102. Seelenmeyer, C. *et al.* Cell surface counter receptors are essential components of the unconventional export machinery of galectin-1. *J. Cell Biol.* (2005). doi:10.1083/jcb.200506026

103. Voss, P. G. *et al.* Dissociation of the carbohydrate-binding and splicing activities of galectin-1. *Arch. Biochem. Biophys.* (2008). doi:10.1016/j.abb.2008.07.003

104. Camby, I., Le Mercier, M., Lefranc, F. & Kiss, R. Galectin-1: A small protein with major functions. *Glycobiology* **16,** (2006).

105. Cousin, J. M. & Cloninger, M. J. The role of galectin-1 in cancer progression, and synthetic multivalent systems for the study of Galectin-1. *International Journal of Molecular Sciences* **17,** (2016).

106. Astorgues-Xerri, L. *et al.* Unraveling galectin-1 as a novel therapeutic target for cancer. *Cancer Treatment Reviews* **40,** 307–319 (2014).

107. Cho, M. & Cummings, R. D. Galectin-1, a β-galactoside-binding lectin in Chinese hamster ovary cells. I. Physical and chemical characterization. *J. Biol. Chem.* (1995). doi:10.1074/jbc.270.10.5198

108. Vyakarnam, A., Dagher, S. F., Wang, J. L. & Patterson, R. J. Evidence for a role for galectin-1 in pre-mRNA splicing. *Mol.Cell Biol.* **17,** 4730–4737 (1997).

109. Rini, J. M. & Lobsanov, Y. D. New animal lectin structures. *Current Opinion in Structural Biology* (1999). doi:10.1016/S0959-440X(99)00008-1

110. López-Lucendo, M. F. *et al.* Growth-regulatory human galectin-1: Crystallographic characterisation of the structural changes induced by single-site mutations and their impact on the thermodynamics of ligand binding. *J. Mol. Biol.* (2004). doi:10.1016/j.jmb.2004.08.078

111. Poirier, F., Timmons, P. M., Chan, C. T., Guenet, J. L. & Rigby, P. W. Expression of the L14 lectin during mouse embryogenesis suggests multiple roles during pre- and post-implantation development. *Development* (1992). doi:10.1109/ICSIPA.2011.6144121

112. Colnot, C., Fowlis, D., Ripoche, M. A., Bouchaert, I. & Poirier, F. Embryonic implantation in galectin 1/galectin 3 double mutant mice. *Dev. Dyn.* (1998). doi:10.1002/(SICI)1097-0177(199804)211:4<306::AID-AJA2>3.0.CO;2-L

113. Puche, A. C., Poirier, F., Hair, M., Bartlett, P. F. & Key, B. Role of galectin-1 in the developing mouse olfactory system. *Dev Biol* (1996).

114. Tenne-Brown, J., Puche, A. C. & Key, B. Expression of galectin-1 in the mouse olfactory system. *Int. J. Dev. Biol.* (1998). doi:10.1073/pnas.030629101030623910 1 [pii]

115. Poirier, F. & Robertson, E. J. Normal development of mice carrying a null mutation in the gene encoding the L14 S-type

lectin. *Development* (1993).

116. McGraw, J. *et al.* Altered primary afferent anatomy and reduced thermal sensitivity in mice lacking galectin-1. *Pain* (2005). doi:10.1016/j.pain.2004.10.009

117. Ozeki, Y. *et al.* Tissue fibronectin is an endogenous ligand for galectin-1. *Glycobiology* (1995). doi:10.1093/glycob/5.2.255

118. Moiseeva, E. P., Williams, B. & Samani, N. J. Galectin 1 inhibits incorporation of vitronectin and chondroitin sulfate B into the extracellular matrix of human vascular smooth muscle cells. *Biochim. Biophys. Acta - Gen. Subj.* (2003). doi:10.1016/S0304-4165(02)00447-6

119. Moiseeva, E. P., Williams, B., Goodall, A. H. & Samani, N. J. Galectin-1 interacts with β-1 subunit of integrin. *Biochem. Biophys. Res. Commun.* (2003). doi:10.1016/j.bbrc.2003.09.112

120. Moiseeva, E. P., Spring, E. L., Baron, J. H. & De Bono, D. P. Galectin 1 modulates attachment, spreading and migration of cultured vascular smooth muscle cells via interactions with cellular receptors and components of extracellular matrix. *J. Vasc. Res.* (1999). doi:10.1159/000025625

121. Maeda, N. *et al.* Stimulation of proliferation of rat hepatic stellate cells by galectin-1 and galectin-3 through different intracellular signaling pathways. *J. Biol. Chem.* (2003). doi:10.1074/jbc.M209673200

122. Wang, P. *et al.* Profiling of the secreted proteins during 3T3-L1 adipocyte differentiation leads to the identification of novel adipokines. *Cell. Mol. Life Sci.* (2004). doi:10.1007/s00018-004-4256-z

123. Perillo, N. L., Pace, K. E., Seilhamer, J. J. & Baum, L. G. Apoptosis of T cells mediated by galectin−1. *Nature* (1995). doi:10.1038/378736a0

124. Fuertes, M. B. *et al.* Regulated expression of galectin-1 during T-cell activation involves Lck and Fyn kinases and signaling through MEK1/ERK, p38 MAP kinase and p70S6kinase. *Mol. Cell. Biochem.* (2004).

doi:10.1023/B:MCBI.0000049376.50242.7f

125. Wilson, T. J., Firth, M. N., Powell, J. T. & Harrison, F. L. The sequence of the mouse 14 kDa beta-galactoside-binding lectin and evidence for its synthesis on free cytoplasmic ribosomes. *Biochem. J.* (1989). doi:10.1042/bj2610847

126. Clerch, L. B. *et al.* Sequence of A Full-length Cdna For Rat Lung β-galactoside-binding Protein: Primary and Secondary Structure of the Lectin. *Biochemistry* (1988). doi:10.1021/bi00402a030

127. Rabinovich, G. A. Galectin-1 as a potential cancer target. *British Journal of Cancer* (2005). doi:10.1038/sj.bjc.6602493

128. Paz, A., Haklai, R., Elad-Sfadia, G., Ballan, E. & Kloog, Y. Galectin-1 binds oncogenic H-Ras to mediate Ras membrane anchorage and cell transformation. *Oncogene* (2001). doi:10.1038/sj.onc.1204950

129. Ose, R., Ohara, O. & Nagase, T. Galectin-1 and Galectin-3 Mediate Protocadherin-24-Dependent Membrane Localization of β -catenin in Colon Cancer Cell Line HCT116. *Curr. Chem. Genomics* **6,** 18–26 (2012).

130. Dagher, S. F., Wang, J. L. & Patterson, R. J. Identification of galectin-3 as a factor in pre-mRNA splicing. *Proc. Natl. Acad. Sci.* (1995). doi:10.1073/pnas.92.4.1213

131. Park, J. W., Voss, P. G., Grabski, S., Wang, J. L. & Patterson, R. J. Association of galectin-1 and galectin-3 with Gemin4 in complexes containing the SMN protein. *Nucleic Acids Res.* (2001).

132. Patterson, R. J., Wang, W. & Wang, J. L. Understanding the biochemical activities of galectin-1 and galectin-3 in the nucleus. *Glycoconjugate Journal* (2002). doi:10.1023/B:GLYC.0000014079.87862.c7

133. Gao, Y. *et al.* Nuclear galectin-1-FOXP3 interaction dampens the tumor-suppressive properties of FOXP3 in breast cancer. *Cell Death Dis.* (2018). doi:10.1038/s41419-018-0448-6

134. Bhat, R. *et al.* Nuclear repartitioning of galectin-1 by an extracellular glycan switch regulates mammary

morphogenesis. *Proc. Natl. Acad. Sci.* (2016). doi:10.1073/pnas.1609135113

135. Paron, I. *et al.* Nuclear localization of Galectin-3 in transformed thyroid cells: A role in transcriptional regulation. *Biochem. Biophys. Res. Commun.* (2003). doi:10.1016/S0006-291X(03)00151-7

136. Lin, H. M., Pestell, R. G., Raz, A. & Kim, H. R. C. Galectin-3 enhances cyclin D1 promoter activity through SP1 and a cAMP-responsive element in human breast epithelial cells. *Oncogene* (2002). doi:10.1038/sj.onc.1205820

137. Thijssen, V. L., Heusschen, R., Caers, J. & Griffioen, A. W. Galectin expression in cancer diagnosis and prognosis: A systematic review. *Biochim. Biophys. Acta - Rev. Cancer* **1855,** 235–247 (2015).

138. Van Den Brûle, F. A., Waltregny, D. & Castronovo, V. Increased expression of galectin-I in carcinoma-associated stroma predicts poor outcome in prostate carcinoma patients. *J. Pathol.* (2001). doi:10.1002/1096-9896(2000)9999:9999<::AID-PATH730>3.0.CO;2-2

139. Sanjuan, X. *et al.* Differential expression of galectin 3 and galectin 1 in colorectal cancer progression. *Gastroenterology* (1997). doi:10.1016/S0016-5085(97)70010-6

140. Spano, D. *et al.* Galectin-1 and its involvement in hepatocellular carcinoma aggressiveness. *Mol.Med.* (2010). doi:10.2119/molmed.2009.00119

141. Berberat, P. O. *et al.* Comparative analysis of galectins in primary tumors and tumor metastasis in human pancreatic cancer. *J. Histochem. Cytochem.* (2001). doi:10.1177/002215540104900414

142. Jung, E. J. *et al.* Galectin-1 expression in cancer-associated stromal cells correlates tumor invasiveness and tumor progression in breast cancer. *Int. J. Cancer* (2007). doi:10.1002/ijc.22434

143. Torres-Cabala, C. *et al.* Proteomic identification of new biomarkers and application in thyroid cytology. *Acta Cytol.*

(2006). doi:10.1159/000326006

144. Mathieu, V. *et al.* Galectin-1 in melanoma biology and related neo-angiogenesis processes. *J. Invest. Dermatol.* (2012). doi:10.1038/jid.2012.142

145. Brown, E. R. *et al.* Association of galectin-3 expression with melanoma progression and prognosis. *Eur. J. Cancer* (2012). doi:10.1016/j.ejca.2011.09.003

146. Kapucuoglu, N., Basak, P. Y., Bircan, S., Sert, S. & Akkaya, V. B. Immunohistochemical galectin-3 expression in non-melanoma skin cancers. *Pathol. Res. Pract.* (2009). doi:10.1140/epjp/i2013-13044-x

147. Kageshita, T. *et al.* Possible role of galectin-9 in cell aggregation and apoptosis of human melanoma cell lines and its clinical significance. *Int. J. Cancer* (2002). doi:10.1002/ijc.10436

148. Irie, A. *et al.* Galectin-9 as a prognostic factor with antimetastatic potential in breast cancer. *Clin. Cancer Res.* (2005). doi:10.1158/1078-0432.CCR-04-0861

149. Zhang, Z.-Y. *et al.* Galectin-9 Acts as a Prognostic Factor with Antimetastatic Potential in Hepatocellular Carcinoma. *Asian Pacific J. Cancer Prev.* (2012). doi:10.7314/APJCP.2012.13.6.2503

150. Rabinovich, G. A. & Conejo-García, J. R. Shaping the Immune Landscape in Cancer by Galectin-Driven Regulatory Pathways. *Journal of Molecular Biology* **428,** 3266–3281 (2016).

151. Demydenko, D. & Berest, I. Expression of galectin-1 in malignant tumors. *Exp. Oncol.* **31,** 74–79 (2009).

152. Ouyang, J. *et al.* Galectin-1 serum levels reflect tumor burden and adverse clinical features in classical Hodgkin lymphoma. *Blood* (2013). doi:10.1182/blood-2012-12-474569

153. Verschuere, T. *et al.* Altered galectin-1 serum levels in patients diagnosed with high-grade glioma. *J. Neurooncol.* (2013). doi:10.1007/s11060-013-1201-8

154. Makoto, W. *et al.* Clinical significance of circulating galectins

as colorectal cancer markers. *Oncol. Rep.* (2011). doi:10.3892/or.2011.1198

155. Chen, L. *et al.* Clinical implication of the serum galectin-1 expression in epithelial ovarian cancer patients. *J. Ovarian Res.* (2015). doi:10.1186/s13048-015-0206-7

156. Saussez, S. *et al.* Serum Galectin-1 and Galectin-3 Levels in Benign and Malignant Nodular Thyroid Disease. *Thyroid* (2008). doi:10.1089/thy.2007.0361

157. Martinez-Bosch, N. *et al.* Increased plasma levels of galectin-1 in pancreatic cancer: Potential use as biomarker. *Oncotarget* **9,** 32984–32996 (2018).

158. Vladoiu, M. C., Labrie, M. & St-Pierre, Y. Intracellular galectins in cancer cells: Potential new targets for therapy (review). *International Journal of Oncology* **44,** 1001–1014 (2014).

159. Fischer, C. *et al.* Galectin-1 interacts with the α5β1 fibronectin receptor to restrict carcinoma cell growth via induction of p21 and p27. *J. Biol. Chem.* (2005). doi:10.1074/jbc.M411580200

160. Kim, H. J. *et al.* High galectin-1 expression correlates with poor prognosis and is involved in epithelial ovarian cancer proliferation and invasion. *Eur. J. Cancer* (2012). doi:10.1016/j.ejca.2012.02.005

161. Xue, X. *et al.* Galectin-1 secreted by activated stellate cells in pancreatic ductal adenocarcinoma stroma promotes proliferation and invasion of pancreatic cancer cells: An in vitro study on the microenvironment of pancreatic ductal adenocarcinoma. *Pancreas* (2011). doi:10.1097/MPA.0b013e318217945e

162. Adams, L., Scott, G. K. & Weinberg, C. S. Biphasic modulation of cell growth by recombinant human galectin-1. *Biochim. Biophys. Acta - Mol. Cell Res.* (1996). doi:10.1016/0167-4889(96)00031-6

163. Griffioen, A. W. & Molema, G. Angiogenesis: potentials for pharmacologic intervention in the treatment of cancer, cardiovascular diseases, and chronic inflammation. *Pharmacol. Rev.* (2000).

164. Carmeliet, P. & Jain, R. K. Molecular mechanisms and clinical applications of angiogenesis. *Nature* (2011). doi:10.1038/nature10144

165. Griffioen, A. W. & Thijssen, V. L. Galectins in tumor angiogenesis. **2,** 1–8 (2014).

166. Thijssen, V. L., Rabinovich, G. A. & Griffioen, A. W. Vascular galectins: Regulators of tumor progression and targets for cancer therapy. *Cytokine and Growth Factor Reviews* (2013). doi:10.1016/j.cytogfr.2013.07.003

167. Thijssen, V. L., Hulsmans, S. & Griffioen, A. W. The galectin profile of the endothelium: Altered expression and localization in activated and tumor endothelial cells. *Am. J. Pathol.* (2008). doi:10.2353/ajpath.2008.070938

168. Thijssen, V. L. *et al.* Tumor cells secrete galectin-1 to enhance endothelial cell activity. *Cancer Res.* (2010). doi:10.1158/0008-5472.CAN-09-4150

169. Hsieh, S. H. *et al.* Galectin-1, a novel ligand of neuropilin-1, activates VEGFR-2 signaling and modulates the migration of vascular endothelial cells. *Oncogene* (2008). doi:10.1038/sj.onc.1211029

170. Croci, D. O. *et al.* Glycosylation-dependent lectin-receptor interactions preserve angiogenesis in anti-VEGF refractory tumors. *Cell* (2014). doi:10.1016/j.cell.2014.01.043

171. Elad-Sfadia, G., Haklai, R., Ballan, E., Gabius, H. J. & Kloog, Y. Galectin-1 augments Ras activation and diverts Ras signals to Raf-1 at the expense of phosphoinositide 3-kinase. *J. Biol. Chem.* (2002). doi:10.1074/jbc.M205698200

172. Liu, F. T. & Rabinovich, G. A. Galectins as modulators of tumour progression. *Nature Reviews Cancer* (2005). doi:10.1038/nrc1527

173. Blaser, C. *et al.* β-galactoside-binding protein secreted by activated T cells inhibits antigen-induced proliferation of T cells. *Eur. J. Immunol.* (1998). doi:10.1002/(SICI)1521-4141(199808)28:08<2311::AID-IMMU2311>3.0.CO;2-G

174. Rabinovich, G. A. *et al.* Specific inhibition of T-cell adhesion to

extracellular matrix and proinflammatory cytokine secretion by human recombinant galectin-1. *Immunology* (1999). doi:10.1007/BF01227337

175. Rabinovich, G. a *et al.* Activated rat macrophages produce a galectin-1-like protein that induces apoptosis of T cells: biochemical and functional characterization. *J. Immunol.* (1998).

176. Pace, K. E., Lee, C., Stewart, P. L. & Baum, L. G. Restricted receptor segregation into membrane microdomains occurs on human T cells during apoptosis induced by galectin-1. *J. Immunol.* (1999). doi:ji_v163n7p3801 [pii]

177. Hernandez, J. D. *et al.* Galectin-1 Binds Different CD43 Glycoforms to Cluster CD43 and Regulate T Cell Death. *J. Immunol.* (2006). doi:10.4049/jimmunol.177.8.5328

178. Rubinstein, N. *et al.* Targeted inhibition of galectin-1 gene expression in tumor cells results in heightened T cell-mediated rejection: A potential mechanism of tumor-immune privilege. *Cancer Cell* (2004). doi:10.1016/S1535-6108(04)00024-8

179. Toscano, M. A. *et al.* Differential glycosylation of TH1, TH2 and TH-17 effector cells selectively regulates susceptibility to cell death. *Nat. Immunol.* (2007). doi:10.1038/ni1482

180. Dalotto-Moreno, T. *et al.* Targeting galectin-1 overcomes breast cancer-associated immunosuppression and prevents metastatic disease. *Cancer Res.* (2013). doi:10.1158/0008-5472.CAN-12-2418

181. Méndez-Huergo, S. P., Blidner, A. G. & Rabinovich, G. A. Galectins: emerging regulatory checkpoints linking tumor immunity and angiogenesis. *Curr. Opin. Immunol.* **45,** 8–15 (2017).

182. Ilarregui, J. M. *et al.* Tolerogenic signals delivered by dendritic cells to T cells through a galectin-1-driven immunoregulatory circuit involving interleukin 27 and interleukin 10. *Nat. Immunol.* (2009). doi:10.1038/ni.1772

183. Cooper, D. *et al.* Multiple functional targets of the

immunoregulatory activity of Galectin-1. Control of immune cell trafficking, dendritic cell physiology, and T-cell fate. in *Methods in Enzymology* (2010). doi:10.1016/S0076-6879(10)80011-4

184. He, J. & Baum, L. G. Endothelial cell expression of galectin-1 induced by prostate cancer cells inhibits T-cell transendothelial migration. *Lab. Invest.* (2006). doi:10.1038/labinvest.3700420

185. Van den Brûle, F. A. *et al.* Galectin-1 modulates human melanoma cell adhesion to laminin. *Biochem. Biophys. Res. Commun.* (1995). doi:10.1006/bbrc.1995.1564

186. Van den Brûle, F. *et al.* Galectin-1 accumulation in the ovary carcinoma peritumoral stroma is induced by ovary carcinoma cells and affects both cancer cell proliferation and adhesion to laminin-1 and fibronectin. *Lab. Investig.* (2003). doi:10.1097/01.LAB.0000059949.01480.40

187. Hood, J. D. & Cheresh, D. A. Role of integrins in cell invasion and migration. *Nature Reviews Cancer* (2002). doi:10.1038/nrc727

188. Roda, O. *et al.* Galectin-1 Is a Novel Functional Receptor for Tissue Plasminogen Activator in Pancreatic Cancer. *Gastroenterology* (2009). doi:10.1053/j.gastro.2008.12.039

189. Wu, M.-H. *et al.* Galectin-1-Mediated Tumor Invasion and Metastasis, Up-Regulated Matrix Metalloproteinase Expression, and Reorganized Actin Cytoskeletons. *Mol. Cancer Res.* (2009). doi:10.1158/1541-7786.MCR-08-0297

190. Hsu, Y. L. *et al.* Galectin-1 promotes lung cancer tumor metastasis by potentiating integrin α6β4 and Notch1/Jagged2 signaling pathway. *Carcinogenesis* (2013). doi:10.1093/carcin/bgt040

191. Glinsky, G. V. Anthi-adhesion cancer therapy. 177–185 (1998).

192. Glinsky, V. V. *et al.* Intravascular metastatic cancer cell homotypic aggregation at the sites of primary attachment to the endothelium. *Cancer Res.* (2003).

193. Tinari, N. *et al.* Glycoprotein 90K/mac-2bp interacts with galectin-1 and mediates galectin-1-induced cell aggregation. *Int. J. Cancer* (2001). doi:10.1002/1097-0215(200002)9999:9999<::AID-IJC1022>3.3.CO;2-Q

194. Glinsky, V. V., Huflejt, M. E., Glinsky, G. V., Deutscher, S. L. & Quinn, T. P. Effects of Thomsen-Friedenreich antigen-specific peptide P-30 on β- galactoside-mediated homotypic aggregation and adhesion to the endothelium of MDA-MB-435 human breast carcinoma cells. *Cancer Res.* (2000). doi:10.1007/s00464-016-5106-4

195. Chiang, W. F. *et al.* Overexpression of galectin-1 at the tumor invasion front is associated with poor prognosis in early-stage oral squamous cell carcinoma. *Oral Oncol.* (2008). doi:10.1016/j.oraloncology.2007.03.004

196. Fitzner, B. *et al.* Galectin-1 is an inductor of pancreatic stellate cell activation. *Cell. Signal.* (2005). doi:10.1016/j.cellsig.2004.12.012

197. Masamune, A. *et al.* Galectin-1 induces chemokine production and proliferation in pancreatic stellate cells. *Am.J.Physiol Gastrointest.Liver Physiol* (2006). doi:10.1152/ajpgi.00511.2005

198. Wu, K. L. *et al.* Circulating Galectin-1 and 90K/Mac-2BP Correlated with the Tumor Stages of Patients with Colorectal Cancer. *Biomed Res. Int.* (2015). doi:10.1155/2015/306964

199. Plattel, W. J. *et al.* Biomarkers for evaluation of treatment response in classical Hodgkin lymphoma: comparison of sGalectin-1, sCD163 and sCD30 with TARC. *Br. J. Haematol.* (2016). doi:10.1111/bjh.14317

200. Chen, K., Cai, Y., Zhang, M., Wu, Z. & Wu, Y. Both serum and tissue Galectin-1 levels are associated with adverse clinical features in neuroblastoma. *Pediatr. Blood Cancer* (2018). doi:10.1002/pbc.27229

201. Martínez-Bosch, N. *et al.* Galectin-1 drives pancreatic carcinogenesis through stroma remodeling and hedgehog signaling activation. *Cancer Res.* **74,** 3512–3524 (2014).

202. Guerra, C. *et al.* Pancreatitis-induced inflammation contributes to pancreatic cancer by inhibiting oncogene-induced senescence. *Cancer Cell* (2011). doi:10.1016/j.ccr.2011.05.011

203. Guerra, C. *et al.* Chronic Pancreatitis Is Essential for Induction of Pancreatic Ductal Adenocarcinoma by K-Ras Oncogenes in Adult Mice. *Cancer Cell* (2007). doi:10.1016/j.ccr.2007.01.012

204. Hingorani, S. R. *et al.* Preinvasive and invasive ductal pancreatic cancer and its early detection in the mouse. *Cancer Cell* (2003). doi:10.1016/S1535-6108(03)00309-X

205. Friedlander, S. Y. G. *et al.* Context-Dependent Transformation of Adult Pancreatic Cells by Oncogenic K-Ras. *Cancer Cell* (2009). doi:10.1016/j.ccr.2009.09.027

206. Habbe, N. *et al.* Spontaneous induction of murine pancreatic intraepithelial neoplasia (mPanIN) by acinar cell targeting of oncogenic Kras in adult mice. *Proc. Natl. Acad. Sci.* (2008). doi:10.1073/pnas.0810097105

207. Carriere, C., Seeley, E. S., Goetze, T., Longnecker, D. S. & Korc, M. The Nestin progenitor lineage is the compartment of origin for pancreatic intraepithelial neoplasia. *Proc. Natl. Acad. Sci.* (2007). doi:10.1073/pnas.0701117104

208. De La O, J.-P. *et al.* Notch and Kras reprogram pancreatic acinar cells to ductal intraepithelial neoplasia. *Proc. Natl. Acad. Sci.* (2008). doi:10.1073/pnas.0810111105

209. Orozco, C. A. *et al.* Targeting galectin-1 inhibits pancreatic cancer progression by modulating tumor–stroma crosstalk. *Proc. Natl. Acad. Sci. U. S. A.* **115,** (2018).

210. Shen, J., Person, M. D., Zhu, J., Abbruzzese, J. L. & Li, D. Protein expression profiles in pancreatic adenocarcinoma compared with normal pancreatic tissue and tissue affected by pancreatitis as detected by two-dimensional gel electrophoresis and mass spectrometry. *Cancer Res.* (2004). doi:10.1158/0008-5472.CAN-04-3262

211. Orozco Castaño, C. A. Deciphering the Role of Stromal Galectin-1 in Pancreatic Cancer Progression and Its Putative

Use As a Therapeutic Target. (Institut de Recerca Hospital del Mar, 2017).

212. Masamune, A., Watanabe, T., Kikuta, K. & Shimosegawa, T. Roles of Pancreatic Stellate Cells in Pancreatic Inflammation and Fibrosis. *Clin. Gastroenterol. Hepatol.* (2009). doi:10.1016/j.cgh.2009.07.038

213. Walker, C., Mojares, E. & Del Río Hernández, A. Role of extracellular matrix in development and cancer progression. *International Journal of Molecular Sciences* (2018). doi:10.3390/ijms19103028

214. Erdogan, B. *et al.* Cancer-associated fibroblasts promote directional cancer cell migration by aligning fibronectin. *J. Cell Biol.* **216,** 3799–3816 (2017).

215. Pickup, M., Novitskiy, S. & Moses, H. L. The roles of TGFβ in the tumour microenvironment. *Nature Reviews Cancer* (2013). doi:10.1038/nrc3603

216. Smyth, G. K., Ritchie, M. & Thorne, N. Linear Models for Microarray and RNA-Seq Data User's Guide. in *R* (2015). doi:10.1093/nar/gkv007

217. Tape, C. J. *et al.* Oncogenic KRAS Regulates Tumor Cell Signaling via Stromal Reciprocation. *Cell* **165,** 910–920 (2016).

218. Recktenwald, C. V., Mendler, S., Lichtenfels, R., Kellner, R. & Seliger, B. Influence of Ki-ras-driven oncogenic transformation on the protein network of murine fibroblasts. *Proteomics* **7,** 385–398 (2007).

219. Horsch, M. *et al.* Overexpressed vs mutated Kras in murine fibroblasts: A molecular phenotyping study. *Br. J. Cancer* **100,** 656–662 (2009).

220. Asem, M. S., Buechler, S., Wates, R. B., Miller, D. L. & Stack, M. S. Wnt5a signaling in cancer. *Cancers (Basel).* **8,** (2016).

221. Griesmann, H. *et al.* WNT5A-NFAT Signaling Mediates Resistance to Apoptosis in Pancreatic Cancer. *Neoplasia* (2013). doi:10.1593/neo.121312

222. Vuga, L. J. *et al.* WNT5A is a regulator of fibroblast

proliferation and resistance to apoptosis. *Am. J. Respir. Cell Mol. Biol.* (2009). doi:10.1165/rcmb.2008-0201OC

223. Ha, G. H., Kim, J. L. & Breuer, E. K. Y. Transforming acidic coiled-coil proteins (TACCs) in human cancer. *Cancer Lett.* **336,** 24–33 (2013).

224. Still, I. H., Hamilton, M., Vince, P., Wolfman, A. & Cowell, J. K. Cloning of TACC1, an embryonically expressed, potentially transforming coiled coil containing gene, from the 8p11 breast cancer amplicon. *Oncogene* (1999). doi:10.1038/sj.onc.1202801

225. Laderach, D. J. *et al.* Dissecting the signal transduction pathways triggered by galectin-glycan interactions in physiological and pathological settings. *IUBMB Life* (2010). doi:10.1002/iub.281

226. ZHANG, W. & LIU, H. T. MAPK signal pathways in the regulation of cell proliferation in mammalian cells. *Cell Res.* (2002). doi:10.1038/sj.cr.7290105

227. Cogoi, S. & Xodo, L. E. G-quadruplex formation within the promoter of the KRAS proto-oncogene and its effect on transcription. *Nucleic Acids Res.* **34,** 2536–2549 (2006).

228. Hoffman, E. K., Trusko, S. P., Murphy, M. & George, D. L. An S1 nuclease-sensitive homopurine/homopyrimidine domain in the c-Ki-ras promoter interacts with a nuclear factor. *Proc Natl Acad Sci U S A* **87,** 2705–2709 (1990).

229. Bailey, T. L., Johnson, J., Grant, C. E. & Noble, W. S. The MEME Suite. *Nucleic Acids Res.* **43,** W39–W49 (2015).

230. Agrawal, P., Yu, K., Salomon, A. R. & Sedivy, J. M. Proteomic profiling of Myc-associated proteins. *Cell Cycle* (2010). doi:10.4161/cc.9.24.14199

231. Nasrabadi, D. *et al.* Nuclear proteome analysis of monkey embryonic stem cells during differentiation. *Stem Cell Rev. Reports* (2010). doi:10.1007/s12015-009-9109-6

232. American Cancer Society. Cancer Facts and Figures 2018. *Am. Cancer Soc.* 1–71 (2018). doi:10.1182/blood-2015-12-687814

233. Martinez-Bosch, N., Vinaixa, J. & Navarro, P. Immune evasion in pancreatic cancer: From mechanisms to therapy. *Cancers* **10,** (2018).

234. Punt, S. *et al.* Galectin-1, -3 and -9 expression and clinical significance in squamous cervical cancer. *PLoS One* **10,** 1–13 (2015).

235. Apte, M. V., Wilson, J. S., Lugea, A. & Pandol, S. J. A starring role for stellate cells in the pancreatic cancer microenvironment. *Gastroenterology* (2013). doi:10.1053/j.gastro.2012.11.037

236. Jolly, L. A. *et al.* Fibroblast-mediated collagen remodeling within the tumor microenvironment facilitates progression of thyroid cancers driven by brafv600e and pten loss. *Cancer Res.* (2016). doi:10.1158/0008-5472.CAN-15-2351

237. Kaukonen, R. *et al.* Normal stroma suppresses cancer cell proliferation via mechanosensitive regulation of JMJD1a-mediated transcription. *Nat. Commun.* (2016). doi:10.1038/ncomms12237

238. Sala Romanyà, L. *et al.* Abrogration of myofibroblast activities in metastasis ans fibrosis by methyltransferase inhibition. In revision. *Int. J. Cancer*

239. Roberts, P. J. & Der, C. J. Targeting the Raf-MEK-ERK mitogen-activated protein kinase cascade for the treatment of cancer. *Oncogene* (2007). doi:10.1038/sj.onc.1210422

240. Serra, R. W., Fang, M., Park, S. M., Hutchinson, L. & Green, M. R. A KRAS-directed transcriptional silencing pathway that mediates the CpG island methylator phenotype. *Elife* (2014). doi:10.7554/eLife.02313

241. Yoo, Y., Wu, X. & Guan, J. L. A novel role of the actin-nucleating Arp2/3 complex in the regulation of RNA polymerase II-dependent transcription. *J. Biol. Chem.* (2007). doi:10.1074/jbc.M607596200

242. Favata, M. F. *et al.* Identification of a novel inhibitor of mitogen-activated protein kinase kinase. *J. Biol. Chem.* (1998). doi:10.1074/jbc.273.29.18623

243. Moutsatsos, I. K., Wadet, M., Schindler, M. & Wang, J. L. Endogenous lectins from cultured cells : Nuclear localization of carbohydrate-binding protein 35 in proliferating 3T3 fibroblasts. *Proc. Natl. Acad. Sci. U. S. A.* (1987). doi:10.1073/pnas.84.18.6452

244. Song, S. *et al.* Galectin-3 modulates MUC2 mucin expression in human colon cancer cells at the level of transcription via AP-1 activation. *Gastroenterology* (2005). doi:10.1053/j.gastro.2005.09.002

245. Douchi, D. *et al.* Silencing of LRRFIP1 reverses the epithelial-mesenchymal transition via inhibition of the Wnt/β-catenin signaling pathway. *Cancer Lett.* (2015). doi:10.1016/j.canlet.2015.05.023

246. Ariake, K. *et al.* GCF2/LRRFIP1 promotes colorectal cancer metastasis and liver invasion through integrin-dependent RhoA activation. *Cancer Lett.* (2012). doi:10.1016/j.canlet.2012.06.012

247. Inoue, K. & Fry, E. A. Tumor suppression by the EGR1, DMP1, ARF, p53, and PTEN Network. *Cancer Invest.* **36,** 520–536 (2018).

248. Adamson, E. D. & Mercola, D. Egr1 transcription factor: Multiple roles in prostate tumor cell growth and survival. *Tumor Biology* (2002). doi:10.1159/000059711

249. Ghatak, S. *et al.* Transforming growth factor β1 (TGF β1) regulates CD44V6 expression and activity through extracellular signal-regulated kinase (ERK)-induced EGR1 in pulmonary fibrogenic fibroblasts. *J. Biol. Chem.* (2017). doi:10.1074/jbc.M116.752451

250. Crnogorac-Jurcevic, T. *et al.* Molecular Analysis of Precursor Lesions in Familial Pancreatic Cancer. *PLoS One* (2013). doi:10.1371/journal.pone.0054830

251. Mourad-Zeidan, A. A., Melnikova, V. O., Wang, H., Raz, A. & Bar-Eli, M. Expression profiling of galectin-3-depleted melanoma cells reveals its major role in melanoma cell plasticity and vasculogenic mimicry. *Am. J. Pathol.* (2008).

doi:10.2353/ajpath.2008.080380

252. Mehrotra, P. *et al.* PARP-14 functions as a transcriptional switch for Stat6-dependent gene activation. *J. Biol. Chem.* (2011). doi:10.1074/jbc.M110.157768

253. Hwang, R. F. *et al.* Cancer-Associated Stromal Fibroblasts Promote Pancreatic Tumor Progression. *Cancer Res.* **68,** 918–926 (2008).

254. Pear, W. S., Nolan, G. P., Scott, M. L. & Baltimore, D. Production of high-titer helper-free retroviruses by transient transfection. *Proc. Natl. Acad. Sci.* (1993). doi:10.1073/pnas.90.18.8392

255. Livak, K. J. & Schmittgen, T. D. Analysis of relative gene expression data using real-time quantitative PCR and the 2-ΔΔCT method. *Methods* (2001). doi:10.1006/meth.2001.1262

256. Schmittgen, T. D. & Livak, K. J. Analyzing real-time PCR data by the comparative CTmethod. *Nat. Protoc.* (2008). doi:10.1038/nprot.2008.73

257. Franco-Barraza, J., Beacham, D. A., Amatangelo, M. D. & Cukierman, E. Preparation of extracellular matrices produced by cultured and primary fibroblasts. *Curr. Protoc. Cell Biol.* (2016). doi:10.1002/cpcb.2

258. Froger, A. & Hall, J. E. Transformation of Plasmid DNA into E. coli Using the Heat Shock Method. *J. Vis. Exp.* (2007). doi:10.3791/253

259. Kopitz, J., Von Reitzenstein, C., Burchert, M., Cantz, M. & Gabius, H. J. Galectin-1 is a major receptor for ganglioside GM1, a product of the growth-controlling activity of a cell surface ganglioside sialidase, on human neuroblastoma cells in culture. *J. Biol. Chem.* (1998). doi:10.1074/jbc.273.18.11205